Investigating the deposition of the extracellular matrix and bone tissue development in vitro using 2D and 3D cell culture methods

CHOONG, KELLY,WOAN,RU

Investigating the deposition of the extracellular matrix and bone tissue development *in vitro* using 2D and 3D cell culture methods

Kelly Woan Ru Choong BSc

A thesis submitted for the degree of Master of Science

Supervisor: Professor Stefan Przyborski

Department of Biosciences

Durham University

DH1 3LE

Abstract

The study of bone tissue development *in vitro* has received much attention over the years due to the increasing incidences of bone disorders worldwide. This has resulted in a growing need for improving the knowledge of bone cell physiology in order to investigate the causes and to develop potential treatments for bone diseases. One approach to this is by modelling osteoblast differentiation *in vitro* which usually involves culturing bone forming cells such as mesenchymal stem cells (MSCs) and bone derived cell lines such as MG-63 on two-dimensional (2D) culture plasticware. However, this culture environment results in alterations to the cell morphology, leading to changes in cell fate and differentiation potential as the microenvironment does not reflect the natural three-dimensional (3D) extracellular matrix in which cells reside *in vivo*. To overcome this, the development of 3D cell culture techniques has been widely investigated to better recapitulate the native environments of bone forming cells, thereby helping to enhance bone formation.

This project describes the culture of bone forming cells on a 3D scaffold to investigate whether osteoblast differentiation and thereby bone formation will be enhanced when compared to 2D. Two types of bone forming cells were used in this study, primary rat MSCs and MG-63s. They were induced to undergo osteogenic differentiation via the use of osteogenic morphogens in both 2D and 3D culture conditions. Results indicated the increase in expression of osteoblast markers such as Collagen I and Alkaline Phosphatase in 3D cultures of MSCs and MG-63s. Additionally, matrix mineralisation was also suggested to be enhanced in 3D cultures. These results suggest bone formation is enhanced in 3D cell culture when compared to 2D methods and reveal the advantages of using a 3D cell culture system to model bone tissue development *in vitro*. However, more data and additional work is required to confirm these findings.

Acknowledgements

I would like to acknowledge and express my gratitude to a number of people who have made this project possible. Firstly, I would like to thank my supervisor Professor Stefan Przyborski for providing me with the opportunity to complete the project, as well as offering advice and guidance throughout this year.

Thank you to all members of the Przyborski group for all your support and making the lab environment a great place to work every day. To Claire Mobbs, for being a lovely friend and someone who I could turn to for advice whenever I needed. To Henry Hoyle, for being my rat buddy and offering ideas even if they were at times somewhat “too creative” for the project. To Ben Allcock, for providing constant jokes and entertainment in the lab. To Nicole Darling, for always looking out for me and providing support when I needed. To Alex Hildago, for always listening and offering to help. To Amy Simpson, for being there whenever I needed a chat. To Lucy Smith, for all her help and technical knowledge especially at the beginning. To Lydia Costello, Kirsty Goncalves, Steve Bradbury, Matthew Freer for all their support and advice.

I would also like to thank my friends for being there and supporting me throughout this year. Thank you to Zoe, for going through this masters with me. Thank you to my family who have always been there in my time of need. Finally, I would like to thank Milan. Thank you for being my rock and for always believing in me. I could not have done this without your endless love and support.

Declaration

This work described herein was carried out in the Department of Biosciences, Durham University between October 2018 and September 2019. All of the work is my own, except otherwise stated. No part has previously been submitted for a degree at this or other universities.

Statement of Copyright

Table of Contents

List of Figures

List of Tables

Abbreviations

ADSCs	Adipose-derived Mesenchymal Stem Cells
ALP	Alkaline Phosphatase activity
APS	Ammonium Persulfate
Asc	Ascorbic acid
ASCs	Adult stem cells
BM	Bone marrow
BMP	Bone morphogenic protein
BMPs	Bone morphogenetic proteins
BSP	Bone sialoprotein
BTE	Bone Tissue Engineering
Dex	Dexamethasone
DMEM	Dulbecco's modified eagle medium
DPBS	Dulbecco's Phosphate-Buffered Saline
ECL	Enhanced chemiluminescence
ELISA	Enzyme-linked Immunosorbent Assay
ESCs	Embryonic stem cells
FAK	Focal Adhesion Kinase
FBS	Fetal Bovine Serum
HSCs	Haematopoietic stem cells
M-CSF	Macrophage colony-stimulating factor
MEM	Modified Eagle Minimum essential Medium
MPER	Mammalian Protein Extraction Reagent
MSCs	Mesenchymal stem cells
MSCs	Rat mesenchymal stem cells
NDP	Nucleoside diphosphate
NGS	Normal goat serum
OCN	Osteocalcin
ON	Osteonectin
OPN	Osteopointin
OS	Osteogenic
PBS	Phosphate buffered saline
PCL	Polycaprolactone
PFA	Paraformaldehyde
PGA	Poly glycolic acid

PLA	Poly lactic acid
*p*NPP	*p*-nitrophenyl phosphate
PTHrP/PTHIR	Parathyroid hormone related-protein
ROS	Reactive oxygen species
RT-qPCR	Real-time quantitative polymerase chain reaction
SDS	Sodium dodecyl sulfate
SDS-PAGE	Sodium dodecyl sulfate – polyacrylamide gel electrophresis
SEM	Scanning electron microscopy
TEMED	N,N,N,N'-tetramethylethane-1,2-diamine
TGFβ1	Transforming growth factor β1

1. Introduction

1.1 Bone anatomy and physiology

Bone is a highly specialised and dynamic connective tissue that undergoes continuous remodelling in the body. Bone is responsible for many different functions in the body, with examples of the most significant roles being:

- Support and protection of vital soft tissues
- Locomotion
- Providing rigidity and shape
- Maintaining calcium and phosphate homeostasis

In order to meet these responsibilities, bone tissue needs to be stiff in order to resist deformation yet flexible enough to absorb energy in response to mechanical stimuli[1]. There are a number of processes which allow for this, such as bone remodelling and mineralisation of its extracellular components which will be explored further. The human skeletal system is comprised of over 200 individual bones, each with a different type (long, short, flat or irregular) and location in the body. Bones can be categorised into two distinct groups through their histology – cortical and trabecular.

1.1.1 Cortical bone

Cortical bone (also known as compact) is found at the dense external layer of long bones and the surfaces of flat bones[2]. It is solid and has a high matrix mass per unit volume, providing the cortical bone with substantial strength and rigidity to carry out its function of supporting muscle action and weight bearing[1]. Cortical bone is composed microscopically of osteons which forms the Haversian system. The Haversian system is arranged with blood vessels and nerves in the centre which are surrounded by concentric layers of calcified bone tissue, referred to as lamellae. This system allows the cortical bone to remain hard while being able to receive nutrients and dispose of waste through osteocytes in the channels[3].

1.1.2 Trabecular bone

Trabecular bone (also known as cancellous) is the internal tissue which is found at the epiphysis (ends) of long bones and inner parts of flat bones. One of the key aspects of trabecular bone is the high porosity contained within the bone, with 50-90% of total trabecular bone volume being made up of pores[4]. The pores are interspersed within an internal highly ordered framework of trabeculae, which are interconnecting horizontal and vertical structural elements. Each trabecula is formed along lines of stress. This gives the trabeculae strength and forms the characteristic spongy-like

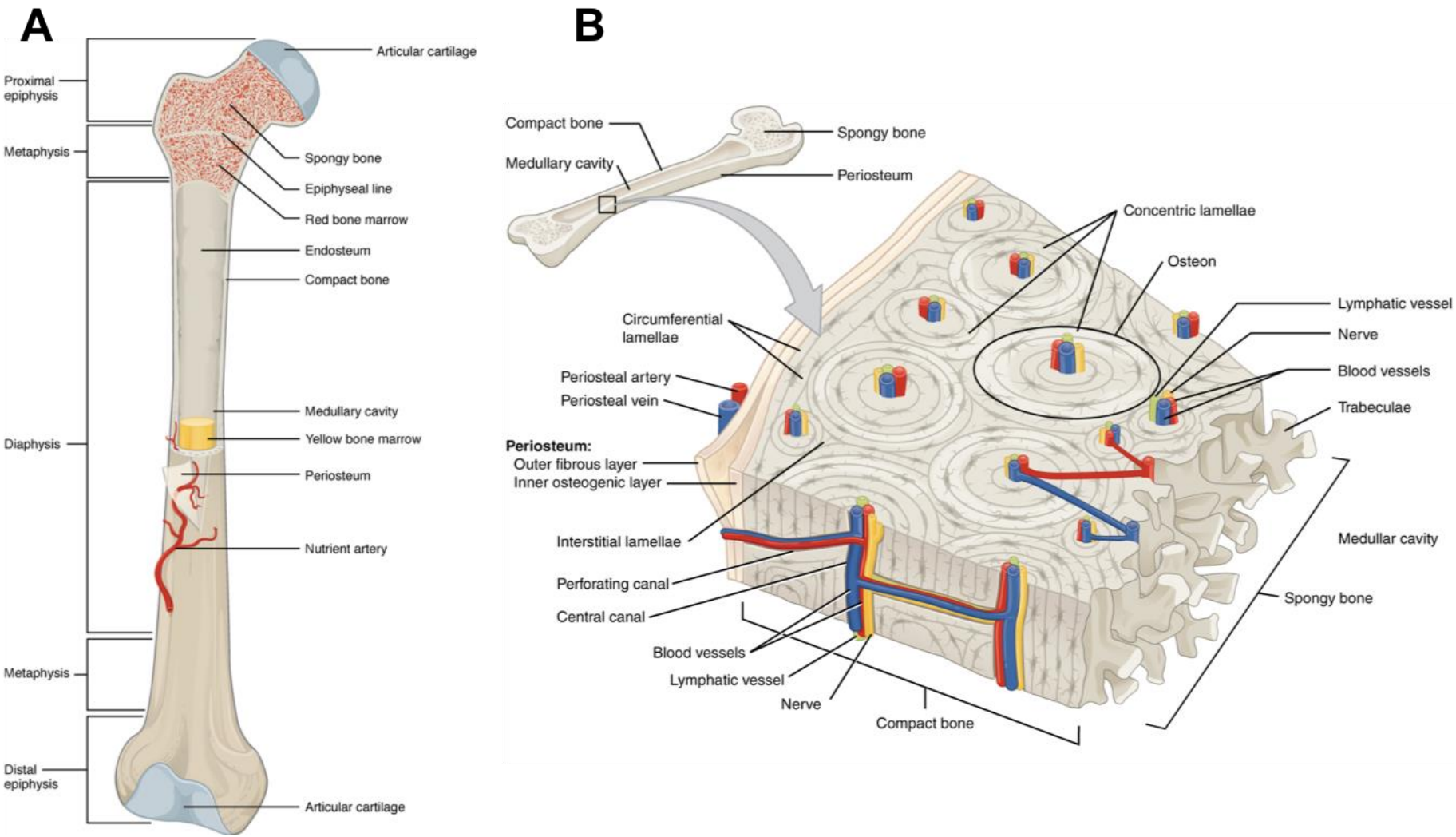

Figure 1.1 Anatomy of a long bone and the microscopic structures involved in cortical bone. The structure of a long bone is shown with the gross anatomical characteristics labelled (A). The components which make up the basic structural unit of cortical (compact) bone (osteon) is shown in (B). Schematic adapted from OpenStax, Anatomy & Physiology. OpenStax CNX. Feb 26, 2016 http://cnx.org/contents/14fb4ad7-39a1-4eee-ab6e-3ef2482e3e22@8.24.

honeycomb appearance[2]. Although trabecular bone possesses less strength compared to cortical bone, one of its roles is to provide secondary mechanical support by offsetting the load and energy experienced by bone during movement. The high porosity of the bone allows trabecular bone to be lighter compared to the heavy, solid cortical bone. Other important functions of trabecular bone include maintaining mineral homeostasis and haematopoiesis[1].

1.1.3 Bone matrix

The surface in which bone cells are embedded is referred to as the bone matrix. The bone matrix is composed of organic and inorganic elements, with the organic component being known as osteoid which is primarily comprised of collagen. Collagen is the major structural component of the osteoid, with type I collagen making up 90% of the organic matrix, along with other types of collagen (III, V, X, and XII)[5]. Collagen is a fibrous structural protein made up of individual collagen fibrils, which consists of 3 polypeptide chains (two $\alpha 1$ chains and one $\alpha 2$ chain) assembled into a triple helix procollagen molecule[6]. Osteoblasts are responsible for secreting the procollagen molecules, which converge together to form a collagen fibre. Collagen propeptides are cleaved off after secretion before the assembly to mature collagen fibres. This highly stable configuration is resistant to proteolytic degradation and provides the bone with flexibility. Intermolecular cross-links between collagens as well as the addition of inorganic minerals to the collagenous network gives the bone the stiffness and strength required for its mechanical properties[7].

The remaining 10% of the organic matrix is composed of noncollagenous proteins, with bone sialoprotein (BSP) and osteocalcin being the most abundant. BSP is a glycoprotein involved in mineralisation of the matrix by binding to calcium and hydroxyapatite, and has been suggested to be involved in osteoblast differentiation[8]. Osteocalcin makes up 20% of the noncollagen matrix proteins and is significant for matrix mineralisation and stabilisation of hydroxyapatite in the matrix[9]. However, its role in regulating osteoblast activity remain uncertain as it was found to decrease bone formation by osteoblasts[10].

The inorganic mineral components of the bone matrix is largely composed of hydroxyapatite, which are salt crystals formed when calcium phosphate and calcium carbonate combine. These crystals are found surrounding and within the collagen fibres, which is responsible for giving the bone the stiffness it requires. The inorganic matrix also acts as a reservoir store of 99% of the total body calcium, along with incorporating other inorganic salts such as phosphate, sodium and magnesium[11,1].

1.1.4. Bone remodelling

Bone is a metabolically active tissue which requires continuous remodelling in order to maintain the integrity of the skeleton and allow for adaptation to mechanical load and strain. This is achieved by 2 processes – bone formation and bone resorption.

1.1.4.1 Bone formation and bone cell types

Bone tissue is composed of the four cell types which make up the "Basic Multicellular Unit" of bone: osteoblasts, osteocytes, osteoclasts and bone lining cells. Bone formation occurs in two stages: 1) production of osteoid matrix, 2) mineralisation of the matrix.

Osteoblasts are cuboidal cells which line along the surfaces of bone formation where they secrete the components of the osteoid and have a role in mineralisation. Active osteoblasts possess a prominent Golgi complex as well as numerous rough endoplasmic reticulum due to their main function of protein secretion[7]. Osteoblasts are polarised cells and only synthesise new organic matrix towards the bone surface during differentiation, which becomes mineralised. A layer of unmineralized matrix separates osteoblasts from the mineralised bone matrix, known as the osteoid seam. As the matrix becomes mineralised during bone formation, 10-20% of active osteoblasts become entrapped and either undergo apoptosis, differentiate into osteocytes[12] or become bone lining cells[7]. Inactive osteoblasts (bone-lining cells) are flattened quiescent cells with little organelles and are found within bone surfaces which are not actively undergoing formation or resorption. These cells are important in forming a barrier between osteoclasts and bone matrix to prevent inappropriate bone resorption[13].

Osteocytes are the most abundant bone cell type, making up 90-95% of the total cells found in bone. Osteocytes carry out two major functions: regulate matrix mineralisation and to form connective cytoplasmic extensions (canaliculi). Osteocytes cells reside in a lacuna (empty space) within the mineralised matrix and form a network of long cytoplasmic extensions called canaliculi, which allows them to maintain contact with adjacent osteocytes and osteoblast on the surface[1]. This sensory network allows the osteocytes to sense local and systemic stimuli which impact the bone (e.g. hormonal/mechanical), causing the osteocytes to release signals to regulate osteoblast and osteoclast activity[14]. Other roles of osteocytes which has been suggested include regulation of local mineral deposition[15] and systemic phosphate levels in the kidneys[16]. Apoptosis of osteocytes which occur in response to local stressors such as microdamage, lack of mechanical stimulation and immobilisation produces a signal to neighbouring non-dying osteocytes to express RANKL, which in turns activates osteoclasts activity of bone resorption[14,17].

1.1.4.2 Bone resorption

Bone resorption is the process in which the mineralised matrix formed by osteoblasts during bone formation is removed by osteoclasts and is replaced by new bone formation. There are three stages which is involved in bone remodelling: 1) Initiation of osteoclasts, 2) transition from resorption to new bone formation, 3) new bone formation by osteoblasts[18].

Osteoclasts are responsible for bone resorption - the process of the breakdown of bone. Osteoclasts can be activated to begin resorption from a range of trigger mechanisms such as mechanical forces, microdamage and systemic hormones[1]. This attracts cells of the haematopoietic lineage such as monocytes/macrophages to the site of resorption which become activated and fuse to differentiate into multinucleated osteoclasts. RANKL and macrophage colony-stimulating factor (M-CSF) are key proteins which are required for osteoclast maturation[2]. RANKL interacts with the RANK receptor located on the cell surface of pre-osteoclast precursors which triggers osteoclast formation, subsequently the precursors express fusion proteins such as DC-STAMP resulting in osteoclast progenitor fusion[13,19]. M-CSF is needed to stimulate osteoclast formation, as suggested by Yoshida *et al* who observed mice with non-functional M-CSF developing osteopetrosis due to lack of osteoclasts[20]. Mature osteoclasts attach to the bone surface via expression of $\alpha_V\beta_3$ integrins binding to matrix proteins containing the RGD amino acid sequence, such as osteopontin (OPN) and bone sialoprotein[21]. Osteoclast-bone interaction activates cytoskeletal reorganisation (podosomes) which are actively assembled and disassembled, resulting in osteoclast movement and resorption across the bone surface[22].

Resorption by osteoclasts involves acidification of the environment between the osteoclast and bone surface through the use of a proton pump. The acidic environment enhances the release of acid hydrolases in lysosomes which degrade the components in the organic matrix. Once resorption has completed, the osteoclasts undergo apoptosis and are removed from the resorption sites[7,23,24]. During bone remodelling, it is vital that bone resorption and bone formation is balanced in order to maintain bone homeostasis or risk the development of pathological conditions, such as osteoporosis. Figure 1.1.4 displays a summary of the processes involved in bone remodelling[25].

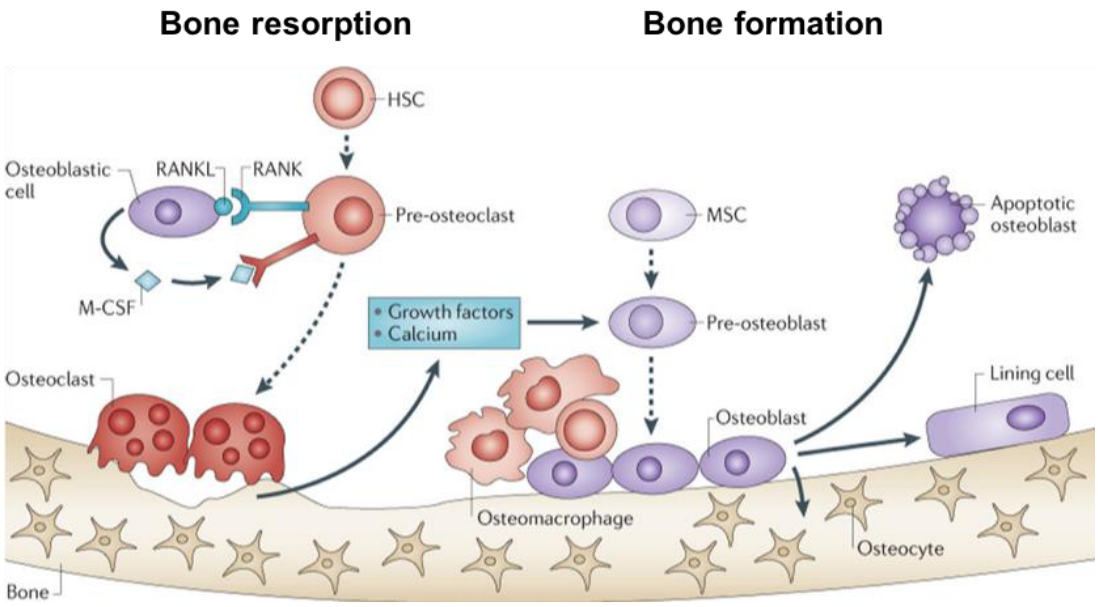

Figure 1.1.4 The processes involved in bone remodelling. Bone remodelling is a finely balanced process which occurs in order to maintain the strength and integrity of bone. Bone resorption involves haematopoietic stem cells (HSC) differentiating into osteoclasts which is responsible for demineralising the bone matrix. Osteoblasts which are derived from MSCs (mesenchymal stem cells) are bone making cells involved in bone formation, which in turn differentiate into osteocytes – cells responsible for maintaining bone. Adapted from Weilbaecher *et al*, 2011[25].

1.2 Bone differentiation *in vitro* using different cell types

Bone formation and osteoblast differentiation is widely studied *in vitro* using various cell types and models. Studies of bone is required in order to elucidate the mechanisms involved in processes such as bone remodelling as there are still uncertainties over the cytokines and hormones which regulate bone activity[13]. Knowledge of the underlying normal physiological mechanisms involved in bone formation and repair will help to develop preventions and treatments for bone disease.

Another important aspect of studying bone differentiation and formation *in vitro* is for the development of regenerating and repairing of bone tissue which is lost due to fractures, tumours and injuries etc[26]. Bone tissue engineering is a highly promising area of science research which has been made possible due to the bone being a tissue which has high potential for regeneration, such as during fracture healing. *In vitro* studies of bone remodelling will help to progress the developments made in the field of bone tissue engineering even further.

1.2.1 Mesenchymal stem cells

Mesenchymal stem cells (MSCs) are widely used to study bone tissue formation *in vitro* and hold great promise for use in bone tissue engineering. MSCs are readily expanded *in vitro*, and their ability to self-renew and differentiate into multiple lineages results in huge therapeutic potential.

1.2.1.1 History and discovery of mesenchymal stem cells

Stem cells are defined as unspecialised cells which possess the ability to self-renew indefinitely and are able to differentiate into multiple specialised cell lineages when stimulated with physiological or experimental conditions[27]. MSCs are multipotent stromal progenitor cells capable of differentiating into cells of three mesodermal lineages – osteogenic, adipogenic and chondrogenic. The discovery of MSCs *in vitro* is credited to Friedenstein *et al* who observed that cells derived from bone marrow stroma were able to generate cells of bone, adipose and cartilage origin after a series of heterotopic transplantations. They showed that these cells were distinct from haematopoietic stem cells which also reside in the bone marrow[28]. These multipotent precursor cells had similar structures to fibroblasts, hence initially being called colony-forming unit fibroblasts (CFU-FU) and could be selected via plastic adherence[29]. However, further studies confirmed their ability to proliferate while differentiating into mesenchymal lineages *in vitro*, therefore suggesting they were actually stem cells and the name "mesenchymal stem cells" was coined [30].

1.2.1.2 Challenges of the characterisation of *in vitro* MSCs

Since the discovery of MSCs in the bone marrow, there have reports of MSCs/MSC-like populations being found in other adult tissues. These include adipose tissue, peripheral blood, heart and kidney[31,32,33,34]. However, the most well characterised source of MSCs remains the bone marrow.

The characterisation of MSCs *in vitro* has remained challenging, mainly due to different laboratories using various isolation and *in vitro* culture methods. This has led to inconsistency in reports of the *in vitro* properties of MSCs which has provided setbacks to MSC research[35]and also makes cross-study comparisons difficult. In order to standardise studies, the International Society for Cellular Therapy provided guidelines for MSC characterisation. This includes three minimal criteria which cells need to possess in order to be defined as "multipotent mesenchymal stromal cells", however the name "mesenchymal stem cells" is still most widely used[36].

These are:

- Plastic-adherent in culture conditions
- Positive for a combination of surface antigens (CD73, CD105, CD90) and negative for haematopoietic markers (CD34, CD45, CD11a, CD19, CD14, HLA-DR)

- Can differentiate into osteoblasts, chondrocytes and adipocytes under the appropriate conditions

1.2.1.3 Bone marrow niche and stimulants of MSC osteoblast differentiation *in vitro*

Like all stem cells, MSCs reside in niches which are local tissue microenvironments which contain the suitable conditions to maintain and regulate stem cells. The bone marrow niche is comprised of a heterogenous population of cells, including haematopoietic stem cells (HSCs), fibroblasts and progenitor cells. MSCs have been consistently reported to lie adjacent to blood vessels, and are thought to contribute to the homeostasis of haematopoietic cells in the bone marrow[37,38].

In the body, MSCs readily differentiate into osteoblasts during bone formation. This multistep process can be modelled *in vitro* through the addition of bone morphogens to the culture media which have been shown to induce osteogenic differentiation by MSCs. The most common cocktail of osteogenic stimulants added to MSC cultures to induce osteogenic differentiation is: dexamethasone, ascorbic acid and β-glycerophosphate[39].

Dexamethasone is a common stimulant which is added to cultures to induce osteogenic differentiation. Dexamethasone is a glucocorticoid steroid which has been shown to stimulate osteogenic differentiation of bone marrow-derived stromal cells by augmenting proliferation and selecting for cells with higher osteogenic capability *in vitro*[40]. It is believed that the dexamethasone upregulates the expression of Runx2, a key transcription factor which is required for osteoblast differentiation[41]. One mechanism which has been identified to elucidate this is through dexamethasone increasing Runx2 co-activator TAZ in rat bone marrow MSCs, which suppresses adipogenic differentiation while promoting osteogenic differentiation[41,42].

Likewise, the addition of ascorbic acid further enhances osteogenic differentiation through promoting MSC proliferation and extracellular matrix synthesis of collagen I fibres[43]. The role of ascorbic acid in osteogenic differentiation is to act as a cofactor for the enzymes which carry out hydroxylation of proline and lysine residues in pro-collagen, allowing the formation of the helical structure of collagen[41]. Without ascorbic acid in the culture media, cells are unable to synthesise and secrete collagen in the extracellular matrix[44] – collagen is a vital component of the bone extracellular matrix, therefore showing the importance of ascorbic acid in stimulating osteogenic differentiation.

Furthermore, the supplementation of β-glycerophosphate in culture media facilitates osteogenic differentiation through hydrolysis by the alkaline phosphatase enzyme (ALP)[45]. This provides a source of inorganic phosphate which is crucial for the production of hydroxyapatite mineral during mineralisation of the bone matrix. A study which cultured rat osteoblast-like cells reported a decrease in *in vitro* mineralisation and loss of calcium phosphate deposition during inhibition of β-glycerophosphate, reducing bone formation[46]. Another important function of inorganic phosphate is to activate the ERK signalling pathway which regulates significant osteogenic genes, such as osteopontin (shown in murine cementoblasts)[47].

Other stimulants of osteogenic differentiation which have been added to MSC culture media includes several members of bone morphogenetic proteins (BMPs). BMP2 and BMP4 added to cultures of primary bone marrow murine cells and were found to be essential for both osteoblast and osteoclast commitment and formation[48]. The addition of growth factors such as transforming growth factor beta (TGF-β) have been shown to stimulate collagen synthesis in cells from fetal rat bone[49]. Notably, the inclusion of TGF-β in cultures of bone marrow stem cells resulted in senescence of cells and production of mitochondrial reactive oxygen species (mtROS)[50]. The role of TGF-β in osteogenic differentiation needs to be explored further for clarification of its effects on osteoblast differentiation[45].

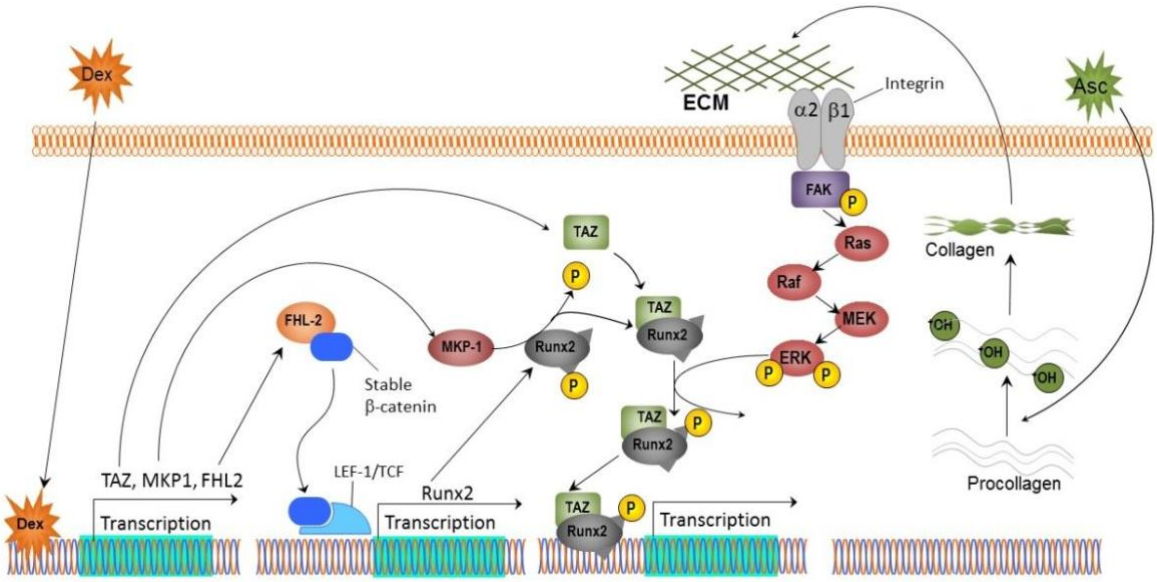

Figure 1.2.1.3 The proposed signalling pathways involved in dexamethasone and scorbic acid inducing osteogenic differentiation of stem cells. For dexamethasone (Dex), there are various transcription factors which dexamethasone can increase the expression of. This includes FHL-2 and Runx2 which are involved in the regulation of osteogenic differentiation. The addition of ascorbic acid (Asc) increases collagen synthesis which in turns increases the signalling pathway which leads to activation of Runx2. Abbreviations: ECM, extracellular matrix; +OH, hydroxylation; MEK, MAPK/ERK Kinase; FAK, Focal Adhesion Kinase; P, phosphate. Adapted from Langenbach *et al*, 2013.

1.2.1.4 The stages and markers of osteogenic differentiation of MSCs *in vitro*

The process of MSCs undergoing osteogenic differentiation to form osteoblasts can be recapitulated *in vitro* through a 3 week culture using osteogenic medium containing dexamethasone, ascorbic acid and β-glycerophosphate[51]. The result of bone formation by MSCs *in vitro* are the presence of mesenchymal condensations which form bone-like nodules[52]. During this time, three key stages occur which result in differentiated osteoblasts – 1) Proliferation, 2) Extracellular matrix development and maturation and 3) Matrix mineralisation[53].

Proliferation is the first stage of osteogenic differentiation of MSCs, whereby cell proliferation genes are upregulated and cells undergo replication to increase cell number. High expression of cell cycle genes such as histones and proto-oncogenes (c-fos and c-myc) can be seen during the first 10-12 days of culture, reflecting the highly proliferative nature of cells[53,54]. Although overexpression of c-Myc in cultures of human MSCs *in vitro* promoted proliferation, osteogenic differentiation was ultimately reduced. This suggests that proliferation needs to be higher at earlier stages but needs to be reduced in order to achieve maximum osteogenic differentiation rates. In control cultures, c-Myc levels naturally declined after day 14 in order to proceed to the next stage (matrix maturation), showing the importance of a reduction in proliferation after the early stage of osteogenic differentiation[55].

Following proliferation, MSCs continue their differentiation into mature osteoblasts through developing the extracellular matrix by the upregulation of key osteoblast proteins. ECM formation begins to accumulate between one to two weeks of culture. This stage is characterised by the production of extracellular deposits, mainly containing calcium and inorganic phosphates[52]. ALP is an metalloenzyme secreted by osteoblasts which is membrane bound and has a phasic expression during differentiation. ALP expression is increased during early osteoblast commitment and extracellular matrix formation but is downregulated during mineralisation and later stages[53]. ALP expression reaching a peak at day 14 of culturing osteogenic-induced MSCs *in vitro* has been widely reported across literature[56–58]. ALP expression is commonly used as an marker of osteoblast differentiation by MSCs. Other important growth factors and proteins secreted by osteogenic-induced MSCs for ECM formation and maturation include fibronectin, vitronectin, collagen and osteopointin (OPN) which are all used as markers of osteoblast differentiation *in vitro*[59]. Fibronectin is a glycoprotein found in the ECM which has been suggested to have a role in osteogenesis, with the expression of fibronectin mRNA being increased during early stages of osteoblast maturation[60]. Fibronectin is believed to be important during the initial attachment of osteoblasts to the matrix,

as it has been shown to be deposited in areas of osteoblast recruitment[61]. Integrins such as BMP-4 have been found to enhance fibronectin assembly into the extracellular matrix by rat osteoblasts[62].

The hallmark of final stage of osteogenesis by MSCs after induction by bone morphogens is mineralisation of the ECM, which involves the generation of calcium phosphate[63]. The main technique used to assess the levels of matrix mineralisation *in vitro* are histological stains, such as Von Kossa and Alizarin Red. The Von Kossa stain involves the use of silver nitrate solution whereby the silver cations replace calcium cations that have been bound to anionic phosphates. This can then be visualised as the silver salts are reduced to metallic silver under light, which are seen as dark brown or black deposits[64,65]. In contrast, Alizarin Red reacts directly with calcium cations by forming chelates which is orange to red in colour[66]. Both histological stains are widely used to visualise calcium deposits, which is an indicator of mineralisation of the extracellular matrix by osteogenic-induced MSCs.

The expression of several genes is also involved during the mineralisation stage of osteoblast differentiation. Osteonectin (ON) (also known as SPARC) is a bone-related protein which reaches a peak during the initiation of mineralisation (16-20 days)[52] which is important for the binding of calcium, hydroxyapatite and fibrillar collagen[67]. Osteocalcin (OCN) is considered as a marker of mature osteoblasts as its expression only occurs after ALP activity and mineral deposition which occurs during the later stages of osteoblast differentiation[68]. The role of OCN in osteoblast differentiation is thought to be involved with regulating bone mineralisation and turnover[69].

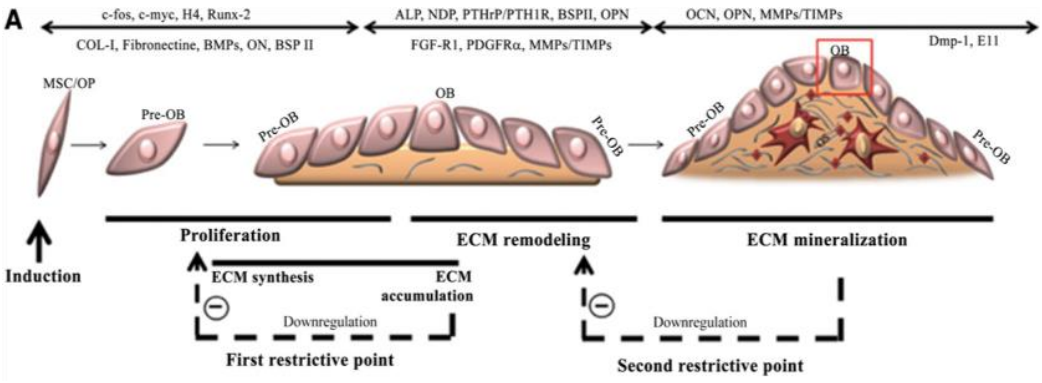

Figure 1.2.1.4 Illustration of the three stages involved in osteogenic differentiation of MSCs *in vitro.* The stages are: 1) Proliferation, 2) ECM remodelling (maturation) and 3) ECM mineralisation. The morphological changes and gene expression involved at each stage is shown above the respective step. Two restrictive points are associated with the osteogenic differentiation. The first point is the downregulation of proliferation in order to increase ECM accumulation while the second refers to the downregulation in ECM remodelling for mineral mineralisation. Abbreviations: ALP, alkaline phosphatase; BMPs, bone morphogenetic proteins; BSPII, bone sialoprotein; COL-I, collagen I; ECM, extracellular matrix; NDP, nucleoside diphosphate; OB, osteoblast, ON, osteopointin; PTHrP/PTHIR, parathyroid hormone related-protein. Adapted from Alami et al, 2016.

1.2.2 Primary cells and cell lines

Other cell types have also been used to model bone tissue formation *in vitro* outside of MSCs. Although primary human MSCs would be the most favourable cell culture model to use as it would be more relevant for clinical studies, there are some disadvantages with using primary human MSCs e.g. limited accessibility and a difficult isolation procedure. The tissue site of human MSC isolation can also exhibit functional differences e.g. MSCs isolated from orofacial bone marrow proliferate faster and have a higher ALP activity compared to iliac crest bone marrow MSCs collected from the same individuals[70]. Similarly, primary mouse/rat MSCs are also widely used and are much more easily available compared to human. However, there are interspecies differences and genomic differences which could make studies less comparable to humans studies[71].

Primary osteoblasts cells have also been investigated for use in *in vitro* bone tissue models as the terminally differentiated cells can be isolated from bone tissue, and are able to be expanded in culture. Osteoblasts can be isolated from rodents such as mouse and rat and have been widely used in studies. Rat osteoblast cells can be isolated from foetal, neonatal/adult calvaria or long bones and have been shown to retain their osteoblastic characteristics in culture, making it a suitable model for *in vitro* bone formation[72]. Similarly, osteoblasts have been isolated from mice, through their calvaria and long bones and were reported to deposit a collagenous ECM and form mineralised bone nodules[73]. However, the osteoblastic phenotype of both rat and murine osteoblasts are influenced by donor age. A comparative study reported osteoblasts isolated from 7 day old rat tibia needed 41 days to form mineralised nodules compared to only 21 days for foetal cells[74]. Likewise, expression of ALP activity was greater from mouse adult long bone compared to adult and neonatal calvarial cells[75]. This could produce results which are hard to compare between studies and may not be clinically relevant to human trials, as well as the issue of interspecies differences.

Additionally, cells from immortalised cell lines have been used to model osteoblast behaviour *in vitro*. There are many advantages to using cell lines instead of primary cells, including the ease of maintaining cultures and the supply of unlimited number of cells. There is also no need for the process of isolating cells which reduces the time needed to set up cultures. Various human cell lines have been isolated and characterised, including SaOs-2 and MG-63.

SaOs-2 is a human osteosarcoma cell line which was first isolated from an 11-year old female in 1975[76]. Cells from SaOs-2 possess a mature osteoblast phenotype and have been shown to express much higher ALP activity compared to human primary osteoblasts after 14 days of culture[77]. SaOS2

cells have been able to produce bone-like mineralised matrix and have been used to investigate osteoblast differentiation into osteocyte-like cells[78].

MG-63 is another cell line derived from human osteosarcoma, originally isolated from the left femur of a 14 year old male[79]. This study also reported the use of MG-63 in the production of human interferon, which have clinical applications in cancer therapy and have been investigated in the treatment of multiple sclerosis[80]. The cells exhibit rapid cell growth[81], which is useful in large scale studies which require an unlimited source of cells. MG-63 cells exhibit similar behaviour to normal primary human osteoblast cells in response to hormones such as 1,25(OH)2 (active form of Vitamin D)[82] and parathyroid hormone treatment[83], suggesting MG-63 cells would be useful in recapitulating the hormonal regulation of the osteoblastic phenotype during bone formation and resorption.

However, a study which characterised the extracellular matrix production of SaOs-2 and MG-63 cells reported differences in production *in vitro* compared to normal primary human osteoblasts. MMP-9 and collagen-X were found in the osteosarcoma cell lines but were not detected in normal osteoblasts. The levels of osteoblast maturity differed between SaOs-2 and MG-63, with SaOs-2 exhibiting the most mature phenotype by displaying positive results for markers such as ALP, osteocalcin and collagen I/III but only in a small population of cells (15%). No ALP activity could be detected in MG-63[84]. The increasing phenotypic heterogeneity with prolonged passaging of cells has been reported[84–86] which may limit the use of osteosarcoma cell lines in resembling the behaviour of primary osteoblast cells. Despite this, they are still commonly used in studies due to their ease of culture compared to primary cells and are a beneficial source of cells for pilot model studies of osteoblast functionality[87].

1.3 Modelling bone development *in vitro* – 2D vs 3D

Since the first isolation and in vitro culture of osteoblast cells from human bone was investigated in 1972 by Bard et al[88] , much efforts in improving the knowledge of bone cell physiology has been derived from experiments cultured using polystyrene substrates. Traditionally, cell culture models have been maintained using techniques which involve growing cells on polystyrene or glass flat two-dimensional (2D) surfaces, creating the traditional monolayer of cells. There are many advantages to using this gold standard *in vitro* cell culture method. This includes:

- Ease of use
- Low costs
- High levels of standardisation

- Allowing for great control over culture environments

However in 2D, cells are cultured on flat and rigid substrates which do not reflect the three-dimensional (3D) extracellular matrix all cells reside *in vivo.* This results in various cell changes such as in gene expression, morphology and polarity, thus providing results which are inconsistent with and nonpredictive for how cells behave *in vivo.* In 2D, cells have been shown to detect the *in vitro* environment which results in forced-polarity due to contact with substrates on one side of the cell and cell flattening and ultimately gene expression changes which do not reflect the cells' usual behaviour *in vivo*[89]. To mitigate these limitations, 3D cell culture aims to bridge the gap between the *in vivo* and *in vitro* cell environments through better recapitulating native microenvironments. This is through incorporating mechanical signals, improving cell-cell and cell-matrix interactions as well as creating spatial gradients of soluble factors in the cell environment[90]. There have been various techniques of 3D cell culture developed, all with the aim of better mimicking the *in vivo* environment.

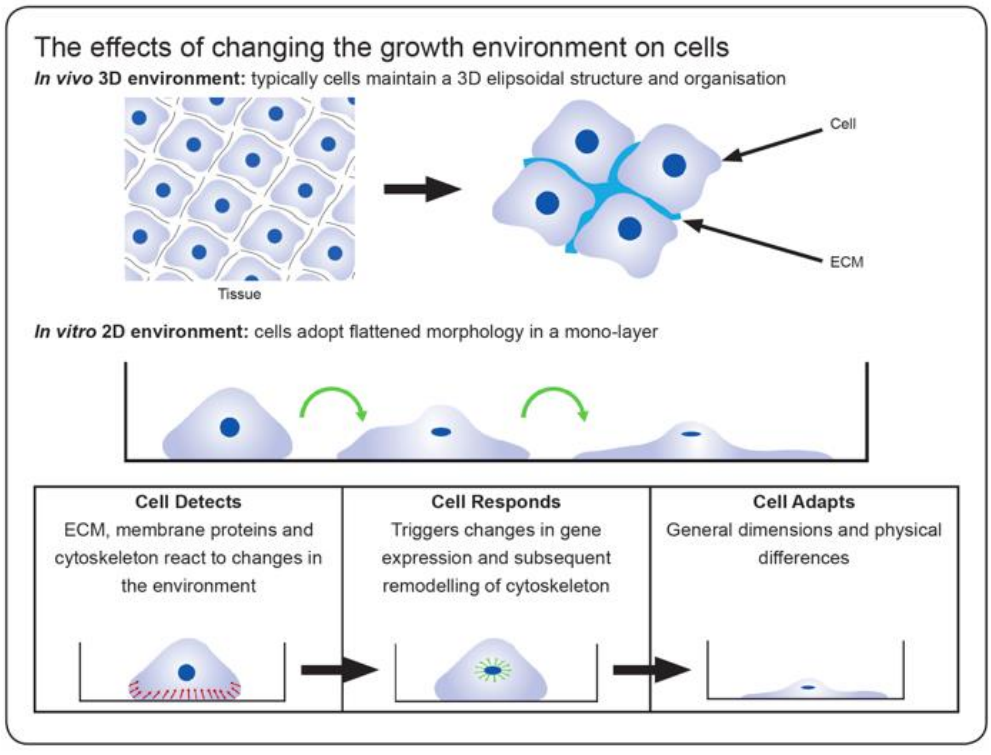

Figure 1.3. Schematic displaying the effect of the 2D and 3D environments on cell morphology. The *in vivo* 3D structure of cells is not reflected in the *in vitro* 2D environments as the cells detect the environment and adapt a flattened morphology as a result. Adapted from ReproCELL Europe Ltd.

1.3.1 2D models of *in vitro* osteoblast differentiation

The process of osteoblast differentiation has been extensively investigated *in vitro* using 2D conditions. The complete stages of osteoblast differentiation (from proliferation to mineralisation) can be recapitulated in the monolayers of bone forming cells. Lian and Stein first reported the sequence of expression of osteoblast markers during each stage of osteoblast differentiation using a monolayer of cells derived from rat calvaria[91], which is now widely used in studies to monitor the development of bone forming cells in culture. Since then, many different cell types have been grown using 2D cell culture which have been shown to undergo the full osteoblast differentiation process (as discussed in Section 1.2). Nonetheless, in some studies involving the culture of adult human derived osteoblasts, cells cultured under 2D conditions produced unsatisfactory levels of late stage osteogenesis[92,93]. Additionally, MSCs propagation using 2D cell culture alters their cell morphology, leading to changes in cell fate and differentiation potential[94]. In particular to bone tissue, bone cells communicate and interact with each other through the ECM via soluble factors or cell-cell/cell-matrix interactions. Evidently, 2D monolayer culture conditions are not able to recapitulate these conditions *in vitro* and is not physiologically relevant, illustrating the need for 3D cell culture systems to create an environment which is more like the *in vivo* niches in which bone cells live.

1.3.2 3D models of *in vitro* osteoblast differentiation - Spheroids

The use of 3D cell culture technologies used to cultivate bone forming cells and model osteoblast differentiation has become increasingly popular. There are many different types of 3D cell technologies, one of the simplest methods is spheroid formation. Maintaining bone forming cells in spheroids involves cells being prevented from adhering to the plastic and instead are stimulated to form multicellular aggregates. There are multiple methodologies for aggregate formation, including the spinner flask method, whereby the cell suspension undergoes continuous agitation to inhibit cellular attachment to the solid surface. Another technique involves using agar to prevent cellular attachment to the culture-plate bottom[95]. One of the most common techniques of generating spheroids is through the hanging drop method whereby the cell suspension is placed in a drop on an inverted tissue culture dish lid, allowing gravity to aid cells to aggregate together at the bottom of the drop[96]. Spheroid formation allows for greater cell-cell and cell-matrix interactions which more closely mimics their cellular niche as the cells are supported by the ECM produced by the cultured cells. Cultivating mouse bone marrow stromal cells in hanging drops resulted in long term survival and stemness, as well as differentiation into multiple lineages including osteogenic[97]. Additionally, culturing human bone precursor and osteoblast cells which are induced with TGFβ1

resulted in the upregulation of bone markers such as alkaline phosphatase, collagen I and osteonectin compared to monolayer cells in 2D[98].

Despite this, there are some limitations of culturing cells in spheroid formation. Due to the structure of the spheroid, the diffusion of nutrients, oxygen and waste through the centre of the spheroids are limited in larger spheroids – with increasing size of spheroids, the greater the decrease in oxygen concentration and cell viability[99,100]. This results in the internal core of spheroids being hypoxic. Spheroid culture of MSCs have reported an upregulation of hypoxia-associated genes such as VEGFA[101] and a stress response is induced[102]. The effect of oxidative stress and the production of reactive oxygen species (ROS) on MSCs has been shown to inhibit proliferation and reduce osteogenic differentiation[103]. Similarly, oxidative stress (as modelled by the addition of exogenous H2O2) suppresses osteogenic differentiation by osteoblastic cells through antagonising Wnt signalling[104] – a vital stimulus for the induction of osteogenesis.

1.3.3 3D models of *in vitro* osteoblast differentiation – Scaffolds

As previously mentioned, the use of spheroids is not suitable for larger 3D models due to the problem of nutrient exchange in the internal structure. To counter this, the use of scaffolds to support 3D growth of cells is common for modelling *in vitro* osteoblast differentiation and for bone tissue engineering. Scaffolds provide a surface for cells to attach and provide a microenvironment which aims to mimic the features found naturally within their native extracellular matrix *in vivo*. When designing scaffolds for 3D cell culture, the properties of the cells which are being cultured must be taken into account. The requirements for 3D scaffolds for culturing bone cells should reflect the natural bone matrix – highly porous with interconnected pores which are able to support cell attachment, proliferation and ECM formation[105]. For osteoblasts, a hard surface scaffold is appropriate to recapitulate the solid surface of bone in which osteoblasts attach to. Scaffolds can be fabricated from a variety of materials – either natural or synthetic[106].

Scaffolds derived from natural materials are typically components of the ECM such as collagen, elastin and fibrin. Type I Collagen scaffolds are one of the most commonly used natural scaffolds for modelling osteogenesis by bone forming cells *in vitro*. 90% of the organic matrix in bone is composed of Type I Collagen[107], therefore it is fundamental to bone formation and suggests it could be useful for 3D cell culture of osteogenic cells. Culturing primary human bone marrow-derived MSCs on a collagen scaffold with immobilised ALP resulted in the enhancement of osteoblast differentiation due to upregulation of several key osteoblastic genes such as ALP, Collagen I and osteocalcin and downregulation of osteogenic differentiation inhibitor tumour necrosis factor-α[108].

Similarly, the cultivation of osteoblastic cell line MC3T3-E1 displayed earlier mineralisation when cultured on a 3D collagen gel compared to 2D. The same study also reported the increased expression of osteoblast genes from primary rat osteoblasts when cultured on the 3D collagen gel compared to 2D[109].

Likewise, the use of natural material and synthetic scaffolds have also been shown to promote osteogenic differentiation. A study by Datta *et al* seeded primary rat MSCs onto scaffolds composed of titanium fibre meshes, in which the MSCs secreted ECM onto the scaffold. The scaffold was then decellularized and re-seeded with fresh MSCs without the osteogenic supplements and only induced to differentiate using the ECM previously deposited on the scaffold. The results of the study illustrated increased expression of osteopontin and calcium deposition compared to cells which were only seeded once on day 16, indicating the bone-like ECM synthesised *in vitro* on scaffolds can be used to enhance MSC osteoblast differentiation[110]. This demonstrates the versatility of scaffolds and how 3D cell culture can be used to enhance osteogenesis *in vitro*.

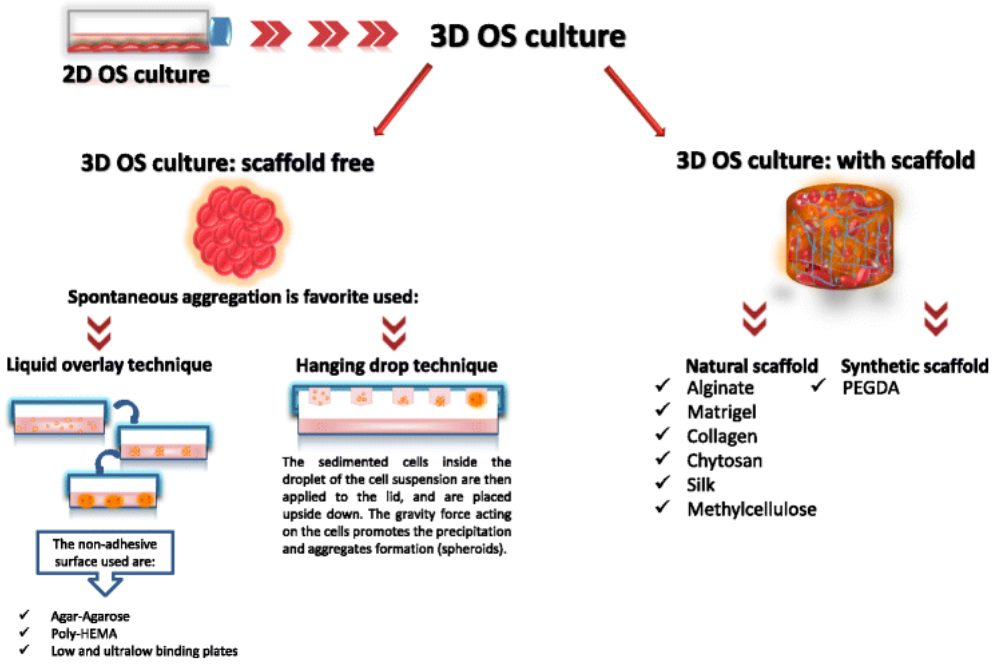

Figure 1.3.3 Overview of 2D and 3D cell culture techniques for osteogenic (OS) cultures. 2D osteogenic cultures involve cultivating cells using plastic tissue flasks which form monolayers. 3D cell cultures can be categorised according to scaffold or scaffold free. An overview of the processes involved and materials used is given. Adapted from De Luca *et al*, 2018[106].

1.3.4 Scaffolds for bone tissue engineering

Not only can 3D cell culture support an *in vitro* osteoblastic model, bone cells cultured on scaffolds can be used for bone tissue engineering (BTE). The fundamental aim of tissue engineering involves being able to replace diseased or damaged tissue with a structure grown on a scaffold regenerated *in vitro* or induced *in vivo*[111]. BTE involves the use of biomaterials and cells to induce new functional bone regeneration either for bone defect repair or for bone grafts. Bone is naturally self-repairing therefore one of the aims of BTE is to promote this process with the induction of materials generated *in vitro.* BTE is a rapidly expanding field due to the increasing worldwide incidence of bone disorders which require bone graft treatment. There are many components which are important to the field of bone tissue engineering[112]:

- Biocompatible scaffold which recapitulates the *in vivo* bone matrix
- Signals that direct osteogenic differentiation of osteogenic cells
- Osteogenic cells to produce the matrix
- Vascularisation in order to supply the nutrients and waste disposal of the tissue

One fundamental aspect of BTE is that if a scaffold is used for implantation for clinical purposes, the scaffold should be biodegradable in order for the implantation to be remodelled by the body and is then replaced by native tissue, thereby restoring original function. The scaffold must not produce any toxic or immunogenic responses during the breakdown in the body[111].

Similar to scaffolds designed for *in vitro* modelling, scaffolds for BTE can be fabricated from a range of natural and synthetic materials. The choice of material for scaffolds should be biocompatible and the body must be able to metabolise the monomeric products without producing an inflammatory response. Commonly used materials for BTE include synthetic polymers such as poly glycolic acid (PGA) and poly lactic acid (PLA) which have been investigated for their excellent mechanical properties. PGA is advantageous for BTE as its fibres exhibit high tensile strength at 7.0 GPa, allowing for a strong and biodegradable material to support BTE[113]. PLA exists in enantiomeric states due to its chirality and these states have comparable tensile strength (4-8 GPa) and a slow crystallising nature which results in a hard and brittle material, useful for fixation-devices such as screws for orthopaedic applications[114]. These polymers also possess characteristics such as biocompatibility, being biodegradable and can be assembled into different shapes[115]. Degradation over time helps with the integration of cells with host tissue during transplantation. The degradation rates of scaffolds manufactured from PGA/PLA can be controlled as higher PGA content degrades faster[111]. Seeding rat osteoblasts onto PGA and PLA substrates resulted in significant attachment, increase in ALP activity and enhanced collagen synthesis compared to cells

grown on normal tissue culture polystyrene[116]. This demonstrates the suitability of PGA/PLA as temporary substrates to transplant osteoblasts *in vivo* for use in bone regeneration.

Natural polymeric scaffolds composed of components of the ECM have been used in BTE due to their osteoinductive properties. There are three classes of natural biomaterials which are proteins (silk, collagen, gelatin etc), polysaccharides (cellulose, dextran, chitin etc) and polynucleotides (DNA,RNA) which have all been used as they naturally enhance the cells function in a biological system[117]. However, natural polymers are either cell-derived or tissue-derived which causes issues with immune rejection if they are not from the same person (allogenous or xenogenous constructs) as well as risk of disease transmission. Autogenous scaffolds require additional surgery and is not as widely available as allogenous scaffolds[115]. The main concern of using natural polymers as scaffolds for BTE is the lack of mechanical support for bone scaffolds as they provide insufficient architectural support for osteogenic cells[118]. To minimise this limitation, natural polymeric scaffolds are usually combined with other materials to produce composite scaffolds which possess excellent mechanical properties such as increasing tensile strength with the addition of polycaprolactone PCL[119] and high osteoconductivity as discussed below.

Bioceramics such as hydroxyapatite and calcium phosphate are naturally occurring in the bone matrix and have been used for their osteoinduction properties. Composite scaffolds containing bioceramics, synthetic polymers and natural polymers have been commonly used during bone repair studies and for BTE purposes[120,121]. An example of this is a study by Phipps *et al* who investigated the use of a nanofibrous bone-mimicking tri-component scaffold comprised of polycaprolactone (PCL), collagen I and hydroxyapatite for culturing MSCs. Compared to culturing MSCs on each component alone, MSCs on the tri-component scaffold displayed faster cell spreading, attachment and greater cell proliferation. An increase in the osteoblastic signalling molecule FAK was also reported. This suggests the combination of materials in the scaffold holds great promise for the delivery of exogenously expanded osteogenic cells as well as potentially inducing bone repair *in vivo*[119].

Although there are many polymeric materials which have the potential to be suitable for BTE, no single polymer possesses all the requirements necessary for successful *in vivo* bone tissue regeneration. Due to this, composite scaffolds can provide a balance between the advantages and disadvantages of each individual component and deliver an overall better suited scaffold for BTE. Moreover, as discussed previously, bone matrix *in vivo* is naturally a mix of organic and inorganic components. This suggests composite scaffolds could become the optimal scaffolds for BTE[122].

1.4 Example of 3D cell culture technology – Alvetex®

Alvetex® (ReproCELL) is a rigid, inert scaffold designed for routine *in vitro* 3D cell culture. It is comprised of a highly porous polystyrene membrane engineered by high internal emulsion templating (polyHIPE)[123]. The scaffold is available as well inserts, designed to fit into conventional 2D cell culture plasticware. Polystyrene has been the fundamental platform used for adherent animal and human cell culture due to its long shelf life, ease of manufacture and low production cost[124] allowing for mass production of Alvetex®. Polystyrene is also a material which is used in 2D culture plasticware, therefore showing its suitability for cell culture and allows comparisons to be made between 2D and 3D. The highly porous nature of Alvetex® is made up of a homogenous network of voids, linked by interconnecting pores which allows cellular attachment and interactions with neighbouring cells. The membrane of Alvetex® is engineered to be 200μm thick, which is thin enough to allows cells to gain access to nutrients and exchange gases and waste products during static culture[125]. Crosslinks in Alvetex® provide structural strength and stability to the thin membrane. The scaffold has been previously applied to a range of *in vitro* models, including co-cultures of dermal fibroblast and keratinocytes in a full thickness skin model[126], neurite outgrowth model[127] and a human airway mucosa model[128].

1.4.1 Alvetex® as a scaffold for an *in vitro* bone tissue model

Alvetex® scaffold is considered to be a suitable material for cultivating bone forming cells in an *in vitro* bone tissue model for a number of reasons. Firstly, one of the requirements for a 3D system for culturing bone cells is the resemblance to the bone matrix[105]. Bone matrix is naturally highly porous with interconnected pores which supports the attachment and proliferation of bone forming cells. Since the membrane of Alvetex® is highly porous and the structure is comparable to the *in vivo* bone matrix, it fulfils this requirement. It has been suggested that scaffolds with a highly interconnected architecture have significant impact on MSC signalling and differentiation and ultimately affects bone formation[129]. The high porosity of Alvetex® also suggests it would allow greater cell-matrix interactions which is vital during osteogenesis. Although the pore sizes differ greatly between Alvetex® scaffold (38μm) and trabecular bone (300 - 600μm)[130,131], the internal organisation of the pores are comparable (Figure 1.4.1). Another property of Alvetex® which makes it an attractive tool for modelling bone tissue *in vitro* is the requirement of a solid material for bone cells to attach. Alvetex® is fabricated from polystyrene material which have been shown to be able to support osteogenic differentiation in 2D cultures[73], therefore suggesting it is an appropriate material for cultivating bone forming cells. Previous work at Durham University involved culturing MSCs[132] and MG-63s[133] on Alvetex®, however the results were only preliminary and the osteogenesis by these bone forming cells on the scaffold requires further extensive characterisation.

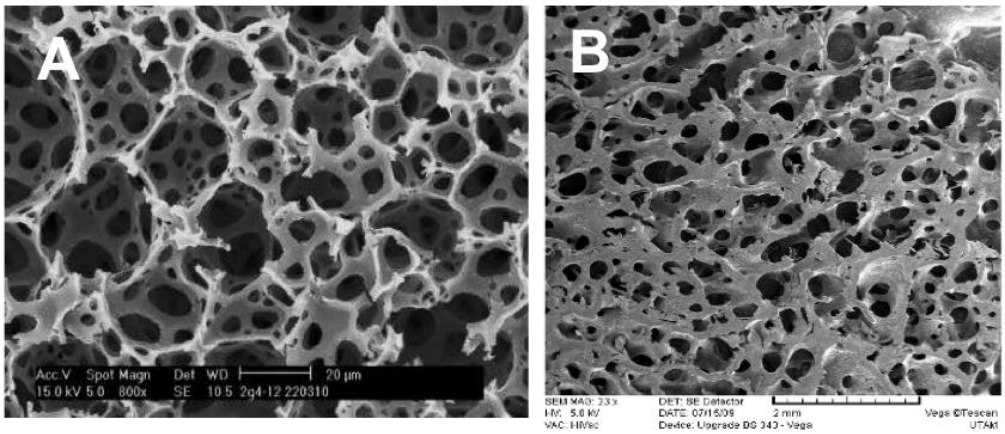

Figure 1.4.1 Comparison of the porous internal structure of Alvetex® and trabecular bone. Scanning electron microscopy images of Alvetex® scaffold (A) and human trabecular bone (B) at 800x magnification and 23x magnification respectively. Similar organisation of the porous networks can be seen between Alvetex® scaffold and human trabecular bone. Images provided by ReproCELL Europe Ltd (A) and adapted from Kytyr *et al*, 2012 (B).

1.5 Project aims and objectives

This project aims to develop an *in vitro* bone tissue model using primary rat MSCs and cells from the human osteosarcoma cell line MG-63. The models will be compared between using 2D tissue culture plasticware and 3D scaffolds to investigate whether bone formation will be enhanced using 3D cell culture. This would allow for an *in vitro* model which could be used to further develop our understanding of the mechanisms behind bone formation and remodelling.

Project objectives:

- To isolate and characterise primary rat MSCs
- To identify and culture a bone derived cell line such as MG-63
- To induce bone formation *in vitro*
- To investigate whether 3D scaffolds will support the growth of bone forming cells
- To analyse the formation and deposition of extracellular matrix by bone forming cells
- To determine whether bone nodule formation is enhanced in 3D cell culture

1.5.1 Project hypothesis

The hypothesis for this project is that culturing bone forming cells on a 3D scaffold which more closely resembles the structure of bone will provide a microenvironment more similar to the *in vivo* bone marrow niche. This will result in the enhancement and increase of the expression of differentiated bone markers in 3D by MSCs and MG63s, compared to growth on a 2D environment.

2. Materials and Methods

2.1 Mesenchymal Stem Cells

2.1.1 Isolation of rat bone marrow MSCs

Rat mesenchymal stem cells (MSCs) were isolated from the femurs and tibiae of adult Wistar rats using established protocols [134]. Rats were euthanised by cervical dislocation method. The femurs and tibiae were extracted from the back limbs and cleaned of connective tissue and muscle. These were placed in a beaker containing 70 % ethanol for a few seconds before being transferred to a beaker of 1 x DPBS (Dulbecco's Phosphate-Buffered Saline). They were kept in PBS and transferred into a sterile class II cell culture hood.

In a cell culture hood, the femurs and tibias were placed in a glass petri dish and the ends of the bones were cut open with scissors. Using forceps, the bones were held over a 50 mL conical tube (Greiner Bio One, Gloucester, UK) and a 22-gauge needle (ThermoFisher Scientific, Cramlington, UK) attached to a 5 mL syringe (ThermoFisher) was inserted into the shaft of the bone and the bone marrow (BM) was flushed out with isolation media. The isolation media consisted of Dulbecco's Modified Eagle Medium (DMEM) (Gibco, Cramlington UK) supplemented with 20 % fetal bovine serum (FBS) (Gibco), 1 % L-glutamine (ThermoFisher), 1 % Penicillin-Streptomycin (ThermoFisher). In total, 20 mL of isolation media was used to flush out the BM into the 50 mL falcon tube. The cell suspension was transferred into a new 50 mL falcon tube using a 100 μm nylon mesh cell strainer (Corning™) to remove bone debris and blood aggregates. The cells were then centrifuged at 200 x g, 4 °C for 5 minutes and supernatant containing thrombocytes and erythrocytes was aspirated. Cells were resuspended in 12 mL isolation media. This was transferred to an adherent petri dish (ThermoFisher) and incubated at 37 °C and 5 % CO_2 in a humidified incubator. This was designated as passage 0 (P0). The dishes were left to allow stromal cells (MSCs) to adhere while the non-adherent haematopoietic cells were removed through media change after two days. The MSCs were isolated by their ability to adhere to plastic culture dishes. Media was changed with isolation media every 3-4 days.

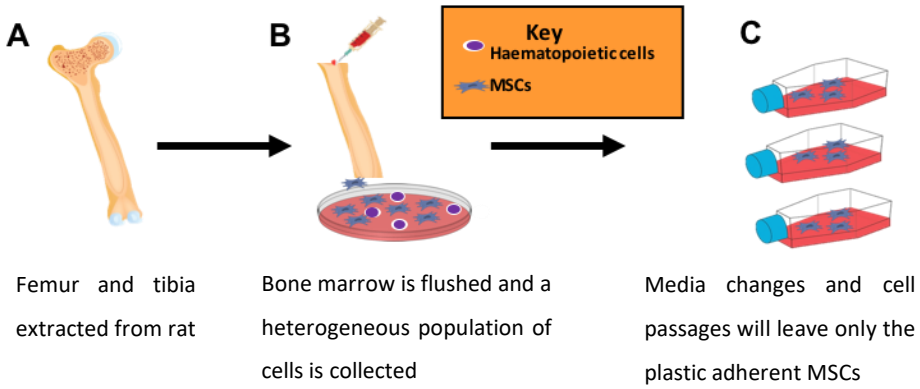

Figure 2.1.1 Schematic diagram of the method used to isolate rat MSCs.

2.1.2 Passaging MSCs

After cells reached 70-80 % confluency, MSCs were passaged and designated as passage 1 (P1). MSCs were washed in sterile 1 xPBS (5 mL) and incubated with 0.25 % trypsin and 0.1 % EDTA (Gibco) (3mL) for 4 minutes at 37 °C. Trypsin was then inactivated by adding 7 mL of isolation media and centrifuged at 1000 rpm for 3 minutes at 21 °C. The supernatant was aspirated, and cells resuspended in 1 mL of isolation media and passaged in a 1:3 ratio. After passage 2, the isolation media was replaced with MSC culture medium (DMEM, 10 % FBS, L-glutamine (1 %) and Penicillin-Streptomycin (1%)). The MSC culture medium was then used for routine expansion along with passaging in a 1:3 ratio. MSCs was used between passages 2 and 8 for all experiments described.

2.1.3 Reviving frozen MSCs stocks

Cryovials were quickly thawed by swirling in a 37 °C water bath for 1-2 minutes and removed when only a small portion of ice remained. The cells were then resuspended with 1 mL of pre-warmed MSC culture medium and this was transferred into a 15 mL falcon (Greiner Bio One) containing MSC culture medium (8 mL). Cells were centrifuged at 200 x g for 5 minutes, media aspirated off and resuspended in 1 mL of media. Subsequently, the cells were seeded 2 x T25 flasks (Greiner Bio One) with 5 mL of media in each flask. Media was changed every 3-4 days.

2.1.4 Freezing MSCs cells

MSCs were frozen down in 1.5 mL cryovials at 1 x 10^6 cells per mL of freezing media. The freezing media consisted of 90 % FBS and 10 % DMSO (Sigma-Aldrich, Dorset, UK). Subsequently, cryovials were stored in Mr.Frosty™ Freezing Container (ThermoFisher) at -80 °C for 24 hours before being moved to long term storage at -150 °C.

2.1.5 Flow Cytometry – Cell surface markers

Flow cytometry was performed to analyse MSC marker expression and to ensure haematopoietic markers were not expressed. Cultures were washed in sterile PBS and incubated in trypsin/EDTA solution at 37 °C for 4 minutes. After cells have detached from the plastic flasks, pre-warmed MSC culture medium was added to inactivate trypsin. Cells were collected in a 15 mL falcon and centrifuged at 1000 rpm for 3 minutes. The supernatant was aspirated and the cell pellet was resuspended in PBS (1 mL) and centrifuged again at 1000 rpm for 3 minutes. This was then repeated once more. The cell pellet was then re-suspended in flow buffer (0.1 % Bovine Serum Albumin in PBS) (BSA, Sigma-Aldrich). Cells were distributed at 1 x 10^5 cells per well in flow buffer onto a U-

bottomed 96-well plate (Greiner Bio-one). 3 wells repeats per antibody was used. A further two additional wells were seeded – one containing cells only for adjusting the settings of the flow cytometer while the other was for the serum control.

After cells have been seeded appropriately, the plate was centrifuged at 4° C for 3 minutes at 1000 rpm. The supernatant was removed by flicking the plate over the sink. Cell pellets were then re-suspended in 50 μL primary antibodies (Table 2.1.4). The cell only control well was re-suspended in 50 μL flow buffer and 50 μl mouse IgG serum (Sigma) was used for the serum control well. The plate was incubated for 1 hour on ice. After this, the plate was centrifuged at 4 °C for 3 minutes at 1000 rpm. Cells were then resuspended in 150 μL of flow buffer and centrifuged again at the same settings. This was repeated twice more. After three washes in total, all cells were re-suspended in 50 μL secondary antibody (Table 2.1.4) apart from the cell only control which was re-suspended in 50 μL flow buffer. The plate was wrapped in foil for protection against light and incubated on ice for 1 hour. After this, the plate was centrifuged at 4 °C for 3 minutes at 1000 rpm. Cells were then re-suspended in 100 μL of flow buffer and centrifuged again at the same settings. This was repeated once more. Following the final wash, cells were re-suspended in 200 μL flow buffer and the plate was read using Guava Technologies EasyCyte Plus flow cytometer according to manufacturer's instructions.

Table 2.1.5 – Summary of primary and secondary antibodies used in flow cytometry
Primary and secondary antibodies used in flow cytometry, with their product code, supplier, species and isotype. All antibodies were diluted in flow buffer. The expected expression of each marker for MSCs is also given.

Antibody	Code	Supplier	Species	Dilution	Expected expression
Anti-CD34 (Primary)	sc-7324	Santa Cruz	Mouse	1 in 100	Negative
Anti-CD45 (Primary)	554875	BD Pharmingen	Mouse	1 in 100	Negative
Anti-CD90 (Primary)	554892	BD Pharmingen	Mouse	1 in 100	Positive
Anti-Mouse IgG Alexa Fluor 488	A11001	Invitrogen	Goat	1 in 100	N/A

2.1.5.1 Analysis of Flow cytometry data and gating

Raw data was analysed by gating to include only the live cells and minimising the background scatter of cells. Plots of the fluorescence in samples was then expressed in histogram form to view the distribution of the signal. The mouse serum only control was used to determine levels of background fluorescence as the peak indicates the level of non-specific signal (Figure 2.1.4.1). Any sample peaks outside the threshold was considered as positive marker expression. Data was also shown to include the % gated of cells which is used to quantify the proportion of cells which display a positive signal (% Marker expression).

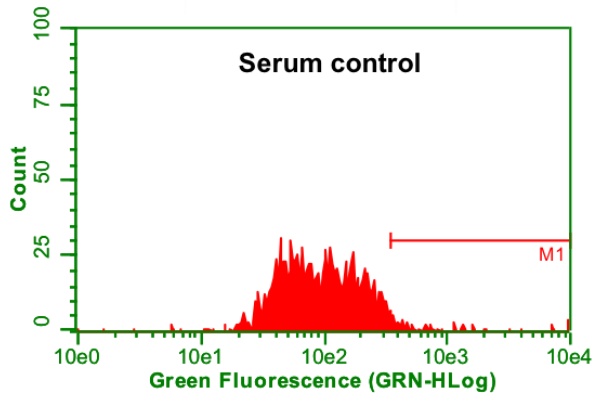

Figure 2.1.5.1 – Flow cytometric analysis of the serum control well. Representative image of the serum control well. The peak is used to gate the levels of background signal. Any signal greater than this was determined as a positive signal and therefore a positive marker expression.

2.1.6 Inducing osteogenic differentiation of MSCs

To induce osteogenic differentiation of MSCs, a previously established protocol was used[132]. MSCs were seeded onto 6 well plates at 3 x 10^3 cells/cm^2 using MSC culture medium (5 mL). For use in 2D staining, cells were seeded onto glass coverslips which were coated overnight at 4 °C with 10 μgmL^{-1} poly-D-lysine (Sigma-Aldrich) before cells were seeded. After 3-4 days when cells have reached 70-80 % confluency, the cell culture medium was switched to osteogenic medium (MSC culture medium supplemented with dexamethasone (100 nM) (Sigma-Aldrich), ascorbic acid 2-phosphate (50 μM) (Sigma-Aldrich) and β-glycerophosphate (10 nM) (Sigma-Aldrich)). Media was changed every 3-4 days and cells were maintained in the osteogenic medium for up to 21 days.

2.1.7 Inducing adipogenic differentiation of MSCs

To induce adipogenic differentiation of MSCs, a previously established protocol was used[132]. MSCs were seeded onto 12 well plates (Greiner Bio-one) at 2 x 10^4 cells/cm^2 using MSC culture medium

(2 mL). For use in 2D staining, cells were seeded onto glass coverslips which were coated overnight at 4 °C with 10 μgmL^{-1} poly-D-lysine (Sigma-Aldrich) before cells were seeded. After 3-4 days when cells have reached 70-80% confluency, the cell culture medium was switched to adipogenic induction medium (MSC culture medium supplemented with dexamethasone (1 μM) (Sigma-Aldrich), indomethacin (0.2 mM) (Sigma-Aldrich), insulin (10 μg/mL) (Sigma-Aldrich) and 3-isobutyl-1-methylxanthine (0.5 mM) (Sigma-Aldrich)). After 3 days, the adipogenic induction medium was removed and replaced with adipogenic maintenance medium (MSC culture medium supplemented with insulin (10 μg/mL)) (Sigma-Aldrich) for 2 days. This cycle of induction medium for 3 days and maintenance medium for 2 days was repeated for 21 days.

2.2 MG-63

2.2.1 Culturing MG-63

MG-63 human osteosarcoma cells were obtained from the American Type Culture Collection (ATCC). Vials of frozen cells were thawed and revived in the same way as described in Section 2.1.2 and 2.1.3. Cells were maintained in media containing Modified Eagle Minimum Essential Media (MEM) (Gibco) supplemented with 10 % FBS (Gibco), 1 % L-glutamine (ThermoFisher) and 1 % Penicillin-Streptomycin (ThermoFisher). When cells reached 70-90% confluency (Figure 2.2.1), cells were routinely passaged in a 1:3 – 1:6 ratio using the method previously described in Section 2.1.2. Medium was changed every 2-5 days as required. MG-63 cells were used between passages 16 and 30 for all experiments described. For use in 2D staining, cells were seeded onto glass coverslips using a density of 2 x 10^4 cells/cm^2 per 6 well plate.

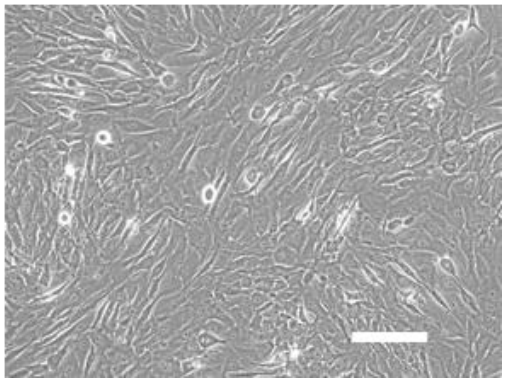

Figure 2.2.1 – Phase contrast image of MG-63 cells in culture. Representative image of confluent MG-63 before passaging. Scale bar = 100 μm. Magnification = 20 x.

2.3 Alvetex® 3D cultures

2.3.1 Seeding cells into Alvetex® membranes

3 types of Alvetex® 3D polystyrene scaffold membranes (ReproCELL Europe, Sedgefield, UK) were used in this project. Cells were seeded onto Alvetex® Scaffold, Alvetex® Strata in the same way. The scaffold membranes were dipped in 70 % ethanol for 5 minutes followed by two washes in sterile 1 x PBS. Alvetex® Scaffold/ Alvetex® Strata 12-well inserts were placed in 12-well culture plates and hydrated by adding 500μL of cell culture media to each membrane for a few minutes. Cells were harvested using trypsin as previously described Section 2.1.2 and were seeded at a density of 5 x 10^5 per 150 μL media per membrane. Plates were then incubated at 37 °C with 5 % CO_2 in a humidified incubator for 3 hours. Following this, each insert was topped with 4 mL of the appropriate cell culture media with media changes every 3 – 4 days.

Alvetex® Polaris 6-well inserts were prepared by clipping the membranes onto the inserts and left in 100 % ethanol overnight. The membranes were then dipped in 70 % ethanol followed by two washes in sterile 1 x PBS. The inserts were placed into 6-well culture plates and hydrated by adding 1 mL of cell culture media. Cells were seeded at a density of 1 x 10^6 per 300 μL media per membrane. Plates were then incubated at 37 °C with 5 % CO_2 in a humidified incubator for 3 hours. Following this, each insert was topped with 10 mL of the appropriate cell culture media with media changes every 3 – 4 days.

For 3D osteogenic differentiation, MSCs were seeded as described previously with MSC culture media. After 3-4 days, the medium was replaced with osteogenic differentiation media. This was cultured for up to 21 days with media changes every 3 – 4 days.

2.3.2 Fixation of Alvetex® 3D scaffolds

Alvetex® scaffold membranes were unclipped from their inserts and washed 2 x with sterile 1 x PBS. The PBS was then replaced with 4 % paraformaldehyde (PFA) and samples were fixed for 2 hours at room temperature. PFA was removed and washed 2 x with 1 x PBS. Samples were stored at 4 °C in PBS until further processed.

2.3.3 Paraffin Wax Embedding and Sectioning of Alvetex® 3D scaffolds

For paraffin embedding, PBS was removed and 30 % ethanol was added for 15 minutes. 30 % ethanol was replaced with 50 % ethanol for a further 15 minutes. Samples were stained with 0.1 % crystal violet (Sigma-Aldrich) in 70 % ethanol for 15 minutes to aid visualisation during sectioning.

The crystal violet was removed and samples were dehydrated through 80 %, 90 %, 95 % and 100 % ethanol at room temperature for 15 minutes each.

Following dehydration, Alvetex® 3D scaffolds were placed into embedding cassettes (ThermoFisher) and transferred to a glass beaker containing Histoclear (National Diagnostics, East Riding, UK) for 30 minutes at room temperature. Subsequently, samples were transferred to a glass beaker containing a 1:1 mixture of liquid paraffin wax (ThermoFisher) and Histoclear for 30 minutes at 60 °C. Samples were further incubated at 60 °C for 1 hour with liquid paraffin wax only. Scaffolds were removed from the cassettes and cut in half and set into paraffin wax using plastic moulds (CellPath, Newton, UK) and the top of the cassettes were placed on top of the moulds. Wax blocks were then left to solidify overnight. Alvetex® scaffolds embedded into wax blocks were sectioned at 6 μm using a Leica RM2125RT Microtome and mounted onto charged Superfrost microscope slides (ThermoFisher).

2.3.4 Haematoxylin and Eosin Staining

Slides were deparaffinised in Histoclear for 10 minutes before being rehydrated in a series of ethanols: 100 % ethanol for 2 minutes, 95 % ethanol for 1 minute, and 70 % ethanol for 1 minute. Samples were then placed in deionised water for 1 minute and stained in Mayer's Haematoxylin (Sigma- Aldrich) for 5 minutes. Following this, slides were rinsed in deionised water for 30 seconds and the nuclei were blued in alkaline ethanol for 30 seconds. Samples were then dehydrated with 70 % ethanol and 95 % ethanol for 30 seconds each before being stained in Eosin solution (Sigma-Aldrich) for 1 minute. Slides were then rinsed in 95 % ethanol for 10 seconds, followed by another rinse in 95 % ethanol for 15 seconds and then dehydrated with 100 % ethanol for 15 seconds and another 100 % ethanol for 30 seconds. Clearing of slides involved 2 incubations in Histoclear for 3 minutes each. Slides were mounted in Omnimount (Scientific Laboratory Supplies, Nottingham, UK) and glass coverslips (ThermoFisher). Images were taken using a Leica ICC50HD microscope.

2.4 Histological and fluorescent stains

2.4.1 Alizarin Red (2D)

Alizarin Red stain solution was prepared through dissolving 1 g of Alizarin Red S powder (Sigma-Aldrich) in 50 mL deionised water to make a 2 % solution. The pH of the solution was adjusted to 4.1 – 4.3 using concentrated hydrochloric acid when the pH needed to be lowered while 10 % ammonium hydroxide was used to increase pH. At the appropriate time points, the cells on coverslips were washed twice with 1 x PBS and fixed with 4 % PFA for 1 hour at room temperature. Glass coverslips were stained with Alizarin Red solution for 2 minutes, dehydrated with acetone,

followed by dehydration in 50:50 acetone: Histoclear for a few minutes. Coverslips were then cleared in Histoclear for before being mounted using Omnimount (Scientific Laboratory Supplies).

2.4.2 Alizarin Red (3D)

Alizarin Red stain solution was prepared using the method described in 2.4.1. Slides were deparaffinised in Histoclear for 10 minutes, rehydrated in 100 % ethanol for 2 minutes, 95 % ethanol for 1 minute, 70 % ethanol for 1 minute and deionised water for 1 minute. Slides were covered in Alizarin Red solution for 2-5 minutes and excess dye was shaken off. Slides were then dipped in acetone for 20 dips and 50:50 acetone: Histoclear for a further 20 dips. Sections were cleared in Histoclear before being mounted using Omnimount (Scientific Laboratory Supplies) and glass coverslips.

2.4.3 Nile Red (2D)

To confirm the adipogenic differentiation of MSCs, the red fluorescent Nile red dye (Sigma-Aldrich) was used. Cells were cultured using the method mentioned previously (Section 2.1.6) on glass coverslips for 21 days. Glass coverslips were coated overnight at 4 °C with 10 $\mu g mL^{-1}$ poly-D-lysine (Sigma-Aldrich) before cells were seeded. Cells were washed in 1 x PBS and fixed with 4 % paraformaldehyde (PFA) for 1 hour at room temperature. 1 in 100 dilution of the stain was used (diluted in PBS) and glass coverslips were stained with Nile red in the wells for 10 minutes at room temperature. The glass coverslips were then washed twice with 1 x PBS and mounted with VECTASHIELD® hardset antifade mounting medium with DAPI (Vector Laboratories, Peterborough, UK).

2.5 Immunofluorescence Staining

2.5.1 Immunofluorescence staining of 2D cultures

Samples on coverslips in 6-well culture plates were washed in PBS and fixed with 4 % PFA for 1 hour at room temperature. Cells were permeabilised with 0.1 % Triton-X100 in 1 x PBS for 10 minutes and blocked for 30 minutes in blocking buffer. Blocking buffer consisted of 1 % normal goat serum (NGS, Sigma-Aldrich) and 0.01 % Tween (Sigma-Aldrich) in PBS. Primary antibody diluted in blocking buffer was then added to each sample (Table 2.5.2) and incubated for 1 hour. Coverslips were then washed three times with blocking buffer for 10 minutes. Following this, samples were incubated with the appropriate fluorescent secondary antibody mixed with nuclear dye Hoechst 33342 (ThermoFisher) (Table 2.5.2.1) diluted in blocking buffer for 1 hour in the dark. Coverslips were then washed with blocking buffer three times for 10 minutes each. After this, samples were mounted onto microscope slides using VECTASHIELD® anti-fade mounting medium (Vector Laboratories).

2.5.2 Immunofluorescence staining of 3D cultures

Paraffin wax sections of samples were first deparaffinised in Histoclear for 10 minutes, rehydrated in 100 % ethanol, 70 % ethanol and 1 x PBS for 5 minutes each. Subsequently, samples were incubated in a 95 °C water bath with citrate buffer for 20 minutes for retrieval antigens. The slides were then slowly cooled to room temperature as the citrate buffer was gradually replaced with deionised water. A hydrophobic pen (Liquid blocker) was used to draw around samples on slides. Samples were then incubated in blocking buffer containing 20 % NGS and 0.4 % Triton X-100 diluted in 1 x PBS for an hour at room temperature. After this, samples were incubated overnight at 4 °C with primary antibody diluted in blocking buffer(Table 2.5.2). Samples were then washed three times in 1 x PBS for 5 minutes each and incubated with secondary antibody mixed with Hoeschst (Table 2.5.2.1) diluted in blocking buffer for an hour at room temperature in the dark. Slides were then washed three times in 1 x PBS for 5 minutes each before mounting with glass coverslips using VECTASHIELD® anti-fade mounting medium. Negative control of immunofluorescence staining of 3D cultures is shown in Figure 2.5.2. Cells were cultured on Alvetex® scaffold and Hoechst antibody was used to stain the nuclei blue.

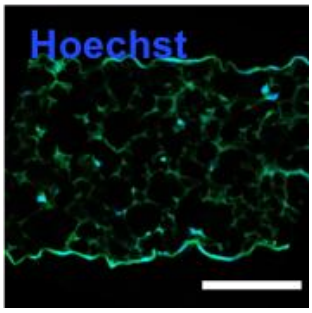

Figure 2.5.2 – Negative control of cells cultured on Alvetex® Scaffold. Representative image of background staining of immunofluorescent staining of cells cultured on Scaffold. Only Hoechst staining of nuclei is shown. Scale bar = 100 μm. Magnification = 20 x.

Table 2.5.2 – Primary antibodies used in immunofluorescence

Summary table of the primary antibodies used in immunofluorescence of 2D and 3D samples, with their respective product code, supplier and host species. All antibodies were diluted in blocking buffer.

Target	Code	Supplier	Host Species	Dilution
Collagen I	ab34710	Abcam	Rabbit	1:100
Collagen III	ab7778	Abcam	Rabbit	1:100
Fibronectin	ab23750	Abcam	Rabbit	1:100

Table 2.5.2.1 – Secondary antibodies and dyes used in immunofluorescence

Summary table of the secondary fluorescent conjugated antibodies and nuclear dye used in immunofluorescence of 2D and 3D samples. The respective product code, supplier and emission wavelengths are given. All antibodies were diluted in blocking buffer.

Antibody	Code	Supplier	Emission Wavelength	Dilution
Alexafluor anti-rabbit 488	A32790	ThermoFisher	488	1:1000
Hoechst 33342	H3570	ThermoFisher	461	1:1000

2.5.3 Cell counting using ImageJ analysis

In order to quantify the amount of cell nuclei in 3D cultures, cultures were stained with Hoechst as previously described. Hoechst immunofluorescently stains nuclei in samples. Digital images of the stains were taken using confocal microscopy and analysed using ImageJ (https://imagej.net), which is a software package used commonly for image processing. The software comes with a "Cell Counter" plugin located under Plugins> Cell counter which is a way of getting an indication of the numbers of cells in an image. Three representative images at the same magnification (20 x) and area of each cell type and timepoint was used. Each image was converted to 8-bit to make it easier to distinguish between nuclei and the scaffold as nuclei is displayed as white. Each nucleus in the image was clicked on directly to count it using the cell counter window. The average number of cells per cell type/time point was calculated and plotted in a bar chart with the standard error of the mean (SEM) bars. Example is shown in Figure 2.5.3.

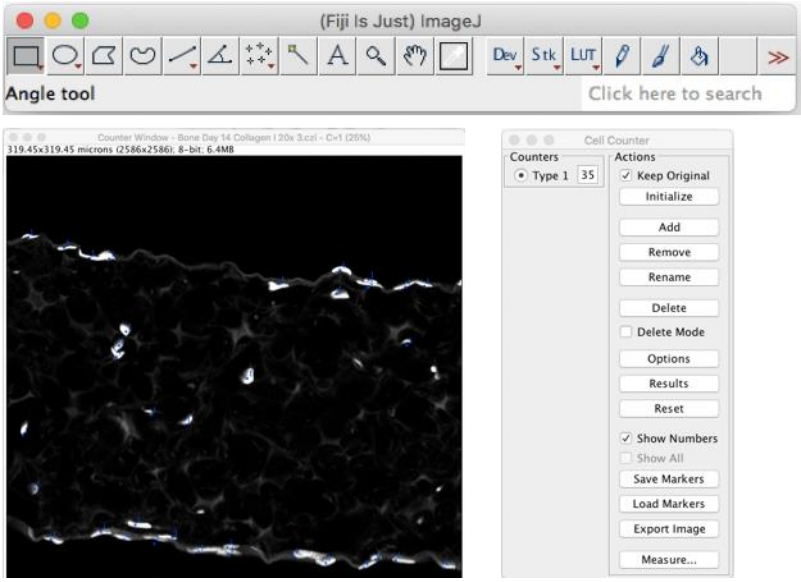

Figure 2.5.3 – Quantification of the number of cells in 3D samples was performed using ImageJ. The in-built cell counter function of the ImageJ processing software was used to count the number of nuclei (white) in each representative sample.

2.6 Alkaline Phosphatase Assay

2.6.1 Running the alkaline phosphatase assay

The level of extracellular alkaline phosphatase (ALP) in cultures was measured as an early marker of osteoblastic differentiation. The assay was performed using the alkaline phosphatase colorimetric assay kit (Abcam, Cambridge, UK) according to the protocol provided by the manufacturer. The kit uses p-nitrophenyl phosphate (*p*NPP) as a phosphate substrate for the ALP enzyme. During this hydrolysis reaction, ALP dephosphorylates *p*NPP to produce *p*-nitrophenol which yields a yellow substrate which can be measured spectrophotometrically at 405 nm. The level of ALP activity in the samples is therefore directly proportional to the absorbance measured.

MSCs were cultured under osteogenic conditions for 7, 14 and 21 days on 6-well plates (2D) vs Alvetex® Scaffold (3D). For MG-63s, cells were cultured using their complete culture medium on 6-well plates (2D) vs Alvetex® Scaffold (3D) for the same time points. The cell culture medium was collected during the last day of experimental culture for each sample. The experimental samples were prepared through diluting by 1:1 for MSCs samples while MG-63 samples were diluted by 1:5 with ALP assay buffer. The samples were prepared in duplicates and sample background control was included using normal culture medium to minimise the interference of the coloured samples. 50 μL of 5 mM *p*NPP solution was added to sample and sample background controls and incubated in the dark for 60 minutes. Standards of known concentrations of *p*-nitrophenol was included for the construction of a standard curve. Absorbance was measured at 405nm using a BioTek, ELx800 microplate reader.

2.6.2 Calculating the concentration of Alkaline Phosphatase activity in samples

The concentration of ALP in samples was calculated through a series of steps:

1. Background was corrected through subtracting the absorbance value from the zero standards from all readings
2. Sample background control value was subtracted from all sample readings and the average of the duplicate absorbance readings for each sample was calculated
3. A standard curve from the standard control values was plotted using GraphPad Prism software An example is shown in Figure 2.6.2.

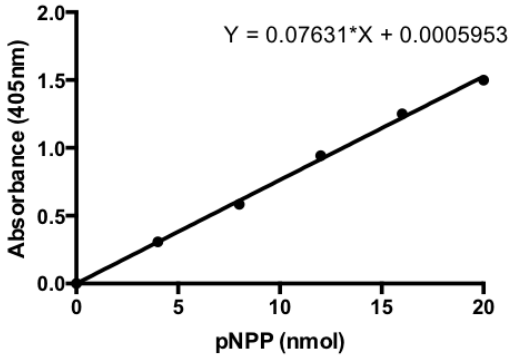

Figure 2.6.2 – Example of standard curve for calculating ALP levels in samples
A typical standard curve plotting the absorbance at 405 nm against the Standards of known concentrations of p-nitrophenol. A linear regression graph was plotted to obtain the equation of the line which is used to determine the concentration of ALP in samples.

4. The equation of the line was calculated and the X value (amount of *p*NPP in sample) was obtained by substituting the Y value (absorbance) for each sample.

5. The ALP activity of each sample was calculated using the following formula provided by the assay kit:

$$ALP\ activity = \left(\frac{X}{\Delta T \times V}\right) \times D$$

Where:

X = amount of *p*NPP in sample calculated from standard curve (μmol)

ΔT = reaction time (minutes) (60 minutes)

V = volume of sample added to the assay well (mL)

D = sample dilution factor

6. ALP activity was normalised to total protein content for each sample (as determined by the Bradford assay) (Section 2.7).

2.7 Bradford Protein Assay

A Bradford Assay was used to quantify the total protein content of osteogenic-induced MSCs and MG63s cultured on 6-well plates (2D) vs Alvetex® Scaffold (3D) for 7,14 and 21 days. At the end of each culture period, cell lysates from each time point and condition was generated.

2.7.1 Generation of Cellular Lysates – 2D cultures

2D cultures on 6-well plates were washed in PBS and trypsinised with 0.25 % trypsin and 0.1 % EDTA (Gibco) (3 mL) for 4 minutes at 37°C. Trypsin was then inactivated by adding 7 mL of isolation media and centrifuged at 1000 rpm for 3 minutes at 21 °C. The number of viable cells in the sample was counted using a sample of the cell suspension (10 μL) and trypan blue solution (10 μL) (Sigma Aldrich). Cell number was determined using a haemocytometer and diluted to a concentration of

100,000 cells in 1 mL media. The cells were then centrifuged at 1000 rpm for 3 minutes at 21 °C and the cell pellet was dissolved in 100 μL lysis buffer containing 1 % protease inhibitor cocktail (Sigma-Aldrich) diluted in Mammalian Protein Extraction Reagent (MPER™, ThermoFisher). Samples were sonicated for 30 minutes and centrifuged at 12000 rpm for 20 minutes at 4 °C. The supernatant was then collected and frozen at -20 °C until use.

2.7.2 Generation of Cellular Lysates – 3D cultures

Alvetex® Scaffold membranes were unclipped from their inserts and washed 2 x with sterile 1 x PBS. The membranes were then placed in 100 μL of lysis buffer and sonicated for 30 minutes. Subsequently, samples were centrifuged at 12000 rpm for 20 minutes at 4 °C and the supernatant was then collected and frozen at -20 °C until use.

2.7.3 Running the Bradford assay

The protein standards (0.125 to 2.0 $mgmL^{-1}$) for the assay was prepared by adding 5 μL of each BSA Protein Standards (Bio-Rad, Hertfordshire, UK) and 250 μL of Quick Start™ Bradford 1x Dye Reagent (Bio-Rad) to a 96-well flat-bottomed plate. This is for producing a standard curve to determine the concentration of protein for each sample. A well containing deionised water only was used as a blank. For running the assay, lysates were thawed on ice and 5 μL of each sample were pipetted onto a well along with 250 μL of Bradford Reagent. Each sample was read in triplicate. The plate was then incubated for 5 minutes and the absorbance was read at 590 nm using a BioTek ELx800 microplate reader.

2.7.4 Quantifying protein content

The absorbance for each sample was calculated by subtracting the blank values from the average absorbance value of each sample. A standard curve was plotted using GraphPad Prism software using the absorbance from the protein standards. The equation of the line was calculated from the standard curve and the protein concentration was calculated (x value) through substituting the absorbance (y value) for each sample.

2.8 Western Blot

2.8.1 Gel casting – SDS Polyacrylamide Gel Electrophoresis

30 μg/mL of protein lysates samples were prepared by diluting the sample in 4x Laemmli sample buffer (Bio-Rad) and 10 % 2-mercaptoethanol (Sigma-Aldrich). Subsequently, samples were boiled at 95 °C for 10 minutes using a heat block. Samples were loaded into polyacrylamide gels along

with a protein ladder (ThermoFisher) and run at 120 V for 2 hours in 1 x running buffer (Bio-Rad). This SDS-PAGE (sodium dodecyl sulphate- polyacrylamide gel electrophoresis) is the first stage of Western blotting for resolving proteins by molecular weight. The components used to make up the gels for running the samples are listed in Table 2.8.1

Table 2.8.1 – Components used to make SDS-PAGE gels and Western blot membranes

Summary table with all the components used to make the stacking and resolving gels used to run the samples and the manufacturers of each component.

Type of Gel	Components
5 % Stacking Gel	▪ 5 % ProSieve™ 50 Gel Solution (Acrylamide) (Lonza, Basel, Switzerland) ▪ 1.5 M Tris, pH 6.8 (ThermoFisher) ▪ 10 % Sodium dodecyl sulfate (SDS) (ThermoFisher) ▪ 10 % Ammonium Persulfate (APS) (ThermoFisher) ▪ 0.1 % N,N,N,N'-tetramethylethane-1,2-diamine (TEMED) (Sigma-Aldrich)
8 % Resolving Gel	▪ 8 % ProSieve™ 50 Gel Solution (Acrylamide) ▪ 1.5 M Tris, pH 8.8 ▪ 10 % SDS ▪ 10 % APS ▪ 0.1 % TEMED

2.8.2 Protein transfer

The proteins on the gel were transferred from the polyacrylamide gel to a nitrocellulose membrane (GE Healthcare, Buckinghamshire, UK) by first discarding the stacking gel and sandwiching the resolving gel in the following order onto a transfer cassette: sponge, blotting paper, stacking gel, nitrocellulose membrane, blotting paper and sponge. The transfer cassette was then placed in a transfer tank topped with transfer buffer (3.03 g Tris, 14.41 g glycine, 200 mL methanol topped with 1 L of deionised water). The transfer was run at 15 V at 4 °C overnight and a further 2 hours at 30 V the following day. As the transfer was run overnight, the electrical current was around 0.4 Amps and the current was kept constant.

2.8.3 Ponceau staining

To check if the proteins did successfully transfer onto the membrane, the membrane was incubated in Ponceau S solution (Sigma-Aldrich) for 5 minutes. The membrane was then washed with deionised water several times and the bands were clearly evident on the membrane, indicating a successful transfer.

2.8.4 Blocking and Immunostaining of membrane

The membrane was blocked in 5 % milk powder (Sainsbury's, London, UK) dissolved in 0.1 % Tween in PBS. This was to prevent non-specific background binding. The membrane was then incubated in primary antibodies (Table 2.8.4) diluted in 5 % milk solution overnight at 4 °C on a rotator. Following this, the membrane was washed 3 times for 5 minutes each in 0.1 % Tween in PBS and incubated in secondary antibody (Table 2.8.4) diluted in 5 % milk solution. This was left for an hour at room temperature. The membrane was washed a further 3 times for 5 minutes in 0.1 % Tween in PBS.

Table 2.8.4 – Antibodies used in western blotting

Primary and secondary antibodies used in western blot. All secondary antibodies were conjugated with horseradish peroxidase (HRP) which allows for chemiluminescence detection.

Target	Code	Supplier	Host Species	Dilution
β - actin	Ab8224	Abcam	Mouse	1:5000
Collagen I	1310 - 01	Southern Biotech	Goat	1:1000
Anti-goat-HRP	AP180P	Sigma-Aldrich	Donkey	1:10000
Anti-mouse-HRP	A4416	Sigma-Aldrich	Goat	1:10000

2.8.5 Blot development

The Clarity ECL (Enhanced chemiluminescence) solution (Bio-Rad) was prepared by adding the two solutions supplied in a 1:1 ratio following manufacturer's instructions. 1 mL of ECL was then added to the membrane for detection and the membrane was developed through exposure with photographic film (ThermoFisher) in a dark room using a film processor (XOMAT).

2.9 Microscopy

2.9.1 Phase contrast microscopy

Phase contrast images were taken using EVOS XL Core Cell Imaging system microscope. The objective lenses x10, x20 and x40 were used.

2.9.2 Brightfield Imaging

Histological samples were imaged using a Leica ICC50 High Definition camera mounted onto a Leica microscope. The objective lenses x10, x20 and x40 were used. Images were captured using Leica EZ software.

2.9.3 Confocal microscopy

Confocal fluorescent images were captured using Zeiss 800 confocal laser-scanning microscope with airyscan. The objective lenses x10, x20 and x63 were used. Zeiss Zen software was used to take the images.

Table 2.8.5 – Technical information for secondary antibody labels

Technical settings for each secondary antibody used during confocal microscopy.

Antibody	Excitation Wavelength/nm	Emission Wavelength/nm	Airy value (AU)	Laser wavelength
Alexafluor anti-rabbit 488	488	525	1	488
Hoechst 33342	350	461	1.2	405

3. Results

3.1 Isolation and characterisation of primary rat MSCs

3.1.1 Cells isolated from rat bone marrow display MSC morphology

MSCs were isolated from the femur and tibiae of Wistar rats as previously described in Section 2.1.1. Plastic adherence of cells to the culture flask was used to select for MSCs as the other cell types in the bone marrow, mainly hematopoietic cells do not possess this characteristic. As a result, with increasing media changes and passages, only true MSCs will be left in cultures while non-plastic adherent cells were washed away. Figure 3.1.1 illustrates the MSCs at different stages during the isolation and passaging process. A heterogenous population of cells of varying morphologies from the bone marrow was collected (Figure 3.1.1A). By day 4 (Figure 3.1.1B), a small population of cells began to differentiate and displayed a long, spindle-shaped morphology (arrowheads) which is in keeping with cells of MSC origin. However, contaminating haematopoietic cells which display a small and round morphology remained. After 9 days (Figure 3.1.1C), the majority of non-adherent cells were removed and MSCs increased in proliferation and expansion. At later time points, MSCs maintained a homogenous fibroblastic morphology which is in agreement of cells of MSC origin (Figure 3.1.1D – F). When cultures reached 70 – 80% confluency (Figure 3.1.1E), which was around 10-13 days after initial plating of bone marrow cells, cells were passaged using methodology previously described (Section 2.1.2) and designated P1. Cells used in experiments were between P2 and P8, whereby the vast majority of cells displayed plastic adherence and fibroblast-like morphology, indicating the cells isolated were of MSC origin.

3.1.2 Cell surface marker expression of isolated cells are negative for haematopoietic markers and positive for MSC marker

Flow cytometry analysis was used to further confirm the cells isolated and used in downstream experiments were of MSC origin. Two haematopoietic markers (CD34 and CD45) and one MSC marker (CD90) was used to assess the purity of the isolated cells. Expression of CD34 and CD45 was largely negative (Figure 3.1.2A-B,D) which indicates cultures used in experiments were not/very minimally contaminated with haematopoietic cells. Although no single definitive marker has been found to be unique for MSCs, there are several cell surface marker antigens which have been widely used to characterise MSCs such as CD90. Expression of CD90 was largely positive (Figure 3.1.2C-D), suggesting the cells obtained from the isolations were of MSC origin.

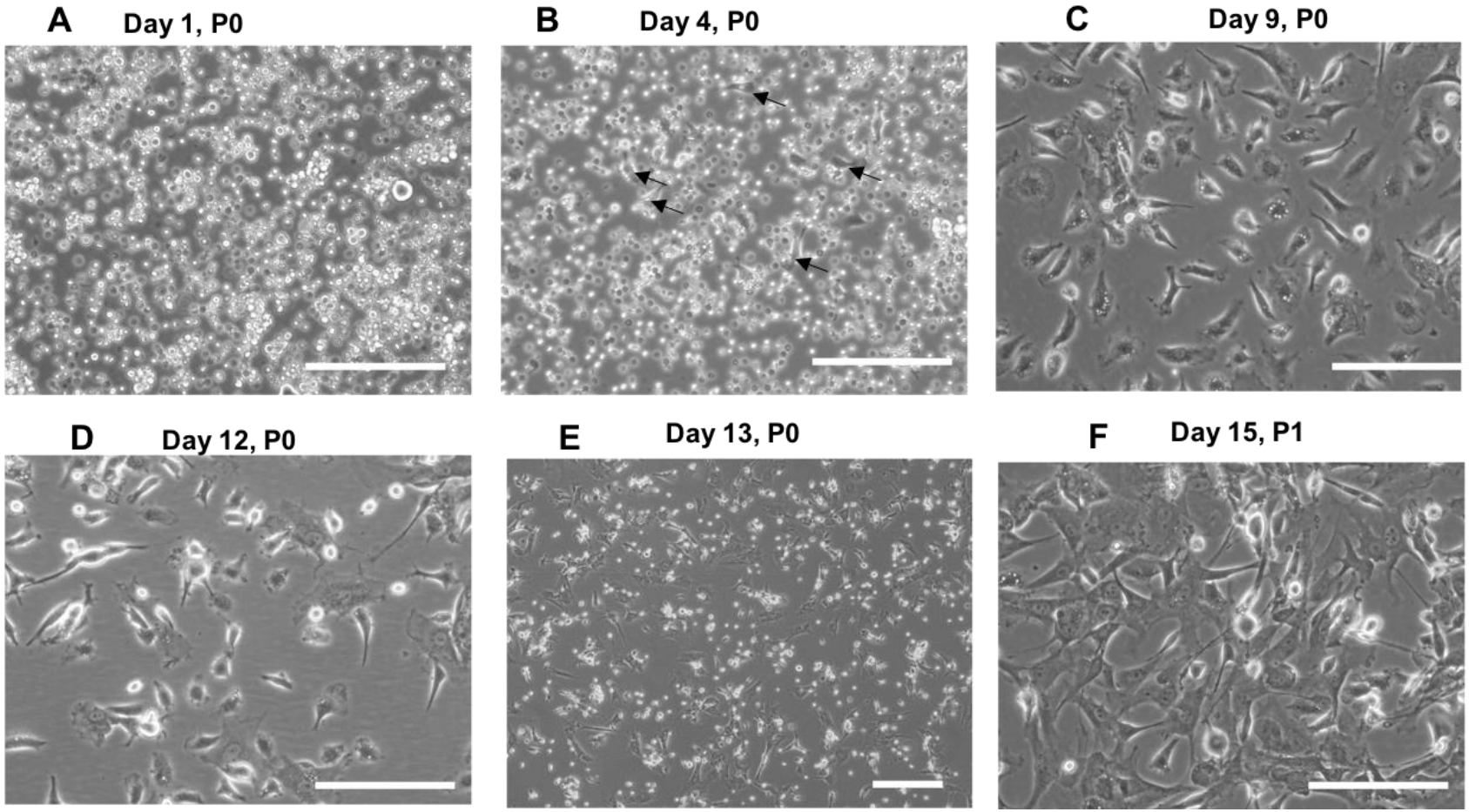

Figure 3.1.1 – Isolation of rat MSCs and expansion process. Phase contrast images showing the cells isolated from rat bone marrow. A heterogenous population of cells can be seen in day 1 (A) and day 4 (B). MSCs are selected for through plastic adherence. By day 9 (C) after several media changes and passages, a more homogenous population of cells remain. As time increases (D – F), MSCs display a large, flattened, fibroblast- like morphology. The passage numbers for each culture is also shown. Scale bars (A – D), (F) = 100 μm, E = 200 μm.

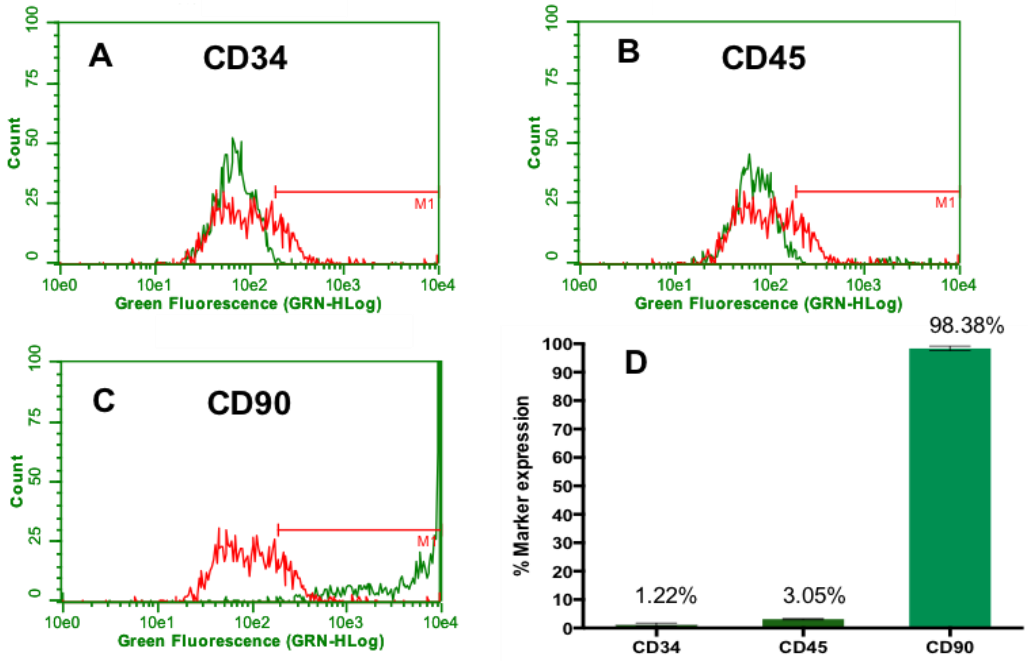

Figure 3.1.2 – Flow cytometric analysis of cell surface marker expression of isolated cells. Representative images displaying the cell surface marker expression for haematopoietic (A – B) and MSC (C) markers of isolated cells. Haematopoietic marker expression was largely negative while MSC marker was very positive. Stained cells are represented in green while the serum control (negative control) is in red. Results of % marker expression over three independent repeats are shown in (D). Data represent the mean ± SEM (n= 3).

3.1.3 Isolated MSCs demonstrate the ability to differentiate into multiple mesodermal cell types such as osteogenic and adipogenic in 2D culture

As shown in previous sections, the isolated cells from the bone marrow display MSC morphology, are negative for haematopoietic cell surface markers and are positive for MSC markers. Another approach to test whether the cells isolated are true MSCs is through assessing their multilineage differentiation potential into mesodermal derivatives such as bone and fat. This is the key characteristic of true MSCs.

Following the method described in Sections 2.1.6 and 2.1.7, MSCs were induced to undergo osteogenic and adipogenic differentiation for up to 21 days. MSCs cultured under osteogenic conditions were assessed using the Alizarin Red histological stain. Deposits of calcium in the extracellular matrix are stained red which is highly indicative of calcified bone nodule formation. Figure 3.1.3A display positive Alizarin Red staining of cells cultured under osteogenic conditions as cells were able to form multiple calcified deposits and displayed cell condensation, suggesting the formation of bone nodules in cultures. Negative controls were stained simultaneously which consisted of cells cultured under MSC culture medium without osteogenic morphogens and this displayed little evidence of positive staining or bone nodule formation (Figure 3.1.3B).

MSCs cultured under adipogenic conditions were assessed using the fluorescent lipophilic Nile red stain. Nile red staining of isolated cells showed intense red globular structures inside cells, resembling intracellular lipid droplets (Figure 3.1.3C). Evidence of lipid droplets was observed from day 7. Negative controls containing MSCs grown using normal MSC culture media did not display any positive staining (Figure 3.1.3D).

The main characteristic of stem cells is the ability to differentiate into multiple cell lineages, therefore by demonstrating that the isolated cells are able to differentiate into mature mesodermal lineages suggest they are true mesenchymal stem cells. Characterising the isolated cells via plastic adherence, morphology, cell surface marker expression and differentiation potential suggests the cells used in further downstream experiments were true MSCs.

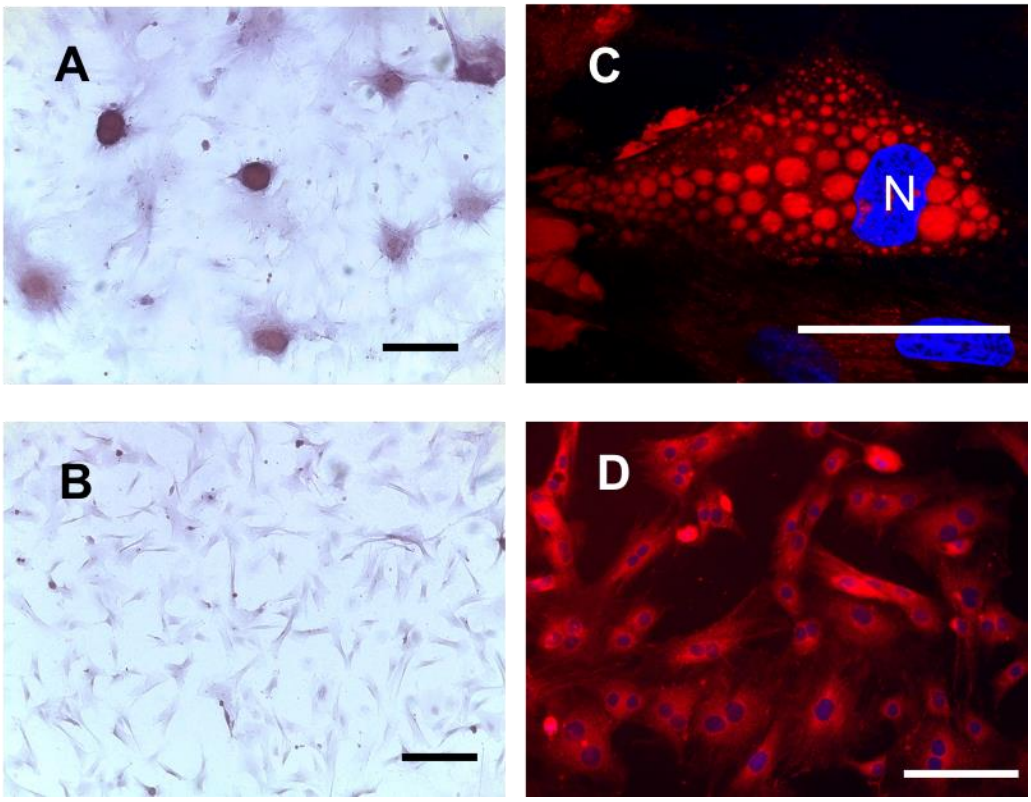

Figure 3.1.3 – Isolated MSCs display multilineage differentiation potential. MSCs cultured under osteogenic conditions in 2D conventional culture (A) display positive Alizarin Red staining and cell condensation, indicative of the early stages of bone differentiation. MSCs cultured under adipogenic conditions display positive Nile red fluorescent staining, showing clearly formation of lipophilic droplets (C). Control MSCs grown using basic medium with no osteogenic morphogens and stained using Alizarin Red (B) and Nile red (D) show negative staining. Scale bars A and B = 200 μm, D = 100 μm, C = 50 μm.

3.2. Selection of the appropriate 3D growth substrate for bone forming cells

3.2.1 3D cell culture is able to support the growth of MG-63 osteoblast-like cell line

To test whether 3D cell culture would be able to support the growth and proliferation of bone forming cells, cells from the human osteosarcoma cell line MG-63 were seeded onto Alvetex® Scaffold for up to 28 days. Since MG-63 cells have a quicker growth rate and are easier to culture compared to primary MSCs, MG-63 cells were first cultured on the 3D scaffold as a preliminary test. Using H&E staining, samples were analysed at day 7, 14,21 and 28 and showed homogenous growth throughout the scaffold at all time points (Figure 3.2.1). As MG-63s are osteoblast-like cells, this suggests that the 3D cell culture scaffold was able to support the proliferation and growth of bone forming cells as healthy cultures were able to be maintained for up to 28 days.

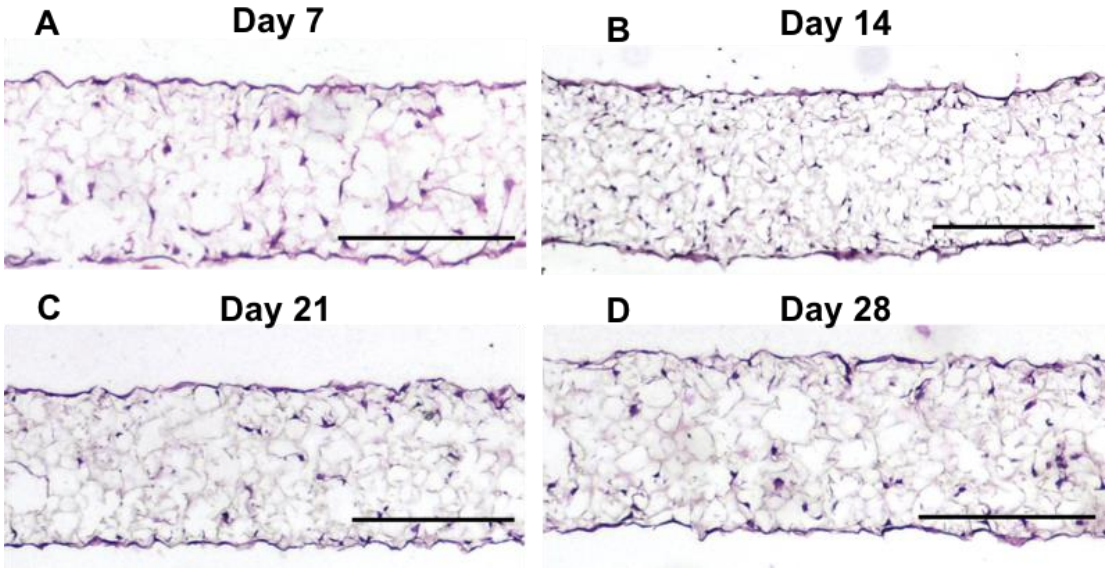

Figure 3.2.1. Histological analysis shows Alvetex® Scaffold supports the proliferation and growth of MG-63 cells. Cells from the human osteosarcoma MG-63 cell line was seeded at $5x10^5$ cells per 12-well insert of Alvetex® scaffold. Cultures were maintained up to 28 days. Cells showed homogenous growth throughout the scaffold at all time points. Scale bar = 200 μm.

3.2.2 The void size differences between the three formats of Alvetex®

Alvetex® is available in three different formats which differ in void size and architecture, allowing for greater range in applications. Scanning electron micrographs (SEM) demonstrate the differences in void and interconnect distribution in the three formats (Fig 3.2.2). Scaffold is the most widely used format and contains the biggest voids (40 μm) linked by 15 μm interconnects. Strata consists of 15 μm voids linked by 5 μm interconnects while Polaris contains the smallest voids at 3 μm with 1 μm interconnects (not commercially available). The values were reported by ReproCell Europe Ltd.

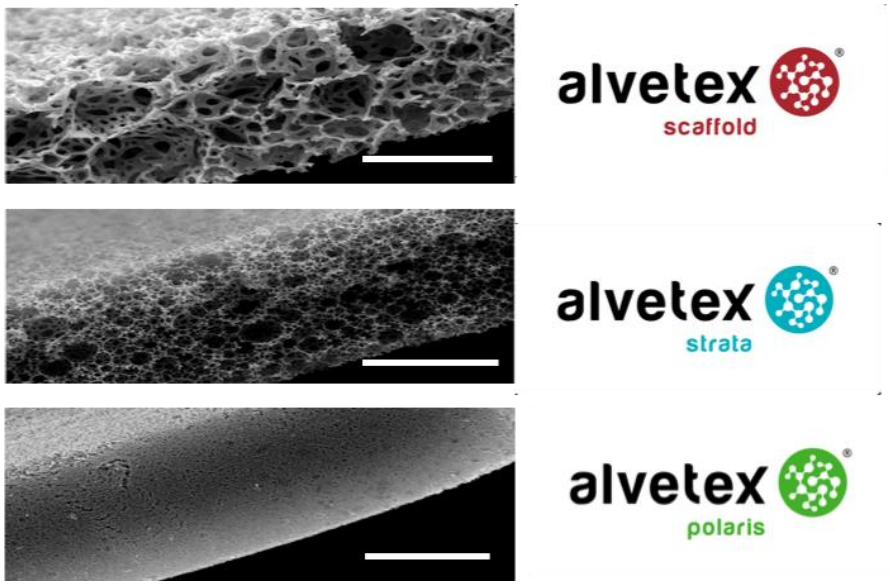

Figure 3.2.2 Scanning electron micrographs of the three formats of Alvetex®. The three formats differ in their void sizes. Images provided by ReproCell Europe Ltd. Scale bar = 200 μm

3.2.3 Scaffold is the most appropriate 3D material for MSCs and MG-63 proliferation

To determine which is the most appropriate format of Alvetex® to use for cultivating bone forming cells, MSCs and MG-63s were cultured on all three formats for 14 days and compared. Cells were seeded at 5 x 10^5 per 12-well insert of Scaffold and Strata, and 1 x 10^6 per 6-well insert of Polaris. Histological analysis of samples showed the distribution of cells inside the scaffolds (Figure 3.2.3). H&E analysis illustrated how MSCs and MG-63 were able to proliferate and grow throughout Scaffold and Strata (Figure 3.2.3 A-D). However, for both cell types, the cells were not able to enter the Polaris scaffold and instead formed a layer of cells on the top of the membrane (Figure 3.2.3E-F). This is due to the size of the cells being too large to enter the membrane. MSCs *in vivo* grow throughout the pores of the bone marrow, therefore Polaris was not considered as an appropriate material for cultivating bone forming cells as the cells were not able to grow in the membrane. Scaffold and Strata were considered as more appropriate materials for recapitulating the *in vivo* environment of bone forming cells. This is due to the cells displaying homogenous growth throughout both membranes which is comparable to *in vivo* conditions. Although the same seeding densities were used for Scaffold and Strata, for both MSCs and MG-63s, cells were more densely packed and covered a greater area of Scaffold compared to Strata. This indicates Scaffold provides a better microenvironment for MSCs and MG-63s as greater proliferation occurred in Scaffold than Strata. Scaffold provides a greater surface area for cells to expand on as cell-cell contact inhibition of growth is minimised, therefore greater proliferation of cells can occur.

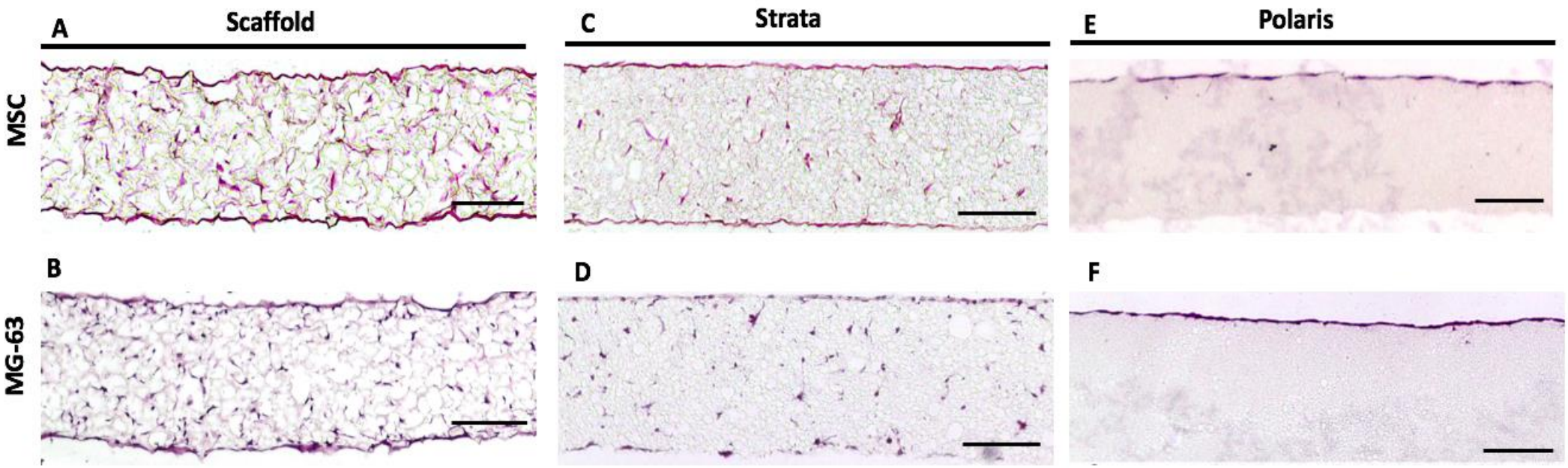

Figure 3.2.3 Histological analysis of culturing MSCs and MG-63s on three formats of Alvetex®. MSCs and MG-63s were seeded onto Alvetex® Scaffold, Strata and Polaris for 14 days. 5 x 10^5 cells were seeded onto Scaffold and Strata while 1 x 10^6 cells were seeded onto Polaris. Cells cultured on Scaffold displayed clearly the greatest homogenous growth and proliferation out of all three membranes for both cell types. Scale bar = 100 μm.

3.2.4 Optimisation of cell seeding density on Scaffold - MSCs

To determine the number of cells needed for each Scaffold insert which yields the greatest number of viable cells, MSCs and MG-63 cells were cultured for 7 and 14 days at densities ranging from 0.25 to 1 million cells per well. Visualisation of MSCs using H&E analysis (Figure 3.2.4) displayed clearly that as time increased (Day 7 to Day 14), the greater the proliferation of cells at each seeding density. Cells maintained at 0.25 million resulted in the least growth across the Scaffold and was therefore deemed as too low (Figure 3.2.4 A and E). At 1 million cells per well (Figure 3.2.4 D and H), MSCs did not populate the Scaffold as much compared to 0.5 million (Figure 3.2.4 B and F) and 0.75 million (Figure 3.2.3 C and G). At the end of each culture period at 1 million cells/well, the media was coloured orange (data not shown). This suggests that 1 million cells/well was too high as it is likely that much cell death occurred and therefore a healthy culture could not be maintained. The seeding densities 0.5 million and 0.75 million displayed the best homogenous growth throughout the Scaffold and healthy cultures could be maintained for up to 14 days. During expansion in flasks, MSCs were found to be difficult to culture as on average, only 3 million cells could be obtained from a T175 flask (data not shown). This increased the difficulty of setting up large scale experiments. Due to this, 0.5 M was determined as the optimum seeding density as it produced a homogenous growth of cells throughout the Scaffold and is feasible for large scale experiments. This density was used for further experiments.

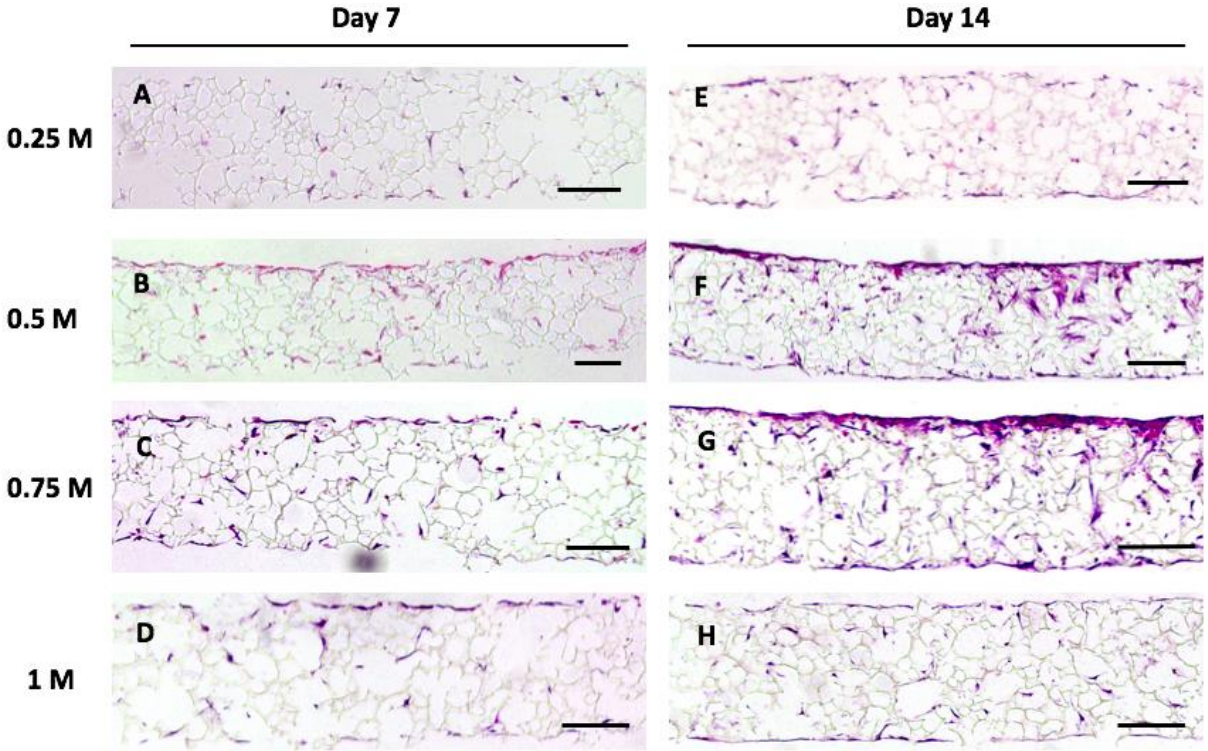

Figure 3.2.4 H&E staining of MSCs seeded on Alvetex® Scaffold at a range of densities. MSCs were seeded at a range of seeding densities at 0.25 million to 1 million for 7 and 14 days. 0.5 million was determined to be the optimal density for cell proliferation and feasibility. Scale bar = 100 μm.

3.2.5 Optimisation of cell seeding density on Scaffold – MG63s

MG-63s were seeded in a range of 0.5 to 1 million per 12-well insert of Alvetex® Scaffold to determine the optimal seeding density. From the H&E images (Figure 3.2.5), 1 million cells per well produced the least proliferation of cells at both Day 7 and Day 14. As MG-63 cells are from a cell line, the growth rate of cells is rapid and is able to reach confluency quickly. When seeding 1 million cells/well, it is likely that the cells did not have enough space to expand and cell-cell contact inhibition prevented further proliferation (Figure 3.2.5C,F) This was evident in the media of the cultures turning orange very quickly (data not shown), which resembles what was seen with MSCs (Figure 3.2.4D,H). Similar to MSCs, 0.5 million cells (Figure 3.2.5A,D) per well produced the greatest proliferation of cells in the scaffold and the colour of the media remained red, indicating a healthy culture. This resulted in 0.5 million cells/well being used for further experiments.

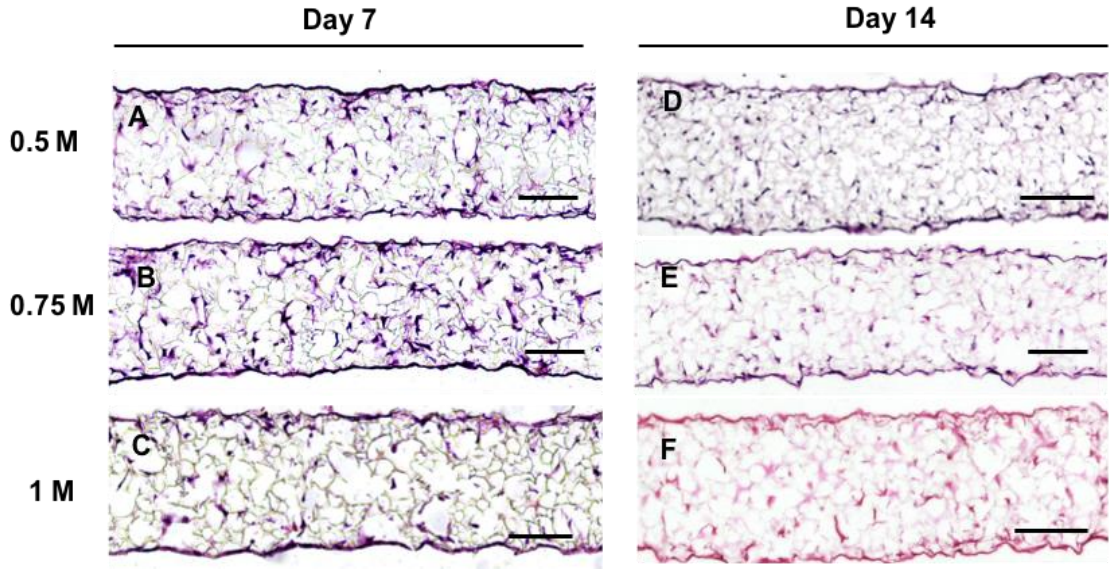

Figure 3.2.5 H&E staining of MG-63s seeded on Alvetex® Scaffold at a range of densities. MSCs were seeded at a range of seeding densities at 0.5 to 1 million for 7 and 14 days. Likewise to MSCs, 0.5 million was determined to be the optimal density for cell proliferation. Scale bar = 100 μm.

3.2.6 Pore sizes of scaffold affects osteogenic proliferation of MSCs

Osteogenic-induced MSCs were cultured on Scaffold and Strata to examine whether porosity of the scaffold affects their proliferation. MSCs were seeded onto Scaffold and Strata following the methodology previously described and cultured for 21 days (Section 2.3.1). Histological analysis of cells revealed clear differences between osteogenic-induced MSCs cultured on Scaffold (Figure 3.2.6A) compared to Strata (Figure 3.2.6B). The osteogenic-induced MSCs cultured on Scaffold produced widespread coverage of the entire membrane and cells were much more elongated and numerous. There were also indications of the production of extracellular matrix around the cells

cultured on Scaffold, seen on the image as wisps of light purple (ECM) around the dark purple (nucleus) which is not seen in Strata. This suggests the larger pores of the Scaffold membrane (Figure 3.2.3) provides a microenvironment which is more conducive to osteogenesis of MSCs as a significant stage of differentiation is the secretion of the ECM. Another key reason why Scaffold may provide a more suited environment for osteogenesis is that MSCs are able to achieve greater proliferation compared to Strata. This is important as the switch to osteogenic differentiation media for MSCs occurs 3 days after seeding of cells, therefore if MSCs are able to proliferate more, there will be more cells for the next stages of osteogenesis.

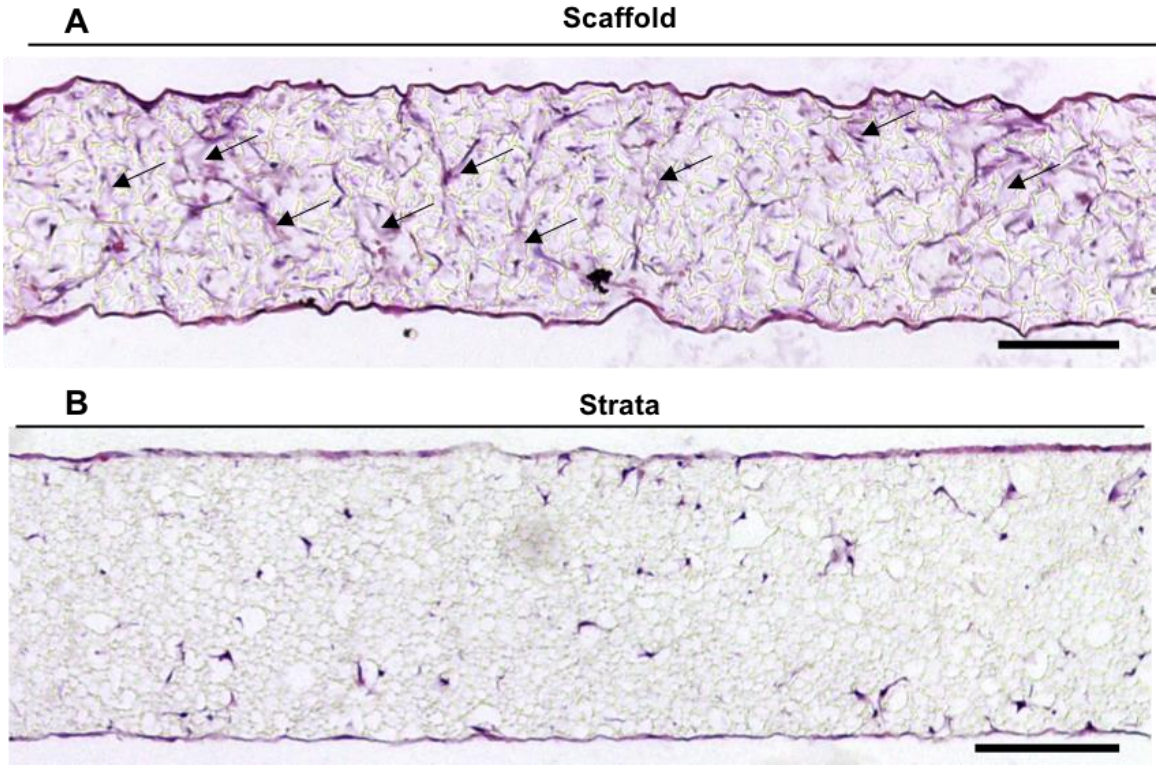

Figure 3.2.6 Histological analysis of osteogenic-induced MSCs cultured on Scaffold vs Strata. MSCs were seeded onto 12-well inserts of Scaffold and Strata and induced to osteogenic differentiation for 21 days. Osteogenic-induced MSCs showed greater proliferation and secretion of extracellular matrix (arrows) on Scaffold compared to Strata. Scale bar = 100 μm.

All results indicate MSCs, osteogenic-induced MSCs and MG-63 cells cultured on Scaffold produced greater proliferation, coverage of the membrane and homogenous growth compared to Strata and Polaris. Osteogenic-induced MSCs for 21 days cultured on Scaffold were able to secrete ECM which is required in order for osteogenic differentiation to take place. Using these results, Alvetex® Scaffold was determined as a suitable 3D cell culture material for culturing bone forming cells.

3.3 Characterisation of osteogenesis by bone forming cells cultured in 2D vs Alvetex® Scaffold

The process of osteogenesis by osteoprogenitor cells can be split into 3 stages. These stages were investigated between 2D and 3D culture methods. These stages are:

- Proliferation
- ECM deposition
- Matrix mineralisation

3.3.1A Proliferation

Proliferation of bone forming cells is the first stage of osteogenesis. During this stage, progenitor cells proliferate and undergo cell division to increase the number of cells in culture. Proliferation must occur before differentiation can take place.

3.3.1. Confluency of proliferation of osteogenic-induced MSCs and MG-63s in 3D is reached at Day 7

MSCs were seeded onto Alvetex® Scaffold and induced for osteogenic differentiation for up to 21 days. H&E analysis shows osteogenic-induced MSCs cultured for 7, 14 and 21 days (Figure 3.3.1). All three timepoints produced similar results whereby cells demonstrated homogenous growth throughout the Scaffold and there were no obvious differences in cell numbers, suggesting proliferation remained at similar levels. This is also reflected in the graph (Figure 3.3.1D) displaying the cell nuclei counts from each timepoint using the method described in Section 2.5.3 . Counts did not produce any statistically significant results between timepoints, suggesting the number of cells remained at similar levels. These results indicate that by day 7, osteogenic-induced MSCs reach their maximum proliferative capacity and subsequently, begin their differentiation stages. This is similar in the osteoblast-like cells MG-63s (Figure 3.3.1.1) which represent a population of osteoblast-like cells which are thought to be more mature. In order for cells to differentiate, proliferation must be reduced. Culturing MG-63s on Alvetex® Scaffold did not show an obvious difference in cell numbers between 7,14 and 21 days from H&E analysis or nuclei cell counts (Figure 3.3.1.1). This suggests the maximum proliferation of cells was achieved by day 7 as the cells appeared to have stopped replicating as they have already differentiated into more mature osteoblasts.

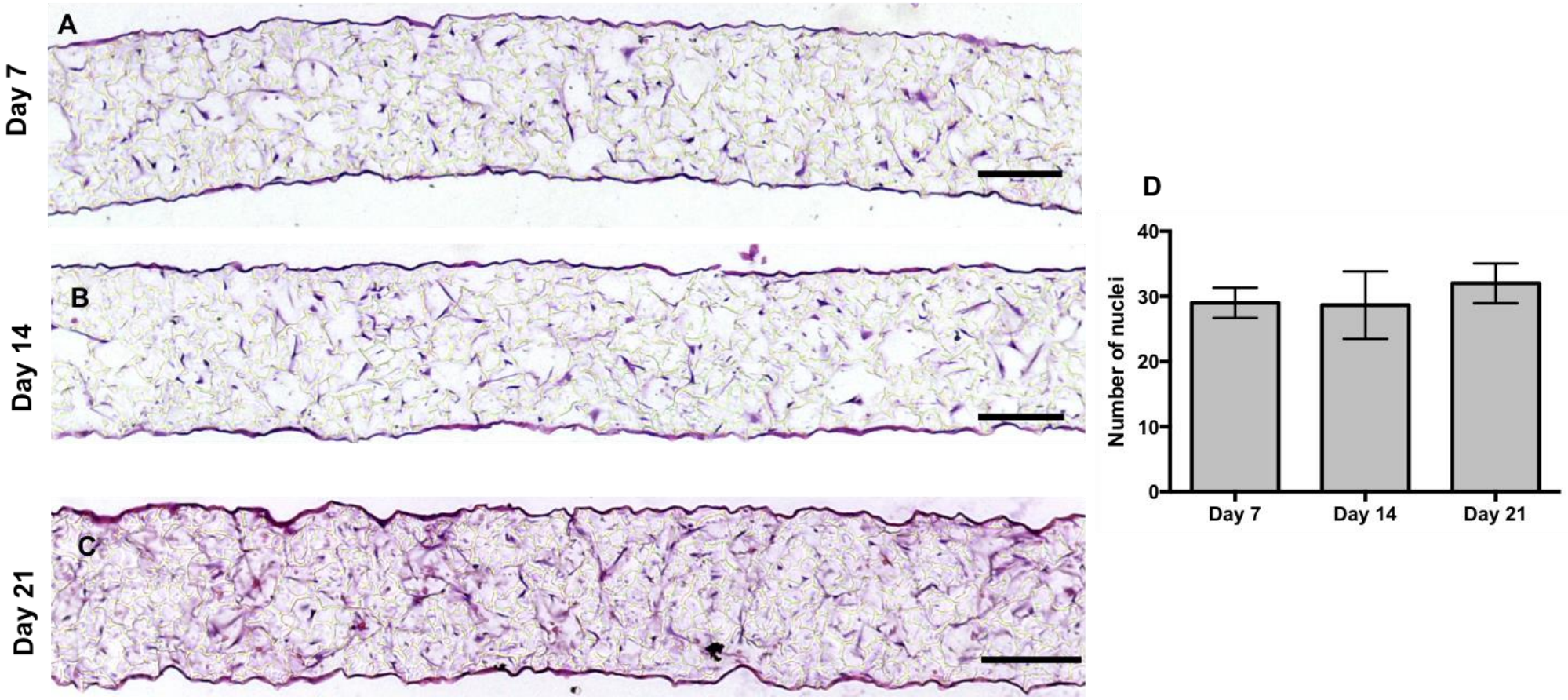

Figure 3.3.1 Osteogenic-induced MSCs cultured on Alvetex® Scaffold. MSCs were seeded onto Scaffold and induced for osteogenic differentiation for up to 21 days and their proliferation was examined. No obvious differences in cell number was seen across the three timepoints. Scale bar = 100 μm. (D) Quantitative analysis of the nuclei number at each time point using ImageJ software cell counter. No statistically significant difference was found between the timepoints ($P>0.05$) . Data represent the mean ± SEM (n= 3).

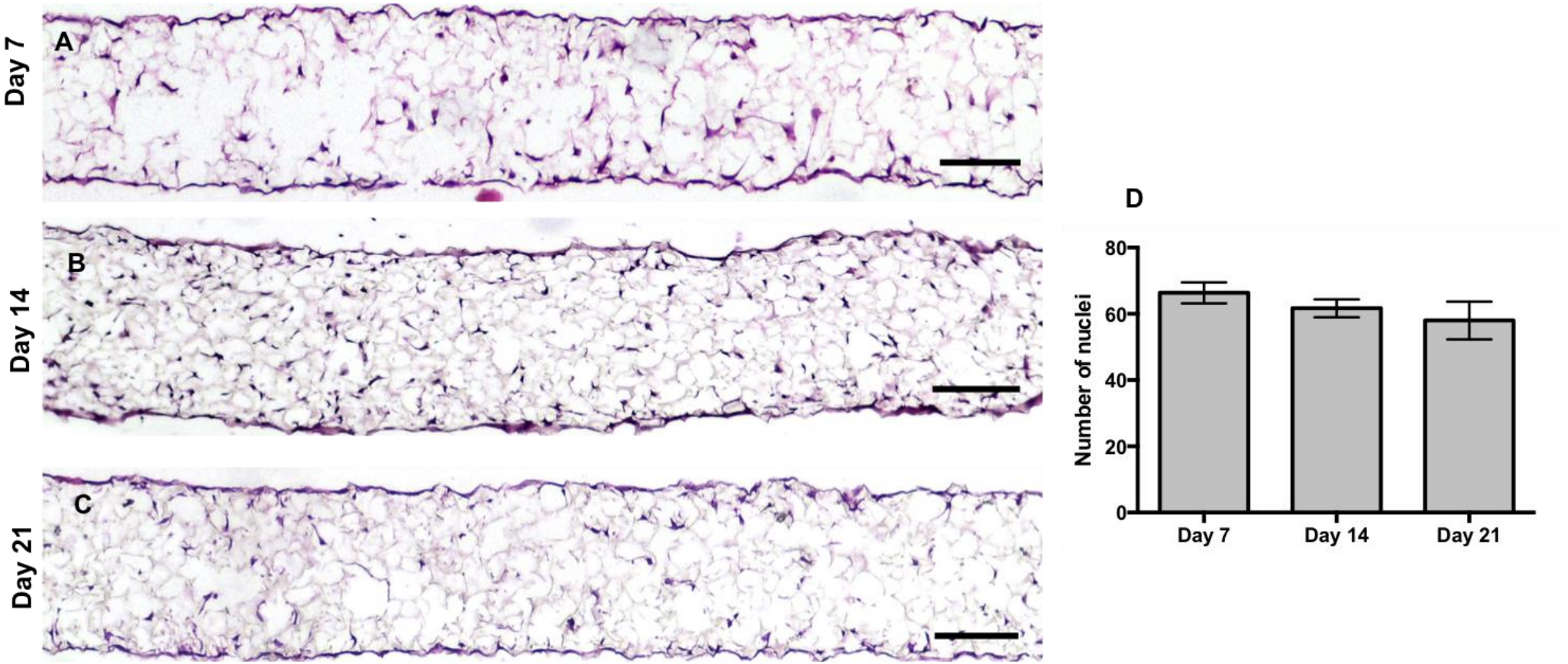

Figure 3.3.1.1 MG-63s cultured on Alvetex® Scaffold. MG-63s were seeded onto Scaffold for up to 21 days and their proliferation was examined. No obvious differences in cell number was seen across the three timepoints (A-C). Scale bar = 100 μm. (D) Quantitative analysis of the nuclei number at each time point using ImageJ software cell counter. No statistically significant difference was found between the timepoints ($P>0.05$) . Data represent the mean ± SEM (n= 3).

3.3.2A ECM deposition

ECM formation is a marker of MSC commitment and differentiation to osteoblasts following proliferation, and this was compared in 2D and 3D cultures. As seen previously in Figure 3.2.6, secretion of ECM by osteogenic-induced MSCs cultured using Alvetex® Scaffold can be observed. The following section aimed to characterise the osteogenic markers found in the synthesised ECM. The 4 markers tested in this project are: fibronectin, collagen I, collagen III and alkaline phosphatase.

3.3.2 ECM deposition – Fibronectin

A major component of the ECM which is highly expressed in bone ECM is fibronectin, particularly during the early stages of osteogenesis. Fibronectin was also deposited in areas of recruitment and commitment of osteoblast precursors, which is involved during formation of mesenchymal condensations, indicative of bone nodule formation.

3.3.2.1 Fibronectin is secreted around condensations by osteogenic-induced MSCs in 2D culture

Immunofluorescence was used to analyse the synthesis of fibronectin by 2D cultures of osteogenic-induced MSCs, up to day 21 (Figure 3.3.2.1). Mesenchymal condensations can be seen by day 7 (Figure 3.3.2.1A), indicating bone nodule formation. With time, the mesenchymal condensations become larger as more cells are recruited and osteogenic-induced MSCs progressively differentiates into osteoblasts (Figure 3.3.2.1A-C). Interestingly, fibronectin secretion is localised to areas in the borders around the mesenchymal condensations formed by osteogenic-induced MSCs and not inside the nodules (Figure 3.3.2.1A-C). In the negative controls of MSCs cultured without osteogenic morphogens, fibronectin is secreted between cells and links are formed using fibronectin (Figure 3.3.2.1D-F). This is suggested to be MSCs secreting fibronectin to locate other cells to actively migrate and come together, resulting in indications of cell condensations by day 21 (Figure 3.3.2.1F). This indicates that rat MSCs may spontaneously differentiate into cells of osteogenic lineage by day 21, without induction by osteogenic morphogens.

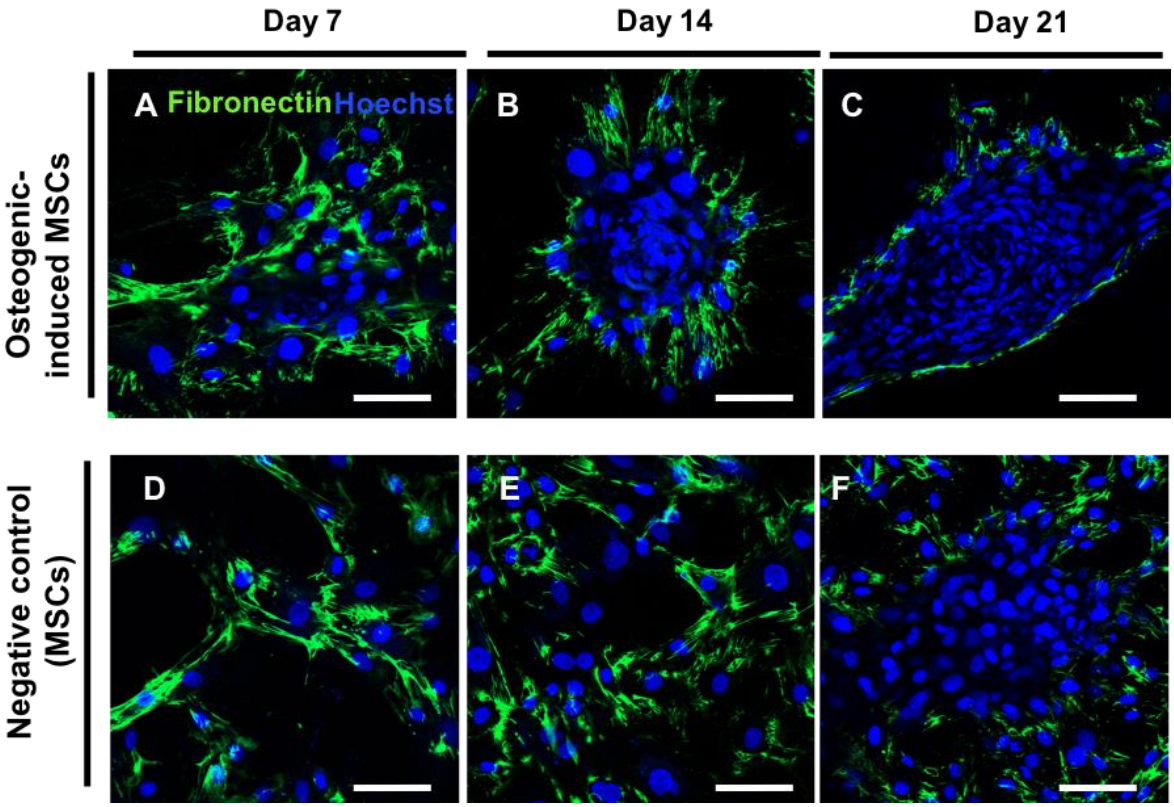

Figure 3.3.2.1 Fibronectin secretion by osteogenic-induced MSCs in 2D. Osteogenic-induced MSCs were cultured for up to 21 days using 2D culture and fibronectin secretion was examined. Fibronectin was produced around condensation of cells during bone nodule formation by osteogenic-induced MSCs (A-C). Negative control of MSCs cultured using media without osteogenic morphogens showed fibronectin secretion between cells at day 7 and 14 (D-E), with indications of mesenchymal condensation being seen by day 21 (F). Scale bar = 200 μm.

3.3.2.2 Fibronectin secretion decreases with time in 3D cultures of osteogenic-induced MSCs

To investigate fibronectin secretion of osteogenic-induced MSCs in 3D culture, MSCs were seeded onto Alvetex® Scaffold and cultured under osteogenic conditions for up to 21 days. Images from immunofluorescence analysis revealed decrease in fibronectin synthesis of osteogenic-induced MSCs from day 7 to day 21 (Figure 3.3.2.2A-C). At day 7, fibronectin production is very evident and occurs throughout the Scaffold (Figure 3.3.2.2A). However, by day 14 (Figure 3.3.2.2B), smaller amounts of fibronectin are deposited in cultures and becomes concentrated at the top and bottom layers of the Scaffold by day 21 (Figure 3.3.2.2C). Fibronectin is involved in early stages of osteogenesis, which suggests that as time in culture progresses, osteogenic-induced MSCs are differentiating into more mature osteoblasts. By day 14 and 21, later stages of osteogenesis occur which results in the decline in fibronectin production by the osteogenic-induced MSCs.

The opposite trend is seen in MSCs cultured without osteogenic morphogens whereby fibronectin production is increased with time. At day 7, fibronectin secretion is limited (Figure 3.3.2.2D) and is much less than osteogenic-induced MSCs at the same timepoint (Figure 3.3.2.2A). By day 14 and 21, fibronectin deposition is greatly increased and covers the area of the Scaffold (Figure 3.3.2.2E-F). The observation from immunofluorescence analysis that non-induced MSCs produce similar levels of fibronectin at day 21 (Figure 3.3.2.2F) compared to osteogenic-induced MSCs at day 7 (Figure 3.3.2.2A) suggest early osteogenesis of non-induced MSCs takes place spontaneously. In agreement with previous findings in 2D, the progressive increase in fibronectin secretion implies MSCs differentiate spontaneously into an osteogenic lineage without stimulation with osteogenic morphogens after 21 days.

3.3.2.3 Fibronectin secretion by MG-63s in 2D and 3D cultures is minimal

Investigation of fibronectin synthesis by osteoblast-like MG-63s was carried out using immunofluorescence. In 3D cultures, little fibronectin production can be seen across the three timepoints (Figure 3.3.2.3A-C). The green staining that is present on the images is likely to be non-specific background staining as some green staining can be detected outside of the Scaffold (arrowheads). This indicates the staining that is present is not genuine fibronectin specific binding and very little positive staining is present. 2D culture of MG-63 at day 14 showed some indications of positive staining of fibronectin between cells (Figure 3.3.2.3D); however this is still quite minimal. Fibronectin expression has been suggested to be involved in early osteogenesis, therefore the observation that MG-63s do not express/only express a small amount of fibronectin in cultures is in agreement with this. MG-63 cells are thought to represent osteoblast-like cells and are considered to be mature osteogenic derivatives. This suggests fibronectin expression should be limited as MG-63 cells have already differentiated.

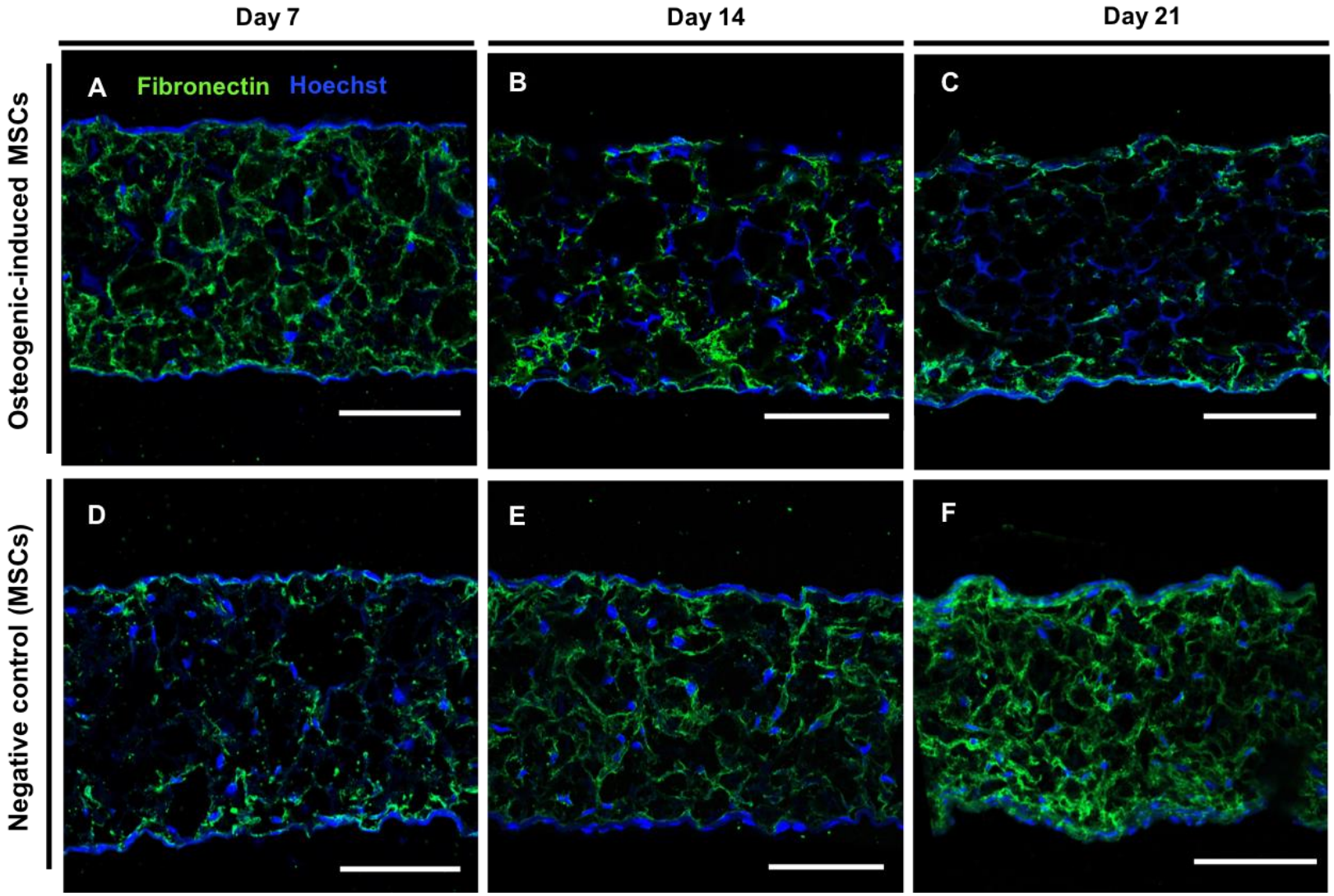

Figure 3.3.2.2 Fibronectin synthesis by osteogenic-induced MSCs cultured using 3D Scaffold. Osteogenic—induced MSCs displayed positive fibronectin staining throughout 3D culture, up to 21 days. Fibronectin production decreased over time (A-C), indicating MSCs differentiating into more mature osteogenic derivatives. Negative controls of MSCs cultured without osteogenic factors displayed increasing fibronectin secretion from day 7 to day 21 (D-F). Scale bar = 100 μm.

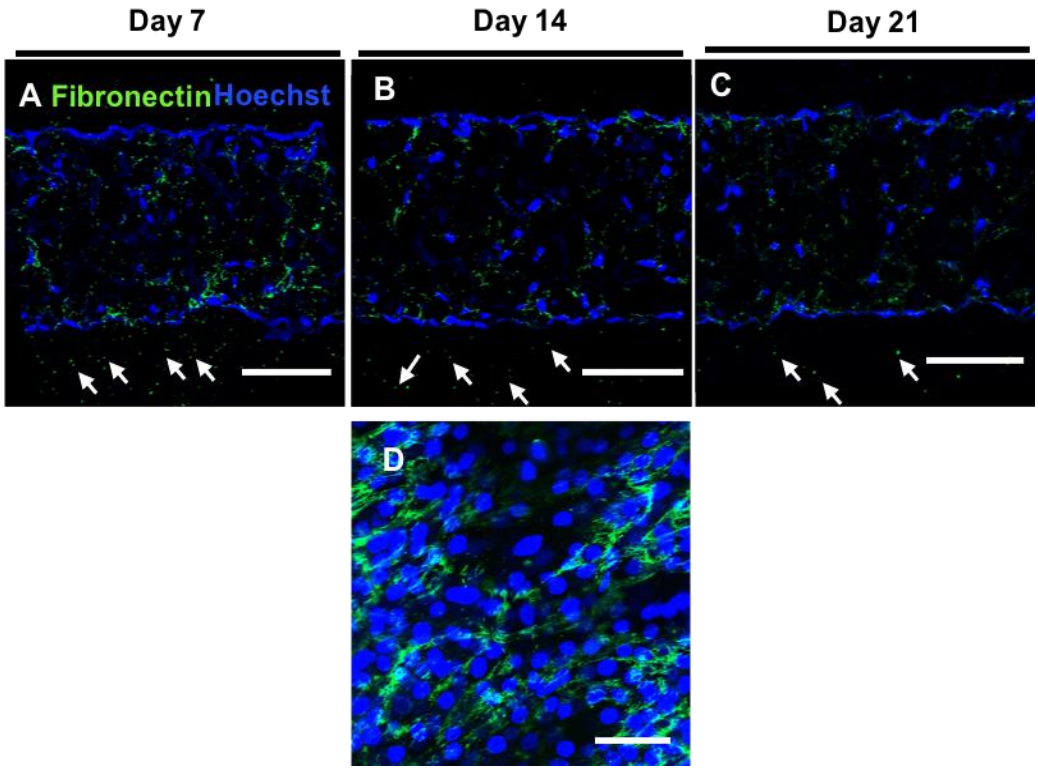

Figure 3.3.2.3 Fibronectin secretion in 2D and 3D cultures of MG-63s. MG-63s displayed little positive expression for fibronectin in both 3D (A-C) and 2D (D) cultures. Non-specific background staining can be seen outside the Scaffold membrane (arrowheads). Scale bar (A-C) = 100 μm, (D) = 200 μm.

3.3.3 ECM Deposition – Collagen I

Collagen I is an essential protein secreted in the bone ECM required for osteogenesis. It is a key ECM marker of osteoblast differentiation and comprises 90% of bone ECM. It is vital for matrix mineralisation which is the final stage of osteoblast differentiation.

3.3.3.1 Collagen I is secreted in 2D cultures of osteogenic-induced MSCs

Osteogenic-induced MSCs were maintained for up to 21 days and collagen I secretion was observed using immunofluorescence staining (Figure 3.3.3.1). Condensation of cells can be readily detected from day 7 (Figure 3.3.3.1A) and collagen I secretion is present at all 3 time points, (Figure 3.3.3.1A-F) indicating bone nodule formation. Collagen I is deposited in the areas of condensations and not outside (data not shown). MSCs cultured with basic media without osteogenic morphogens displayed no condensations of cells and mainly negative staining of collagen I (Figure 3.3.3.1G-I). However at day 21 (Figure 3.3.3.1I), there are some indications of positive staining in the culture. This suggests MSCs may spontaneously begin differentiating into an osteogenic lineage without stimulation with osteogenic morphogens after 21 days, which is in agreement with previous findings.

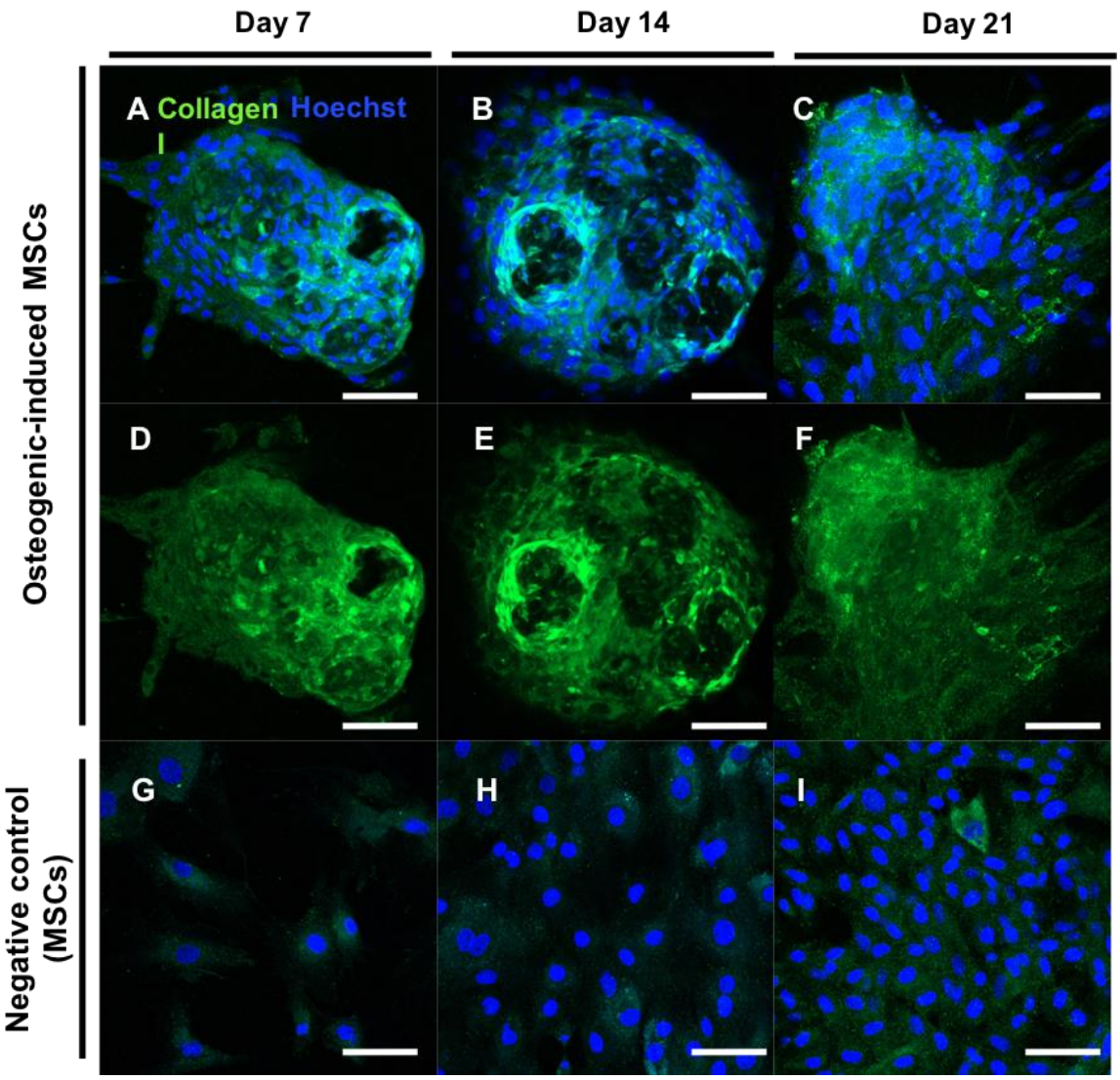

Figure 3.3.3.1 Collagen I is produced by osteogenic-induced MSCs in 2D cultures. Representative immunofluorescent images showing osteogenic-induced MSCs secreting collagen I up to 21 days during differentiation into osteoblasts (A-F). Clear condensation of cells into bone nodules is seen. Collagen I staining without Hoechst (nuclei) is shown (D-F). Negative controls containing MSCs cultured in basic media without osteogenic morphogens did not show collagen I secretion up to day 14, with some indications of positive staining at day 21 (G-I). Scale bar = 200 μm.

3.3.3.2 Collagen I is secreted increasingly over time in 3D cultures of osteogenic-induced MSCs

Collagen I deposition by osteogenic-induced MSCs in 3D cultures was investigated at day 7, 14 and 21 (Figure 3.3.3.2). Immunofluorescence analysis displayed clear collagen I secretion (green) into the scaffold by the osteogenic-induced MSCs at day 7,14 and 21 (Figure 3.3.3.2A-C). The levels of positive staining appear to accumulate with time, suggesting the MSCs are differentiating into more mature osteoblasts as there is a greater production of collagen I in the ECM. At day 21, osteogenic-induced MSCs are able to secrete enough collagen I to cover the Scaffold, leaving collagen I being

densely packed in the ECM (Figure 3.3.3.2C). Similar to 2D cultures, the negative controls containing MSCs cultured without osteogenic morphogens showed little/no positive staining in day 7 – 14 (Figure 3.3.3.2D and E) but by day 21 (Figure 3.3.3.2F), there is some collagen I being secreted into the ECM. This agrees with the previous finding that by day 21, unstimulated MSCs begin to differentiate in an osteogenic lineage without stimulation from osteogenic morphogens. However, the amount of collagen I being secreted in the scaffold at day 21 (Figure 3.3.3.2F) is still minimal compared to day 7 (Figure 3.3.3A) of osteogenic-induced MSCs.

3.3.3.3 Deposition of collagen I is evident in 2D and 3D cultures of MG-63 cells

Secretion of collagen I by MG-63s maintained in 2D and 3D cultures was also examined. From immunofluorescence analysis, MG-63s appear to produce similar amounts of collagen I across the three timepoints in 3D (Figure 3.3.3.3A - C), suggesting production of collagen I reaches a maximum saturation point in 3D as MG-63s are already differentiated. MG-63s cultured using 2D methods also secreted collagen I at day 14 (Figure 3.3.3.3D). Condensation of cells can also be observed as the nuclei (blue) are in close proximity to each other, and collagen I is secreted in this condensation. This is similar to results observed with osteogenic-induced MSCs as in both types of cells, collagen I secretion is localised to the inside of the condensations.

3.3.3.4 Collagen I expression is greater in 3D cultures than 2D for osteogenic-induced MSCs

To assess the whether there are differences in collagen I expression between 2D and 3D cultures, osteogenic-induced MSCs were maintained in 2D and 3D cultures for up to 21 days. Protein lysates of each condition was generated after 7,14 and 21 days and western blotting was used to measure the amount of collagen I expressed in each sample. The antibody used for measuring collagen I expression cross reacts with different epitopes of collagen I, resulting in numerous bands being shown on the blot. Western blot analysis revealed increased expression of collagen I for 3D culture at day 7, 14 and 21 compared to their respective 2D culture condition (Figure 3.3.3.4). The bands are less prominent for 2D cultures and only had one band, suggesting lower levels of collagen I expression whereas the 3D cultures produced clearer bands with the characteristic numerous collagen I epitope bands. Results suggest osteogenic-induced MSCs cultured using Alvetex® Scaffold not only increased collagen I expression compared to their 2D counterparts, but also expresses more than one epitope of collagen I. As collagen I is a marker for MSC differentiation into osteoblasts, another implication of this is that 3D culture conditions is able to support greater differentiation of MSCs into osteoblasts as collagen I is expressed more compared to 2D conditions. The molecular weight of the bands corresponds to mature collagen and the antibody recognises epitopes in both alpha-1 and alpha-2 collagens.

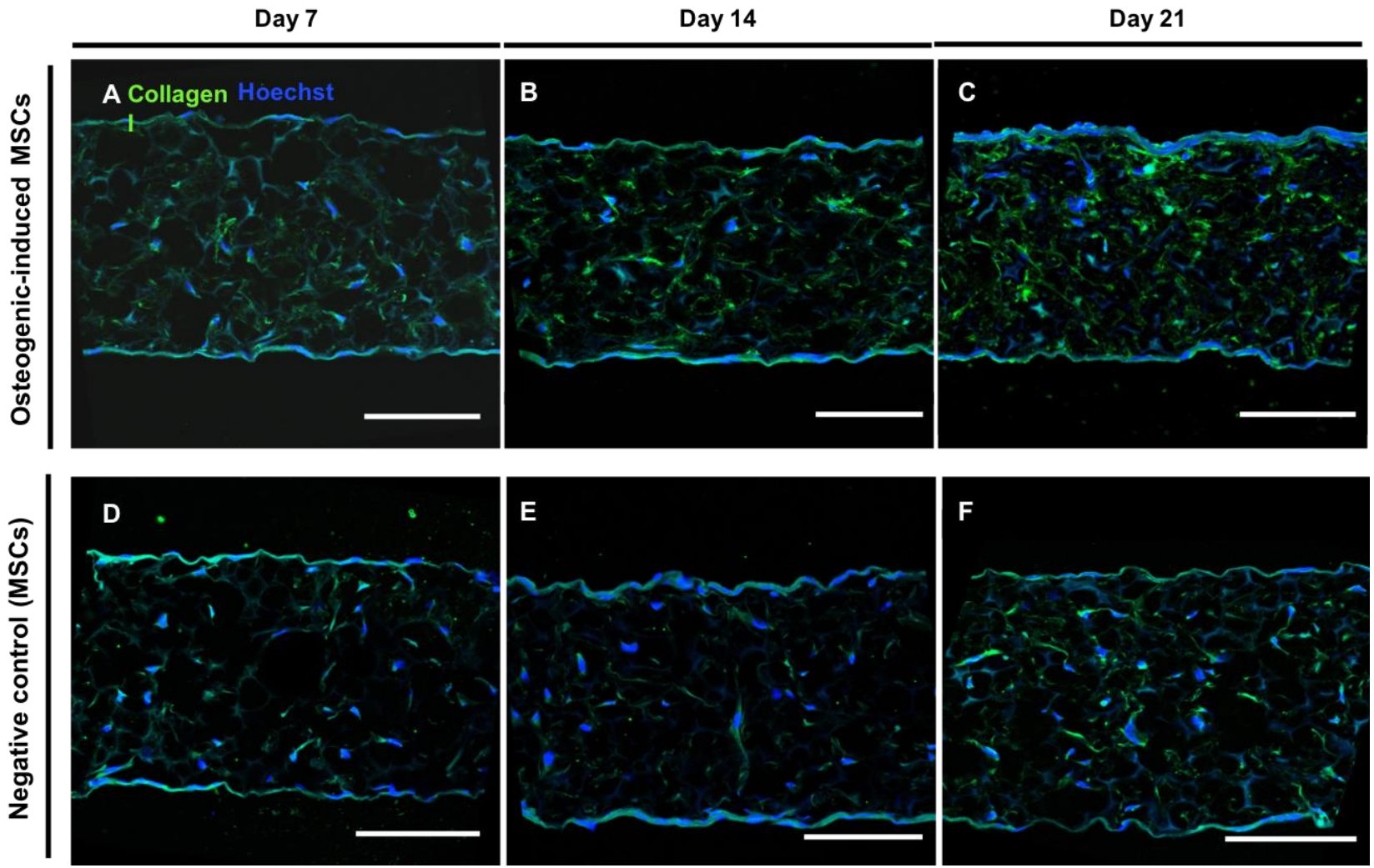

Figure 3.3.3.2 Collagen I deposition by osteogenic-induced MSCs in 3D cultures increase over time. Representative immunofluorescent analysis of increasing collagen I secretion by osteogenic-induced MSCs over time, up to day 21 (A-C). Negative controls containing MSCs cultured in basic media omitting osteogenic morphogens show little or no secretion of collagen I (D-F). Scale bar = 100 μm.

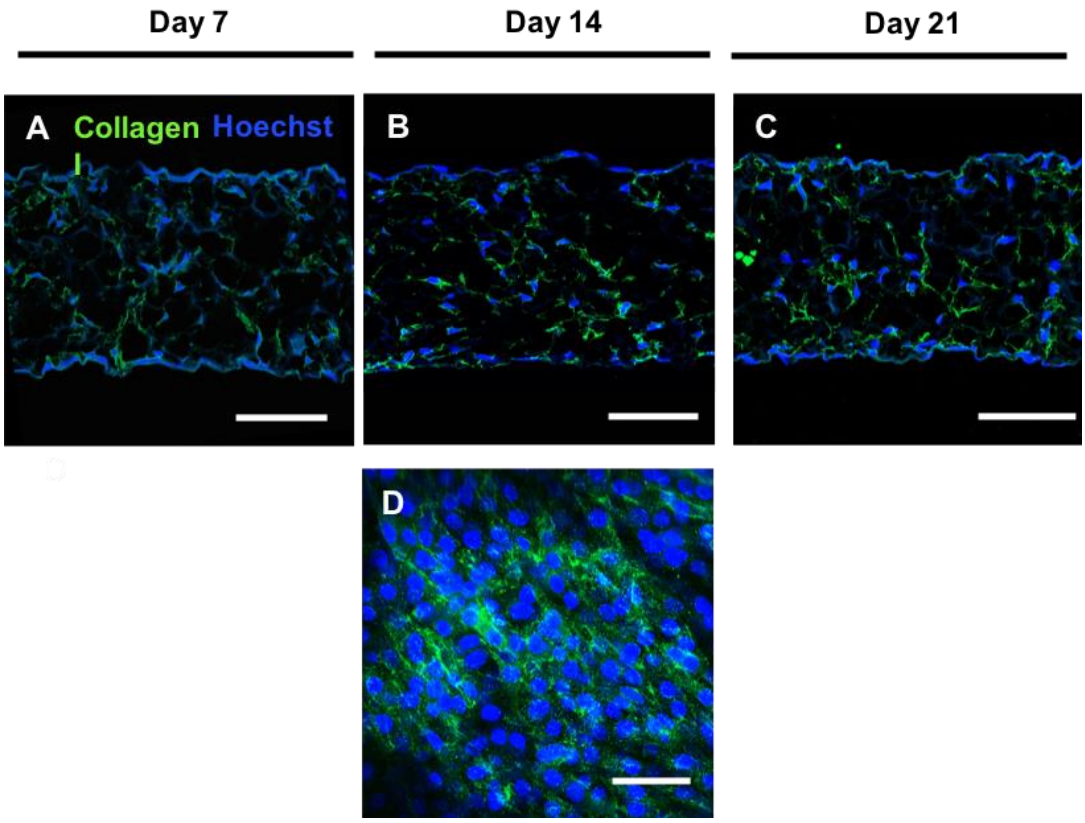

Figure 3.3.3.3 Collagen I deposition in 2D and 3D cultures of MG-63s. MG-63 displayed positive staining for collagen I for both 2D (D) and 3D (A-C) cultures. MG-63s appeared to produce similar levels of collagen I across the timepoints in 3D culture. In 2D culture, at day 14, MG-63 also displays positive staining for collagen I. Scale bar (A-C) = 100 μm, (D) = 200 μm.

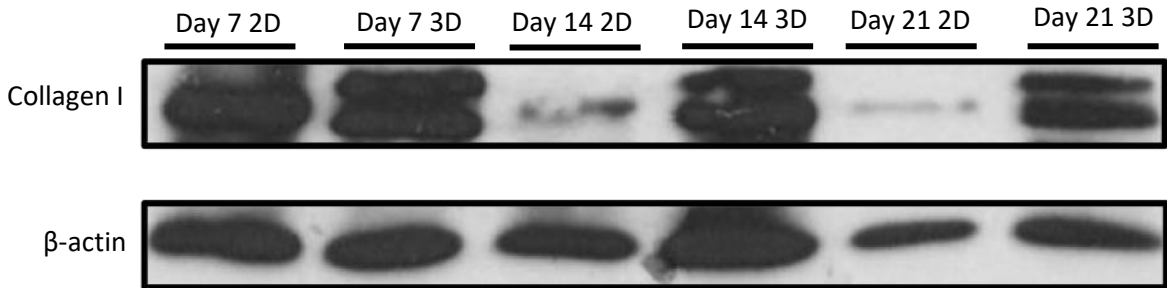

Figure 3.3.3.4 Expression of Collagen I is greater in 3D cultures than 2D counterparts for osteogenic-induced MSCs. Representative western blot analysis of collagen I appeared to be greater in 3D cultures at each time point compared to 2D cultures. The different epitopes of collagen I can be clearly seen for 3D cultures but not 2D. β-actin was used as a loading control.

3.3.4 – ECM deposition – Collagen III

Collagen III is another major ECM component which is expressed by osteoblasts during differentiation. It has been shown to be present in mesenchymal condensations in cultures. Expression of collagen III by bone forming cells was also investigated in 2D and 3D cultures.

3.3.4.1 Collagen III is expressed in 2D cultures of osteogenic-induced MSCs

Secretion of collagen III in the ECM by osteogenic-induced MSCs was investigated in 2D cultures. Collagen III deposition could be identified by day 7 (Figure 3.3.4.1A and D) as well as mesenchymal condensations, indicating bone nodule formation. Collagen III expression is highly localised to the inside of the condensations of cells for up to day 21 (Figure 3.3.4.1C and F) which is similar to the findings for collagen I expression in 2D cultures by osteogenic-induced MSCs discussed previously (Section 3.3.3.1). Negative controls were also included in which MSCs cultured with basic media without osteogenic morphogens was stained with the same collagen III antibody. Small amounts of positive staining can be seen in all three time points (Figure 3.3.4.1G-I), and at day 21, there is an indication of cells beginning to aggregate together to form a condensation. This agrees with the previous notion suggested whereby by day 21, MSCs may naturally begin differentiation towards an osteogenic lineage without induction by osteogenic morphogens.

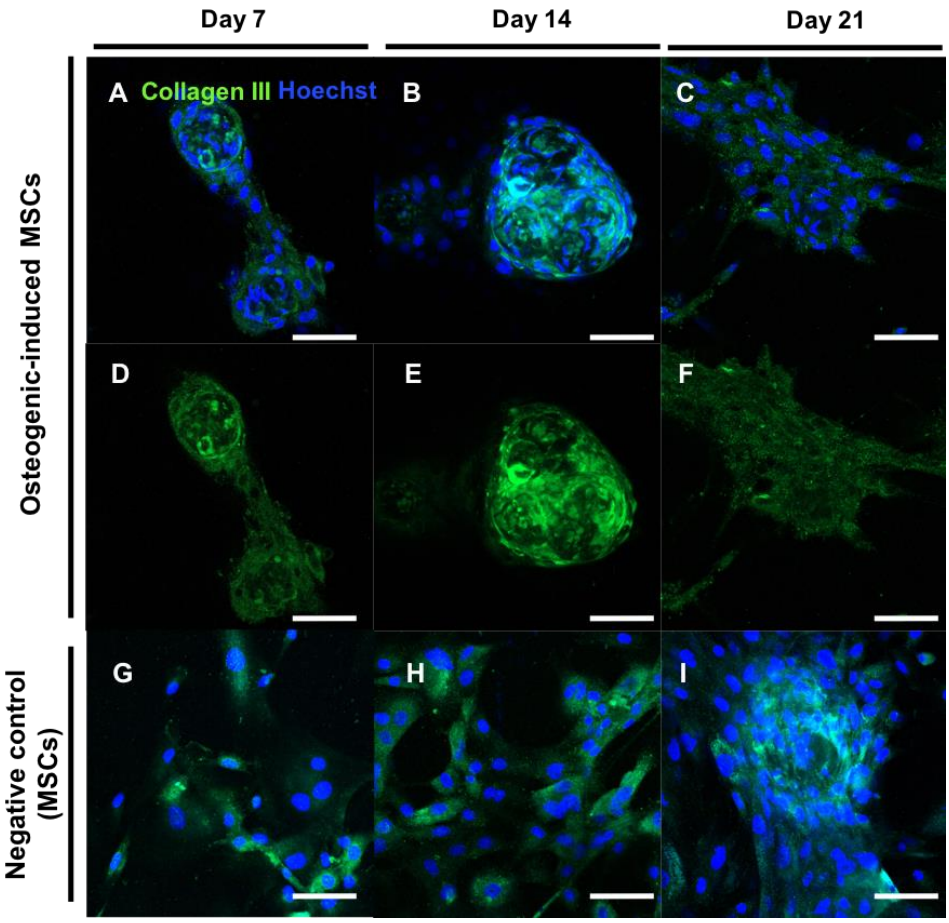

Figure 3.3.4.1 – Collagen III is deposited in 2D cultures of osteogenic-induced MSCs. Representative immunofluorescence analysis of collagen III deposition (green) and cell nuclei (blue). Osteogenic-induced MSCs were cultured up to day 21 (A-F), with collagen III staining only shown in (D-F). Negative controls of MSCs cultured using basic media without osteogenic morphogens is also shown (G-I). Scale bar = 200 μm.

3.3.4.2 Collagen III is increasingly deposited in 3D cultures of osteogenic-induced MSCs

Collagen III production in the ECM of 3D cultures of osteogenic-induced MSCs was also assessed. At day 7, minimal amounts of positive staining can be seen, suggesting little collagen III is produced in the ECM as cells are only beginning to differentiate (Figure 3.3.4.2A). By day 14 and 21, collagen III secretion is more much evident in cultures as cells are differentiating into more mature cells of osteogenic lineage (Figure 3.3.4.2B-C). This provides further evidence to suggest MSCs are acquiring an osteogenic phenotype and are progressively differentiating into osteoblasts. Collagen I deposition (Figure 3.3.3.2) displayed similar results of secretion of collagen III which is expected as collagen I and III production are closely linked. Both collagen III and collagen I secretion covers the whole area of the Scaffold and is not concentrated in one area. Negative controls containing MSCs cultured without osteogenic morphogens show little or no positive staining across all three timepoints (Figure 3.3.4.2D-F).

3.3.4.3 Collagen III is secreted at similar levels across 3D cultures and is evident in 2D cultures of MG-63

To examine further the ECM produced by osteoblast-like cells, MG-63 cells were cultured in 2D and 3D for up to day 21 (Figure 3.3.4.3). Staining for collagen III by immunofluorescence displayed similar findings to collagen I (Figure 3.3.3.3). For 3D cultures, collagen III production at day 7,14 and 21 was comparable between them (Figure 3.3.4.3A-C) as the amount of staining between the timepoints remained at similar levels. No significant differences between the samples can be seen from the immunofluorescence analysis. Collagen III deposition is also present in 2D cultures of MG-63s (Figure 3.3.4.3D).

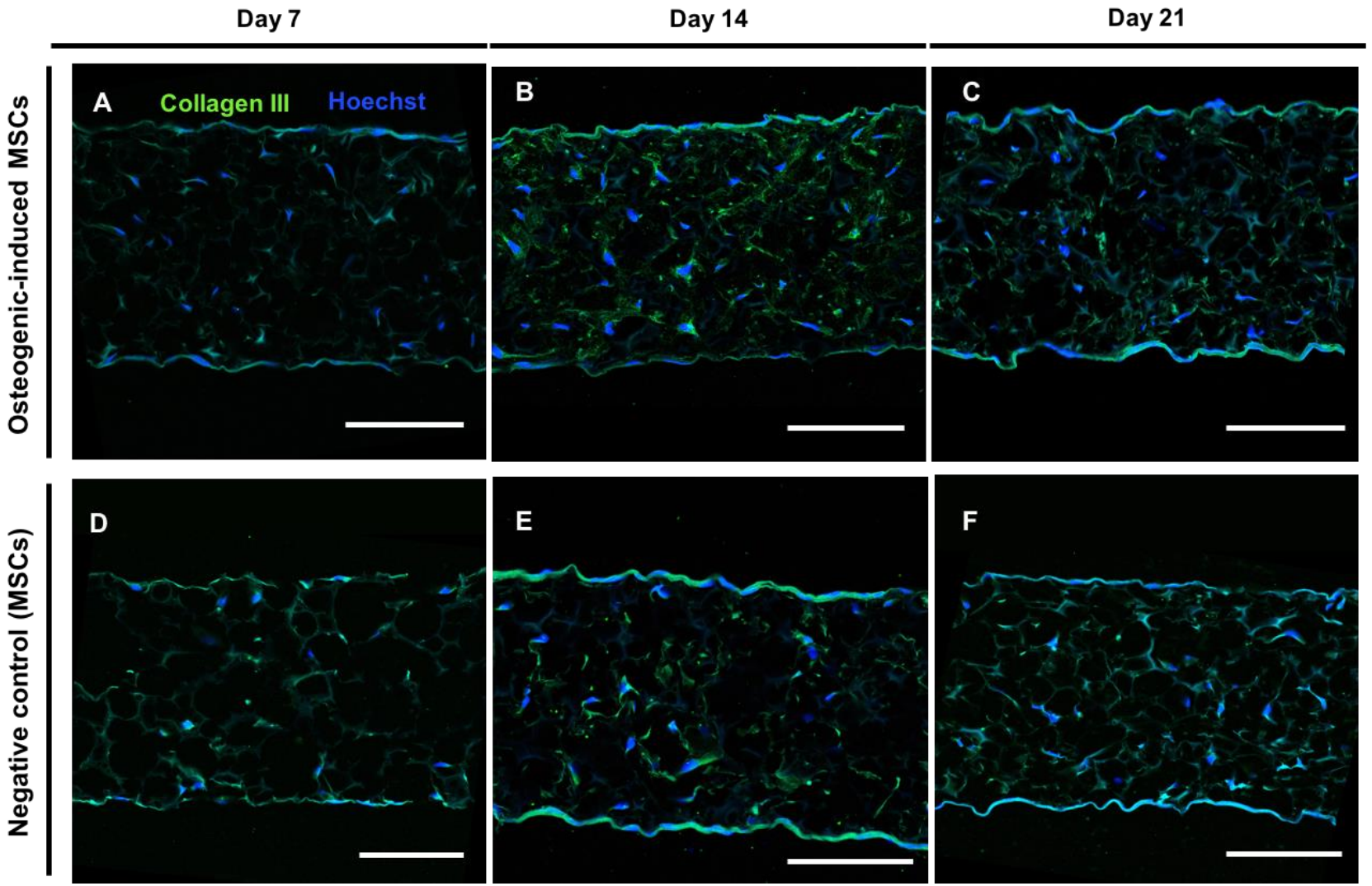

Figure 3.3.4.2 – Collagen III is deposited by osteogenic-induced MSCs in 3D cultures. Representative immunofluorescent analysis of collagen III secretion by osteogenic-induced MSCs over time, up to day 21 (A-C). Negative controls containing MSCs cultured in basic media omitting osteogenic morphogens show little or no secretion of collagen III (D-F). Scale bar = 100 μm.

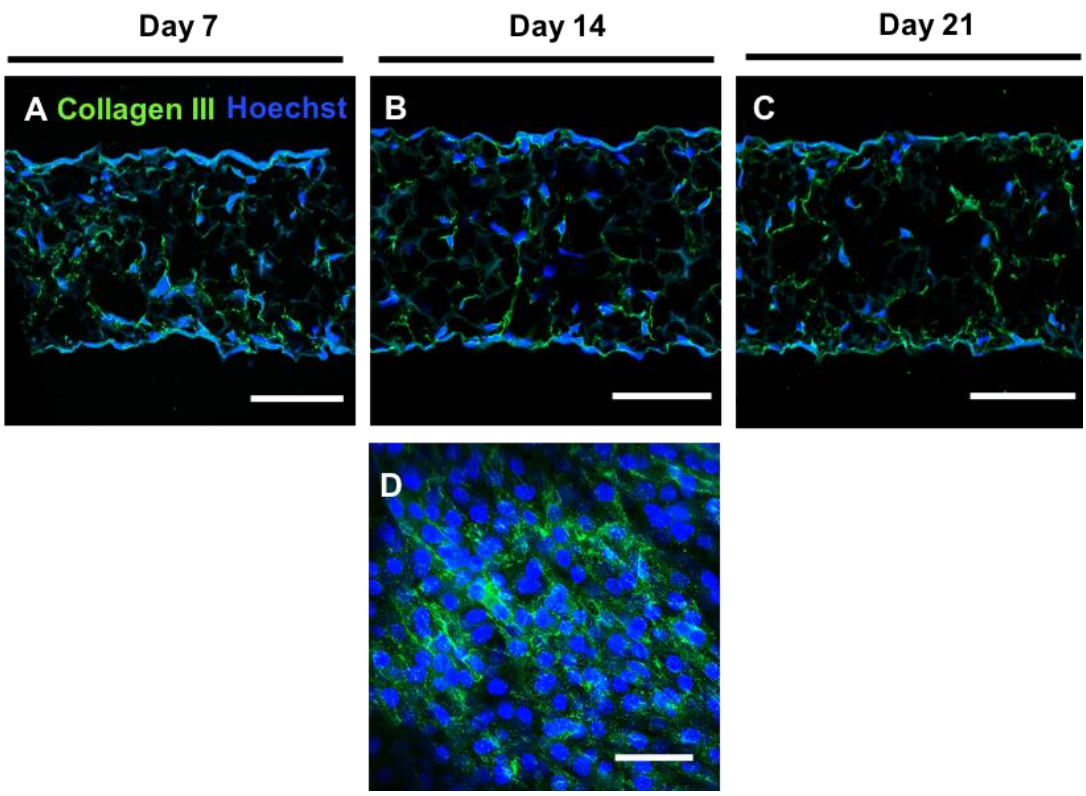

Figure 3.3.4.3 – Collagen III deposition in 2D and 3D cultures of MG-63s. MG-63 displayed positive staining for collagen III for both 3D (A-C) and 2D (D) cultures. MG-63s appeared to produce similar levels of collagen I across the timepoints in 3D culture. In 2D culture, at day 14, MG-63 also displays positive staining for collagen III. Scale bar (A-C) = 100 μm, (D) = 200 μm.

3.3.5. ECM deposition – Alkaline Phosphatase (ALP)

Alkaline phosphatase (ALP) is another important marker in the ECM expressed during early osteoblast differentiation, needed to supply phosphate for bone mineralisation – the next stage of osteogenesis. The expression of alkaline phosphatase in cultures was measured using a colorimetric alkaline phosphatase assay kit as previously described (Section 2.6).

3.3.5.1 Alkaline phosphatase expression is indicative of greater osteoblast differentiation by osteogenic-induced MSCs in 3D cultures

To investigate osteogenesis in 2D and 3D cultures further, the expression of alkaline phosphatase was measured in cultures of osteogenic-induced MSCs, up to 21 days. Although no statistical significance could be calculated between 2D and 3D at the respective timepoints, the trend of the graph still provides useful information (Figure 3.3.5.1). ALP expression in 2D cultures increased over time, reaching peak at 21 days whereas in 3D cultures, ALP expression reached its maximum at day 14 and decreased at day 21. Alkaline phosphatase is expected to increase during osteoblast differentiation while decreasing during matrix mineralisation – the stage of osteogenesis which

following osteoblast differentiation. The trend seen from the ALP assay suggests that in 2D, MSCs continue to differentiate into osteoblasts past day 21 and greater matrix mineralisation may take place in 3D by day 21 as a decrease in ALP secretion is observed. At day 7 and day 14, osteogenic-induced MSCs produce greater ALP expression in 3D compared to 2D. This could indicate greater osteoblast differentiation in 3D, however this is not statistically significant.

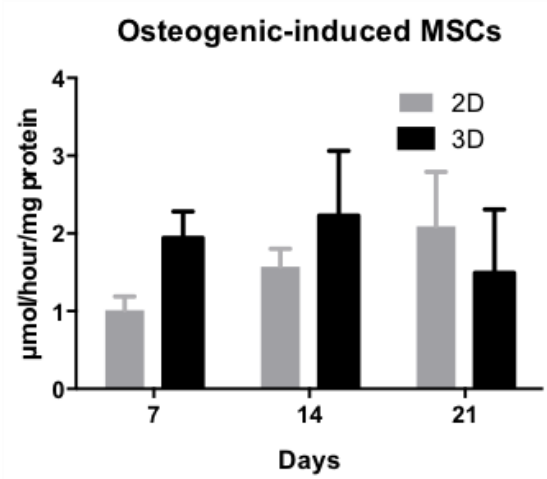

Figure 3.3.5.1 Alkaline Phosphatase expression by osteogenic-induced MSCs in 2D vs 3D cultures. Although no statistical significance was found between the data, the trend seen on the graph is indicative of greater osteoblast differentiation in 3D cultures. At day 7 and 14, 3D culture of osteogenic-induced MSCs resulted in greater alkaline phosphatase production compared to 2D. By day 21, MSCs may have differentiated more to form mature osteoblasts, resulting in decreased ALP production compared to 2D. Data represent the mean ± SEM (n= 3).

3.3.6A Matrix mineralisation

Matrix mineralisation is the last stage of osteogenesis. During this, osteoblasts mineralises the extracellular matrix by laying down minerals such as calcium and phosphate. There are several markers for matrix mineralisation, one of which is the deposition of calcium which was investigated in 2D and 3D cultures of bone forming cells.

3.3.6.1 Detection of calcium deposition in 2D and 3D cultures

Mineralisation of the extracellular matrix was visualised using Alizarin Red staining in 2D and 3D cultures. Osteogenic-induced MSCs were maintained using 2D and 3D cultures, as well as MG-63s on 3D cultures. After 21 days, cultures were fixed and stained with Alizarin Red stain following the methods described in Section 2.4.1 and 2.4.2. Alizarin Red stains calcium deposits a bright red colour, indicative of bone matrix mineralisation. Results are illustrated in Figure 3.3.6.1. At 21 days, both 2D and 3D cultures of osteogenic-induced MSCs demonstrate calcification of the matrix due

to clear positive red staining (Figure 3.3.6.1A and B). In 2D, multiple mesenchymal condensations can be seen and calcium deposition can be detected inside the condensations. However, only 2 of the nodules contain an intense red colour, whereas the other condensations are much lighter in colour which indicates less calcium being stained (Figure 3.3.6.1A). In 3D cultures, calcium deposition can be readily detected by osteogenic-induced MSCs at a much darker red colour (Figure 3.3.6.1B) compared to 2D culture. This is preliminary evidence to suggest greater calcium deposition occurs in 3D compared to 2D, however quantifiable data is needed to support this. MG-63s cells cultured in 3D also display positive Alizarin Red staining (Figure 3.3.6.1C), with an intense red colour which is similar to osteogenic-induced MSCs (Figure 3.3.6.1B).

Previous work which involved culturing osteogenic-induced rat MSCs on Alvetex® Scaffold was able to display bone nodule formation in 3D cultures using Von Kossa staining. Similar to Alizarin Red, the Von Kossa histological stain is used to identify the formation of calcified bone nodules which appear as densely dark areas (Figure 3.3.6.1D arrowhead). Using wholemount staining, MSCs cultured under osteogenic conditions for 21 days in 3D demonstrated condensation of cells and calcium deposition.

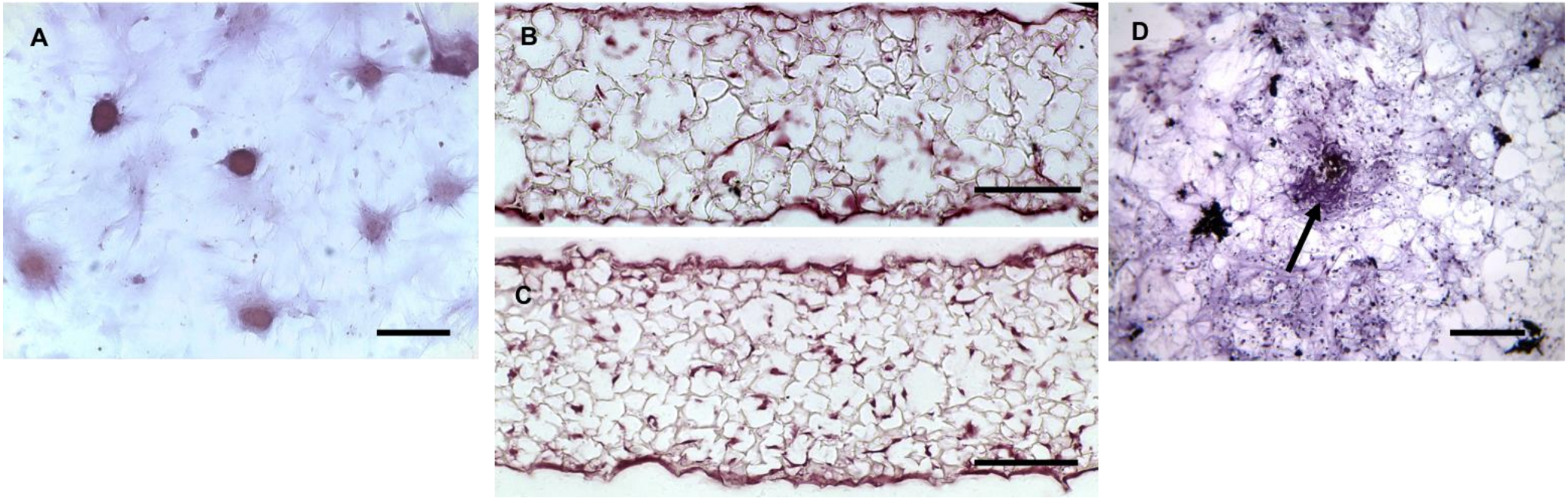

Figure 3.3.6.1 Histological stains of 2D and 3D cultures of bone forming cells suggests matrix mineralisation. Osteogenic-induced MSCs were cultured in 2D (A) and 3D (B) as well as MG-63s (C) for 21 days and stained with Alizarin Red. Alizarin Red stains calcium deposits bright red which is seen in both 2D and 3D cultures. Previous work showed Von Kossa staining of osteogenic-induced MSCs in 3D which similarly shows calcium deposition (D, arrowhead). Credit: Hardy, S. (2010). Scale bar A and D = 200 μm, B and C = 100 μm.

4. Discussion

The overall aim of this study was to develop and characterise an *in vitro* bone tissue model using bone forming cells such as primary rat MSCs and cells from the human osteosarcoma cell line MG-63, to investigate whether 3D cell culture could enhance bone formation. In order to meet this aim, several objectives were required to be met. The first was to isolate and characterise primary rat MSCs and to identify and culture a bone derived cell line such as MG-63s to provide the bone forming cells required for the project. The second objective was to investigate whether 3D scaffolds would support the growth and proliferation of bone forming cells. The third objective of the study was to compare and analyse the stages of osteoblast differentiation by bone forming cells between 2D and 3D culture.

By meeting all these objectives, the hypothesis that 3D cell culture techniques would enhance bone development by bone forming cells can be investigated by comparing the expression of key osteoblast markers between cells cultured by 2D and 3D methods.

4.1 Isolation and culture of bone forming cells

4.1.1 Isolated cells were confirmed to be true MSCs

As discussed in Section 1.2, there is a wide variety of representative cell types which are used to study osteoblast differentiation and bone tissue formation *in vitro*. Primary MSCs are a common type to use as they have the most physiological relevance in modelling osteoblast differentiation *in vitro*. MSCs from rat bone marrow have been characterised and used commonly to investigate *in vitro* osteoblast differentiation[59]. Specifically, the bone marrow was chosen as the source of isolated cells over adipose tissue as rat BM-MSCs have been shown to proliferate faster and possess higher multilineage potential compared to rat adipose MSCs[135].

The first stage of the project was to isolate primary rat MSCs as they are much more widely available compared to human MSCs. Cells were isolated from rat femurs and tibiae using a commonly used methodology[134] and MSC-like cells were identified through plastic adherence, morphology, cell marker expression and multilineage differentiation potential. Plastic adherence is commonly used to characterise isolated MSCs[136], which was assessed through the cells' ability to remain in the plastic flasks after extensive passages. Cells displaying fibroblastic-like, spindle shaped morphology could be seen using phase contrast microscopy, which has been reported to be the morphology MSCs exhibit *in vitro*[137]. Analysing the cell-surface marker expression is another method employed to isolate MSCs. Flow cytometric analysis revealed the largely positive expression from isolated cells

of the mesenchymal marker CD90 (Thy-1), which has been suggested to be involved in early MSC differentiation towards osteogenic cells[138]. The expression of commonly used HSC markers, CD34 and CD45 were found to be largely negative in isolated cells, confirming the depletion of HSCs from culture. However, the use of $CD34^-$ being a marker of MSC has attracted controversy, with some papers reporting $CD34^+$ MSCs formed greater fibroblastic colonies than $CD34^-$ MSCs and CD34 should be considered a positive marker for MSC[139]. However, the predominant opinion still accepts $CD34^-$ as an *in vitro* MSC marker especially for cells isolated from the bone marrow[140], and a large number of papers have indicated an absence of CD34 in cultured MSCs[29,141,142]. CD45 is a HSC surface marker, suggested to play a key role in the proliferation and differentiation of haematopoietic cells[143]. The high purity of the MSCs isolated was confirmed as 98.38% of isolated cells had expressed CD90, while only 3.05% and 1.22% expressed the haematopoietic markers CD45 and CD34 respectively (Figure 3.1.2D). This suggests the isolated cells were overwhelming MSCs and the continuous passages had removed contaminating haematopoietic cells. One of the most important characteristic of true MSCs is the ability to differentiate into cells of multiple lineages, including osteogenic and adipogenic. Using the histological stains Alizarin red and Nile red, MSCs were confirmed to be able to differentiate into osteogenic and adipogenic cells respectively.

Since the isolated cells display plastic adherence, fibroblast-like morphology, mesenchymal markers cell surface expression and multilineage differentiation ability, the cells comply with the minimum criteria set by the International Society for Cellular Therapy (Section 1.2.1.2) for cells to be considered as true MSCs. This confirms the isolated cells used in the study are true MSCs.

4.1.2 Selection and culture of a bone derived cell line

As discussed in Section 1.2.2, primary cells are limited in their availability and their isolation method increases the time needed for culture, whereas immortalised cells lines are able to grow for an indefinite number of passages. Due to this, a bone derived cell line was also used for preliminary tests and to use as a comparison for MSCs to an osteoblast-like cell line (MG-63), which is considered to have express some mature osteoblastic features[84]. MG-63s were successfully cultured following the method described in Section 2.2 and used in downstream experiments, along with MSCs. Other bone derived cell lines were also considered for use, such as SaOs-2 cell line. As previously mentioned, SaOs-2 is similar to MG-63s as it is also derived from human osteosarcoma. A study by Pautke *et al*[84] compared the use of osteosarcoma cell lines to human osteoblasts and found the SaOs-2 cell line represented the most mature phenotype and displayed similar cytokine and growth factor expression to primary normal human osteoblast cells. However, ALP levels in SaOs-2 were much higher than primary cells and they do not mirror the whole range of osteoblast

phenotypic changes[86]. Another potential cell line which could have been used in the project is MC3T3-E1 which is a common osteoblast cell line used in studies. This cell line was originally derived from mouse calvaria cells, however a disadvantage to their use is that they are considered as pre-osteoblastic[87]. This would have prevented comparisons made between the primary rat MSCs and a more mature phenotype. Overall, due to time and availability of cells MG-63s were chosen as the most appropriate cell line to use. A potential future work would be to repeat the study with cells from SaOs-2 cell line as this is considered a more mature osteoblast phenotype.

4.2 3D scaffolds supported the growth of bone forming cells

The project then investigated whether 3D cell culture was able to support the growth of bone forming cells. As previously discussed in Section 1.3.2 and 1.3.3., there are various methods of 3D techniques which have been shown to support bone growth *in vitro*. Aggregate formation via spheroids is a common technique employed to study bone formation *in vitro*. However, there are issues with this technique such as the limited nutrient diffusion across the centre of the spheroids which results in a concentrated hypoxic region of the spheroids, which have been shown to upregulate hypoxia-associated genes[101]. As a result, this project chose to focus on the use of scaffolds as cells grown using scaffolds have a much more direct access to nutrients due to the porous environment. Another advantage to scaffolds is due to its hard surface which recapitulates the bone environments on which osteoblasts attach to. There are various natural and synthetic materials which have been used to make the scaffolds. Polystyrene was chosen as the most appropriate scaffold material for this project as it is the same material which is used in 2D culture, therefore allowing direct comparisons between 2D and 3D – any differences seen with 3D culture will most likely be due to the 3D environment and not the material in which the scaffold is made of. Alvetex® was chosen as the most appropriate 3D cell culture technology to use in the project due to its properties such as its polystyrene material and highly porous network resembling the *in vivo* bone matrix, which suggested it would be a suitable scaffold to use for an *in vitro* bone tissue model (Section 1.4.1). Preliminary results with culturing MG-63s on Alvetex® scaffold displayed homogenous growth throughout the scaffold for up to 28 days, suggesting 3D scaffolds are able to support the growth of bone forming cells.

4.2.1 Porosity of scaffolds affect the distribution and proliferation of bone forming cells

The pore sizes and porosity of 3D scaffolds has been reported to be significant in the regulation of the morphology and behaviour of cells of osteogenic lineage[144]. Porosity is vital for modelling bone formation as it allows cellular infiltration, proliferation and matrix deposition[145]. Alvetex® also contains high interconnectivity between the pores, which is a property of scaffolds which has been

shown to promote osteogenic tissue growth[105,146]. Since Alvetex® is available in three formats which have varying void sizes and interconnected distributions, bone forming cells were cultured using all three formats to determine the effect of porosity on the proliferation. Scaffold was chosen as the most appropriate format as it produced the greatest proliferation and homogenous growth for both MSCs and MG-63s. This is due to the larger pore size being closer to the mean pore size of 96 - 150μm which has been suggested to facilitate optimal attachment for bone tissue engineering[147]. The larger pore size also allows the cells to migrate in towards the scaffold[148], allowing for homogenous growth throughout the scaffold and not only on the top of the membrane like with Polaris. Since Strata has a smaller void size than Scaffold and cells were still able to proliferate and grow on the Strata membrane, this suggests cells on Scaffold were actively migrating in and not just falling through. Similarly, osteogenic-induced MSCs also showed better proliferation and coverage when cultured on Scaffold rather than Strata as well as secretion of ECM.

Alvetex® Scaffold was designed for the dissociation of mammalian cells within the scaffold, while Strata and Polaris allows for cell growth on the surface of the membrane in order to form layers either on the top or bottom of the membrane (ReproCELL Europe Ltd). Due to the hypothesis of the project being that a more similar microenvironment to the *in vivo* bone niche of the 3D cell culture technology will enhance bone formation, Scaffold was also chosen as cells are able to penetrate the membrane and dissociate in a way which is similar to the normal behaviour of bone forming cells in the bone marrow. Previous work with osteogenesis on Alvetex® also chose to use Scaffold[132,133], suggesting that it is the best format to use and allowing for cross-study comparisons.

4.3 Osteogenic differentiation in 2D vs 3D

4.3.1 3D cell culture supports the proliferation stage of osteogenesis

Proliferation is the first stage of osteogenesis, whereby bone forming cells replicate and undergo cell division to increase the number of cells in culture (Section 1.2.1.4). For the study, comparing the proliferation rates accurately between 2D and 3D was faced with difficulty. This is due to the large difference in seeding number between 2D and 3D (3×10^3 cells/cm^2, 2×10^4 cells/cm^2 and 5×10^5 cells) (MSC and MG-63, 2D and 3D respectively). This made it difficult to draw accurate comparisons between the proliferation rates from images alone as the 2D images were not representative - they could not capture the entire culture of the cells. In general, bone forming cells cultured on 2D was seen to proliferate during the earlier stages of culture and reduced during later stages (data not shown).

However, for 3D, proliferation of cells could be indicated by assessing the nuclei distribution from H&E images and nuclei counts. As osteogenesis is a gradual and progressive process, three time points were used to represent the early, middle and end stages of osteoblast differentiation (Day 7, 14 and 21). From the results shown in Figure 3.3.1 and Figure 3.3.1.1, osteogenic-induced MSCs and MG-63s were suggested to reach peak proliferation levels by day 7 and remained at similar levels up to day 21. As discussed in Section 1.2.1.4, proliferation by osteogenic cells are required to increase during the early stages of osteogenic differentiation but is needed to decline/remain at similar levels in order to proceed to the next stage[55]. These results suggest Alvetex® scaffold is able to support the proliferation stage of osteogenesis in both 2D and 3D; however, more information and analysis is required to compare the proliferation rates between 2D and 3D. A more quantitative approach could have been used to measure the proliferation rates between 2D and 3D, to further improve the accuracy of results. One such method which could be used is the PicoGreen assay, which is a fluorescent probe which binds to dsDNA for use in DNA quantitation[149]. This quantitation assay is easy to use as you add the dye to the sample, incubate for 5 minutes and read using a microplate reader, therefore it is viable option for quantifying the proliferation rates in 2D and 3D as the greater the proliferation, the greater the reading will be from the assay.

4.3.2. ECM maturation and deposition by bone forming cells in 2D vs 3D

Following proliferation, the next stage of osteogenesis by bone forming cells is the maturation and deposition of bone ECM. To assess the levels of ECM deposition by bone forming cells, numerous osteoblast markers which are important in this stage can be detected and identified. The 4 markers used in this project are: fibronectin, collagen I, collagen III and alkaline phosphatase, which have been commonly used in studies to assess osteoblast differentiation[108,119]. As previously discussed in Section 1.2.1.4, there are many markers which are commonly used to assess levels of maturation of osteogenic differentiation *in vitro*. Fibronectin is an important glycoprotein found in the bone ECM which is shown to have a role in osteoblast recruitment[61]. Collagen is the major structural component of the organic bone matrix, therefore a highly important marker of osteoblast maturation and bone matrix formation. Collagen I and collagen III were used as a markers of osteoblast maturation as it is vital for matrix mineralisation and those are the types of collagen which are the most abundant in natural bone [150]. Alkaline phosphatase is one of the most commonly used markers of osteoblast maturation as it needed for the production of hydroxyapatite and consequently the mineralisation of bone matrix (Section 1.2.1.3). ALP was used as a marker in this project as it has been shown to have a critical role in bone formation[151], thereby ALP expression by cells is highly indicative of osteoblast maturation and bone nodule formation.

4.3.2.1 Fibronectin secretion can be detected in 2D and 3D cultures of bone forming cells

As mentioned previously, fibronectin is a key marker of osteogenesis which is thought to be involved during the early stages of osteogenesis. In 2D cultures of osteogenic-induced MSCs, fibronectin secretion was localised to areas around the mesenchymal condensations and not inside (Figure 3.3.2.1), as seen with the positive green staining. This is in agreement with the roles of fibronectin that have been suggested by the literature, as several papers have reported that fibronectin is deposited in areas of recruitment and commitment of osteoblast precursors. This is due to their function in regulating the adhesion, migration and maturation of osteoblasts[61]. In 2D, with time, the condensations of cells increase and fibronectin was only detected around the borders of the bone nodules. This allows fibronectin to communicate to and recruit precursors outside of the nodules to migrate in and expand the condensations.

In 3D, fibronectin secretion was seen to decrease with time which complies with findings in the literature where the expression of fibronectin mRNA reduced with time[152]. In this paper, fibronectin was reported to increase during proliferation and early differentiation, and decline as cells mature. This indicates that after day 7 in 3D, osteogenic-induced MSCs are differentiating into more mature osteoblast derivatives as their fibronectin secretion sharply reduces at day 14 and even more so at day 21 (Figure 3.3.2.2). The finding that fibronectin deposition decreases with maturing osteoblast differentiation is supported by the lack of detection of fibronectin secretion by MG-63 cells in both 2D and 3D. MG-63 are considered to be more mature osteoblast-like cells, therefore it is expected that fibronectin expression to be limited as they are no longer at the early stages of osteogenesis. Comparing fibronectin secretion between 2D and 3D using immunofluorescence alone is not accurate as the images do not provide a representation of all the cells in each culture. In order to compare 2D and 3D fibronectin secretion, quantitative data is needed such as measuring mRNA expression. Since there are some indications of little positive staining in 2D culture of MG-63 and none in 3D cultures, this suggests 3D culture of MG-63 could allow cells to differentiate further into more mature osteoblasts. However, more data analysis to fully support this.

4.3.2.2 Collagen I and III secretion can be detected in 2D and 3D, with increased Collagen I in 3D

Collagen I and III are important proteins in bone ECM, with 90% of the organic bone matrix being made up of collagen I[5]. Additionally, cells must be in connection with a collagen I-containing matrix in order to differentiate[45,59] – osteogenic-induced MSCs and MG-63s were seen to secrete collagen I and III in both 2D and 3D. This further indicates that cells are differentiating towards more mature osteoblast derivatives in both 2D and 3D cell culture. For osteogenic-induced MSCs in 2D, collagen I and III secretion could be detected in the condensations of osteogenic-induced cells which are

indicative of bone nodule formation[52]. In 3D, an increase in collagen I and III secretion over time could be seen in osteogenic-induced MSCs which suggests the 3D scaffold is able to support ECM deposition and matrix maturation as collagen I and III could accumulate over time. To compare collagen I expression between 2D and 3D, a western blot analysis was carried out for osteogenic-induced MSCs (Figure 3.3.3.4). The results suggest in 3D, osteogenic-induced MSCs produce more collagen I as the bands are more prominent and included numerous epitope bands compared to 2D. This indicates that culturing osteogenic-induced MSCs on a 3D scaffold is able to produce more collagen I and is able to differentiate into more mature osteoblast derivatives, a finding which has been reported in literature using different types of 3D scaffolds[108,153]. For MG-63s on 3D, no significant differences could be seen for collagen I and III points between day 7, 14 and 21. This suggests that as MG-63 cells have already differentiated by the time they are seeded on the Scaffold, the cells secrete a consistent level of collagen I and III across the increasing timepoints.

4.3.2.3 Alkaline phosphatase activity is indicated to be greater in 3D cultures

ALP is a very important enzyme in the bone matrix which is widely used as a marker of osteoblast differentiation. From the results presented in Figure 3.3.5.1, osteogenic-induced MSCs produced a higher expression of ALP in 3D compared to 2D at day 7 and 14, while decreasing at day 21. Although the results were not statistically significant, the trend presented is still indicative of osteogenesis by the osteogenic-induced MSCs. According to the sequence of osteoblast marker expression which was first defined by Lian and Stein[91], ALP activity reaches a maximum peak at 14 days during osteoblast differentiation and subsequently decreases during matrix mineralisation at day 21, a finding which has also been widely reported in literature (Section 1.2.1.4). The decrease at day 21 is associated with the acquisition of a more mature osteoblastic phenotype. This trend was seen in osteogenic-induced MSCs in 3D, whereas MSCs in 2D continue to increase ALP expression past day 14. This indicates that the osteogenic-induced MSCs cultured on Scaffold has reached maximum matrix maturation by day 14 and undergoes the matrix mineralisation stage by day 21. In contrast, the increasing trend of ALP activity seen in 2D suggests osteogenic-induced MSCs may not have matured as greatly as 3D at day 21 and matrix maturation is reduced. The ALP expression is also greater for 3D than 2D at day 14, suggesting 3D does enhance bone formation. However since this is not statistically significant, more repeats will need to be conducted to reduce the error bars and increase significance.

ALP activity has been reported to increase in osteogenic-induced MSCs cultured on Alvetex® Scaffold. Ruminski *et al* cultured human adipose-derived mesenchymal stem cells (ADSCs) using the routine 2D environment and 3D culture (Alvetex® Scaffold) and induced the cells with osteogenic

differentiation medium. They reported an elevated ALP activity at their longest time point (day 7) for cells cultured on Scaffold compared to 2D[154], which is similar to the results presented in this study. Similarly, an increase ALP activity and mineral deposition was seen in ADSCs cultured on 3D scaffolds (made of reduced graphene oxide/polydimethylsiloxane)[155].

Previous work carried out at Durham University involved culturing osteogenic-induced rat MSCs on Alvetex® Scaffold which reported a statistically significant enhancement of ALP activity on cells cultured on 3D compared to 2D at day 5, 7, 14 and 21. Since this study used the same method of cell culture, osteogenic differentiation and same type of cells, this suggests the lack of statistically significant results in Figure 3.3.5.1 could be due to human error and requires more than 3 repeats to improve the size of the error bars. This study showed that MSCs cultured on Scaffold display an enhanced osteoblastic functional behaviour[156]. Likewise, culturing MG-63s on Scaffold resulted in significantly greater levels of ALP compared to 2D plastic surfaces, further indicating Alvetex® Scaffold is able to enhance osteoblast maturation of bone forming cells[133].

4.3.3 Matrix mineralisation can be seen in both 2D and 3D cultures

Matrix mineralisation is considered to be the last stage of osteogenesis, whereby osteoblasts deposit minerals such as calcium and phosphate into the organic matrix. As discussed previously in Section 1.2.1.4, the commonly used methods to assess matrix mineralisation in *in vitro* cultures is through histological stains such as Von Kossa and Alizarin Red. Alizarin Red was used to stain both 2D and 3D cultures of bone forming cells at day 21, which binds to calcium deposits and stains an intense red colour[66]. In 2D of osteogenic-induced MSCs, bone nodules can be readily seen with some containing an intense red colour, while others are express lighter shades of red. In comparison, osteogenic induced MSCS and MG-63s on 3D produce a much darker red colour, which is indicative of greater calcium deposition by the cells (Figure 3.3.6.1A-C). As MG-63s are considered to be osteoblast-like, this indicates that by day 21, osteogenic-induced MSCs have differentiated into mature osteoblasts in 3D similar to MG-63. However, these findings are only preliminary and requires other data to support this such as through quantifying the amount of Alizarin Red staining.

Previous work at Durham university demonstrated positive Von Kossa staining on wholemount 3D cultures of rat osteogenic-induced MSCs[156]. Figure 3.3.6.1D displays clear condensation of cells cultured on Alvetex® Scaffold, which was stained an intense black colour which is indicative of calcium production. This further supports the finding that MSCs cultured in 3D are able to complete all stages of osteogenesis, with calcium deposition being a marker of matrix mineralisation which is the final stage. This preliminary result suggests culturing osteogenic-induced MSCs in 3D could

produce greater calcium deposition. However, in order to compare levels of matrix mineralisation between 2D and 3D, other methods such as quantifying histological stains is required to make accurate comparisons. One common method that is used to quantify histological stains is through eluting the stain and reading the amount present using a spectrophotometer[157]. This results in a standard curve and the amount of calcium deposition can be expressed as equivalent to the amount of calcium bound to Alizarin Red/Von Kossa.

4.3.4 Spontaneous osteogenic differentiation by rat MSCs *in vitro*

Another key finding of the study which has been supported throughout is the spontaneous osteogenic differentiation by rat MSCs. In 2D immunofluorescence images of fibronectin, collagen I and collagen III, condensations of MSCs cultured using media without osteogenic morphogens can be seen by day 21 (Figures 3.3.2.1F, 3.3.3.1I, 3.3.4.1I), which is indicative of bone nodule formation. Similar findings have been reported in literature as a behaviour of rat MSCs. Karaoz *et al* described the expression of bone morphogenic proteins (BMP2 and BMP4) by rat bone marrow MSCs without stimulation by osteogenic morphogens which are considered to be key osteogenesis markers[158]. Huang *et al* demonstrated spontaneous cellular aggregation and calcification in rat bone marrow MSCs cultured using media without osteogenic morphogens by day 21 by phase contrast microscopy and positive Alizarin Red staining[159]. This behaviour was not observed in goat or human bone marrow MSCs cultured using the same system[160]. These results support the finding that rat bone marrow MSCs possess a tendency of spontaneous calcification *in vitro* and differentiate into an osteogenic lineage spontaneously.

4.4 Conclusions

This study investigated the use of a 3D scaffold to culture bone forming cells in order to develop an *in vitro* bone tissue model, with an aim to model the stages of osteoblast differentiation and bone tissue formation. The findings of the study demonstrated successful isolation of primary rat MSCs and culture of a human osteosarcoma cell line (MG-63) to provide the bone forming cells required for the study. The 3D scaffold was able to support the proliferation of both primary rat MSCs and MG-63 cells, suggesting it would be an appropriate material to use to develop a bone tissue model. Successful osteogenic differentiation in both 2D and 3D was demonstrated though the use of different methods such as histological stains and immunofluorescence. Porosity of the Scaffold was seen to affect the proliferation and distribution of bone forming cells. Overall, using the results of the study and previous work at Durham University, comparisons of osteogenic differentiation in 2D and 3D by bone forming cells showed indications of increased collagen I and alkaline phosphatase secretion and greater matrix mineralisation in 3D. However, other techniques such as qualitative methods should be used to further improve the accuracy of comparisons made between 2D and 3D.

Collectively, the use of Alvetex® Scaffold to culture bone forming cells reported indications of enhanced bone formation compared to 2D methods. This highlights the relevance of using 3D cell culture systems to model bone tissue development *in vitro*.

4.5 Future Directions

The data presented in this study provides a foundation for studying bone tissue development *in vitro* using a 3D cell culture system. Due to the time constraints of the project, there are additional investigations that can be conducted in order to support the findings and further enhance bone formation in 3D.

As mentioned previously, further comparisons are needed to measure the differences in levels of osteogenesis between 2D and 3D. Although, histological stains, immunofluorescence, Western blot and ALP assays were techniques used to measure osteogenesis in 2D and 3D, the data provided is largely qualitative which makes it difficult to see small differences between 2D and 3D and results could be interpreted differently. One common quantitative method used is using specific bone marker enzyme-linked Immunosorbent Assay (ELISA) systems. Sandwich ELISA Kits are highly specific for secreted markers and widely used as quantitative assessments of bone formation. One such ELISA kit which is commonly used is for osteocalcin[161], which would be another useful marker to use to compare osteogenesis between 2D and 3D. Another quantitative method which could be used is real-time quantitative polymerase chain reaction (RT-qPCR)[162] which measures the mRNA levels of bone markers to quantify the difference in bone marker expression between 2D and 3D.

Since the majority of bone markers used in this study are largely involved in the early stages of osteogenesis, a beneficial further investigation for the study is to use markers associated with later stages. One such marker is osteocalcin, which is considered to be a bone-specific marker indicative of mature osteoblast differentiation as it is involved in matrix mineralisation[163]. Other bone markers which could be measured in 2D and 3D osteogenesis are: runx2[78], BMP-2[164], BSP[8] and osteopointin[165] which are all commonly used as osteoblast differentiation markers. If higher levels of these markers are found in 3D, this will further support the finding that 3D cell culture is able to enhance bone nodule formation.

There have been suggestions of interactions between fibronectin and collagen as fibronectin binding to collagen I and III has been reported *in vitro*. Fibronectin has been shown to be required for collagen organisation and deposition[166]. Another potential further work for the project is to investigate the interactions between collagen and fibronectin in osteoblast differentiation by rat MSCs and MG-63s and test whether these interactions are enhanced in 3D.

Several conditions have been shown to enhance bone formation *in vitro* which could be further investigated in this study. One example of this is to induce hypoxic conditions during osteogenic

differentiation of MSCs, which has been shown to enhance proliferation and promote osteogenic differentiation in human mesenchymal stromal cells. Osteoblasts have been shown to operate under low oxygen (hypoxic) microenvironments *in vivo* and express hypoxia-inducible factors (HIF1) and HIF2, whereby HIF1 is thought to be a positive regulator for bone formation[167]. By recapitulating these hypoxic conditions in the *in vitro* bone tissue model, bone formation may be enhanced even further in 3D as the osteoblast microenvironment will be more of an accurate representation of *in vivo* conditions.

Another potential further investigation which could be carried out to enhance bone formation further in 3D is through coating the Alvetex® Scaffold with osteoinductive materials such as collagen and hydroxyapatite. Collagen-based scaffolds have been shown to increase bone formation and are widely used in bone tissue engineering. Culturing rat MSCs on a collagen coated porous scaffold resulted in enhanced ALP activity and cell number, as well as upregulation in gene expression of osteocalcin and collagen I thereby increasing osteoblast differentiation[168]. A study by Lee *et al* investigated the effects on osteoblast differentiation by MG-63 by the addition of hydroxyapatites onto porous scaffolds, including Alvetex® Scaffold. The study reported enhancement and early onset of mineralisation and osteoblastic cell proliferation when hydroxyapatite was incorporated into the Scaffold[169]. This could be a potential further work for the project.

5.0 References

1. Fuchs, R. K., Thompson, W. R. & Warden, S. J. Bone biology. in *Bone Repair Biomaterials* 15–52 (Elsevier Ltd, 2019). doi:10.1016/B978-0-08-102451-5.00002-0
2. Datta, H. K., Ng, W. F., Walker, J. A., Tuck, S. P. & Varanasi, S. S. The cell biology of bone metabolism. *Journal of Clinical Pathology* **61**, 577–587 (2008).
3. Ascenzi, M.-G. & Roe, A. K. The osteon: the micromechanical unit of compact bone. *Frontiers in Bioscience* **17**, 1551–1581 (2012).
4. Kim, T. R. *et al.* Evaluation of structural and mechanical properties of porous artificial bone scaffolds fabricated via advanced TBA-based freeze-gel casting technique. *Applied Sciences (Switzerland)* **9**, 1–17 (2019).
5. Tzaphlidou, M. Bone architecture: collagen structure and calcium/phosphorus maps. *Journal of Biological Physics* **34**, 39–49 (2008).
6. Shoulders, M. & Raines, R. Collagen structure and stability. *Annual Reviews Biochemistry* **78**, 929–958 (2009).
7. Craig, L. E., Dittmer, K. E. & Thompson, K. G. Bones and joints. *Jubb, Kennedy & Palmer's Pathology of Domestic Animals: Volume 1* **1**, 16-163.e1 (2016).
8. Gordon, J. A. R. *et al.* Bone sialoprotein expression enhances osteoblast differentiation and matrix mineralization in vitro. *Bone* **41**, 462–473 (2007).
9. Zoch, M., Thomas, C. & Riddle, R. New Insights into the biology of osteocalcin. *Bone* **82**, 42–49 (2016).
10. Ducy, P. *et al.* Increased bone formation in osteocalcin-deficient mice. *Nature* **382**, 448–452 (1996).
11. Feng, X. Chemical and biochemical basis of cell-bone matrix interaction in health and disease. *Current Chemical Biology* **3**, 975–990 (2010).
12. Mackie, E. J. Osteoblasts: Novel roles in orchestration of skeletal architecture. *International Journal of Biochemistry and Cell Biology* **35**, 1301–1305 (2003).
13. Florencio-Silva, R., Sasso, G. R. D. S., Sasso-Cerri, E., Simões, M. J. & Cerri, P. S. Biology of bone tissue: structure, function, and factors that influence bone cells. *BioMed Research International* **2015**, (2015).
14. Schaffler, M. & Kennedy, O. Osteocyte signaling in bone. *Current Osteoporosis Reports* **10**, 118–125 (2012).
15. Feng, J. Q. *et al.* Loss of DMP1 causes rickets and osteomalacia and identifies a role for osteocytes in mineral metabolism. *Nature Genetics* **38**, 1310–1315 (2006).
16. Liu, S. & Quarles, L. D. How fibroblast growth factor 23 works. *Journal of the American Society of Nephrology* **18**, 1637–1647 (2007).
17. Goldring, S. R. The osteocyte: key player in regulating bone turnover. *RMD Open* (2015). doi:10.1136/rmdopen-2015-000049
18. Hadjidakis, D. & Ioannis, A. Bone remodeling. *Annals of the New York Academy of Sciences* **396**, 385–396 (2006).
19. Boyce, B. F. & Xing, L. Functions of RANKL/RANK/OPG in bone modeling and remodeling. *Archives of Biochemistry and Biophysics* **473**, 139–146 (2008).
20. Yoshida, H. *et al.* The murine mutation osteopetrosis is in the coding region of the macrophage colony stimulating factor gene. *Nature* **345**, 422–444 (1990).
21. Davies, J. *et al.* The osteoclast functional antigen, implicated in the regulation of bone resorption, is biochemically related to the vitronectin receptor. *Journal of Cell Biology* **109**, 1817–1826 (1989).
22. Gil-Henn, H. *et al.* Defective microtubule-dependent podosome organization in osteoclasts leads to increased bone density in Pyk2−/− mice. *Journal of Cell Biology* **178**, 1053–1064 (2007).
23. Czupalla, C. *et al.* Proteomic analysis of lysosomal acid hydrolases secreted by osteoclasts: Implications for lytic enzyme transport and bone metabolism. *Molecular and Cellular Proteomics* **5**, 134–143 (2006).

24. Blair, H., Teitelbaum, S., Ghiselli, R. & Gluck, S. Osteoclastic bone resorption by a polarized vacuolar proton pump. *Science* **245**, 855–857 (1989).
25. Weilbaecher, K. N., Guise, T. A. & McCauley, L. K. Cancer to bone: a fatal attraction. *Nature Reviews Cancer* **11**, 411–425 (2011).
26. Mishra, R. *et al.* Study of in vitro and in vivo bone formation in composite cryogels and the influence of electrical stimulation. *International Journal of Biological Sciences* **11**, 1325–1336 (2015).
27. Wei, X. *et al.* Mesenchymal stem cells: A new trend for cell therapy. *Acta Pharmacologica Sinica* **34**, 747–754 (2013).
28. Friedenstein, A. J., Petrakova, K. V, Kurolesova, A. I. & Frolova, G. P. Heterotopic of bone marrow. Analysis of precursor cells for osteogenic and hematopoietic tissues. *Transplantation* (1968). doi:10.1097/00007890-196803000-00009
29. Pittenger, M. F. *et al.* Multilineage potential of adult human mesenchymal stem cells. *Science* (1999). doi:10.1126/science.284.5411.143
30. Caplan, A. I. Mesenchymal stem cells. *Journal of Orthopaedic Research* (1991). doi:10.1002/jor.1100090504
31. Li, A. I., Hokugo, A., Jarrahy, R. & Zuk, P. A. Human adipose tissue as a source of multipotent stem cells. in *Stem Cells in Aesthetic Procedures: Art, Science, and Clinical Techniques* **9783642452079**, 67–83 (Springer-Verlag Berlin Heidelberg, 2014).
32. NJ, Z. *et al.* Mesenchymal precursor cells in the blood of normal individuals. *Arthritis Research* **2**, 477–88 (2000).
33. Chen, W. C. W. *et al.* Human myocardial pericytes: multipotent mesodermal precursors exhibiting cardiac specificity. *Stem Cells* **33**, 557–573 (2015).
34. Stefanska, A. *et al.* Human kidney pericytes produce renin. *Kidney International* **90**, 1251–1261 (2016).
35. Salem, H. K. & Thiemermann, C. Mesenchymal stromal cells: current understanding and clinical status. *Stem Cells* (2010). doi:10.1002/stem.269
36. Dominici, M. *et al.* Minimal criteria for defining multipotent mesenchymal stromal cells. The International Society for Cellular Therapy position statement. *Cytotherapy* (2006). doi:10.1080/14653240600855905
37. Corselli, M., Chen, C. W., Crisan, M., Lazzari, L. & Péault, B. Perivascular ancestors of adult multipotent stem cells. *Arteriosclerosis, Thrombosis, and Vascular Biology* (2010). doi:10.1161/ATVBAHA.109.191643
38. Nombela-Arrieta, C., Ritz, J. & Silberstein, L. E. The elusive nature and function of mesenchymal stem cells. *Nature Reviews Molecular Cell Biology* 126–131 (2011). doi:10.1038/nrm3049
39. Marion, N. W. & Mao, J. J. Mesenchymal stem cells and tissue engineering MSCs: definition and therapeutic Promise. **6879**, (2014).
40. Yuasa, M. *et al.* Dexamethasone enhances osteogenic differentiation of bone marrow-and muscle-derived stromal cells and augments ectopic bone formation induced by bone morphogenetic protein-2. *PLoS ONE* (2015). doi:10.1371/journal.pone.0116462
41. Langenbach, F. & Handschel, J. Effects of dexamethasone, ascorbic acid and β-glycerophosphate on the osteogenic differentiation of stem cells in vitro. *Stem Cell Research and Therapy* (2013). doi:10.1186/scrt328
42. Hong, J. H. *et al.* TAZ, a transcriptional modulator of mesenchymal stem cell differentiation. *Science* (2005). doi:10.1126/science.1110955
43. Fujisawa, K. *et al.* Evaluation of the effects of ascorbic acid on metabolism of human mesenchymal stem cells. *Stem Cell Research and Therapy* **9**, (2018).
44. Franceschi, R. T. & Iyer, B. S. Relationship between collagen synthesis and expression of the osteoblast phenotype in MC3T3-E1 cells. *Journal of Bone and Mineral Research* (1992). doi:10.1002/jbmr.5650070216
45. Vater, C., Kasten, P. & Stiehler, M. Culture media for the differentiation of mesenchymal stromal cells. *Acta Biomaterialia* (2011). doi:10.1016/j.actbio.2010.07.037

46. Chang, Y. L., Stanford, C. M. & Keller, J. C. Calcium and phosphate supplementation promotes bone cell mineralization: implications for hydroxyapatite (HA)-enhanced bone formation. *Journal of Biomedical Materials Research* **52**, 270–278 (2000).
47. Fatherazi, S. *et al.* Phosphate regulates osteopontin gene transcription. *Journal of Dental Research* (2009). doi:10.1177/0022034508328072
48. Abe, E. *et al.* Essential requirement of BMPs-2/4 for both osteoblast and osteoclast formation in murine bone marrow cultures from adult mice: antagonism by noggin. *Journal of Bone and Mineral Research* **15**, 663–673 (2010).
49. Centrella, M., McCarthy, T. L. & Canalis, E. Transforming growth factor beta is a bifunctional regulator of replication and collagen synthesis in osteoblast-enriched cell cultures from fetal rat bone. *Journal of Biological Chemistry* (1987).
50. Wu, J. *et al.* TGF-β1 induces senescence of bone marrow mesenchymal stem cells via increase of mitochondrial ROS production. *BMC Developmental Biology* (2014). doi:10.1186/1471-213X-14-21
51. Song, I. H., Caplan, A. I. & Dennis, J. E. In vitro dexamethasone pretreatment enhances bone formation of human mesenchymal stem cells in vivo. *Journal of Orthopaedic Research* (2009). doi:10.1002/jor.20838
52. Alami, S., Gangloff, S., Laurent-Maquin, D., Wang, Y. & Kerdjoudj, H. Concise review: in vitro formation of bone-like nodules sheds light on the application of stem cells for bone regeneration. *Stem Cells Translational Medicine* **5**, 1587–1593 (2016).
53. Stein, G. S. & Lian, J. B. Molecular Mechanisms Mediating Developmental and Hormone-Regulated Expression of Genes in Osteoblasts. *Cellular and Molecular Biology of Bone* (ACADEMIC PRESS, INC., 1993). doi:10.1016/b978-0-08-092500-4.50006-1
54. Aubin, J. E. & Heersche, J. N. M. Osteoprogenitor cell differentiation to mature bone-forming osteoblasts. *Drug Development Research* **49**, 206–215 (2000).
55. Melnik, S. *et al.* Impact of c-MYC expression on proliferation, differentiation, and risk of neoplastic transformation of human mesenchymal stromal cells. *Stem Cell Research and Therapy* **10**, (2019).
56. Shafiee, A. *et al.* A comparison between osteogenic differentiation of human unrestricted somatic stem cells and mesenchymal stem cells from bone marrow and adipose tissue. *Biotechnology Letters* (2011). doi:10.1007/s10529-011-0541-8
57. Loebel, C. *et al.* In vitro osteogenic potential of human mesenchymal stem cells is predicted by Runx2/Sox9 Ratio. *Tissue Engineering, Part A* **21**, 115–123 (2014).
58. Chen, J. *et al.* Angiogenic and osteogenic synergy of human mesenchymal stem cells and human umbilical vein endothelial cells cocultured on a nanomatrix. *Scientific Reports* (2018). doi:10.1038/s41598-018-34033-2
59. Hanna, H., Mir, L. M. & Andre, F. M. In vitro osteoblastic differentiation of mesenchymal stem cells generates cell layers with distinct properties. *Stem Cell Research and Therapy* **9**, 1–11 (2018).
60. Winnard, R. G., Gerstenfeld, L. C., Toma, C. D. & Franceschi, R. T. Fibronectin gene expression, synthesis, and accumulation during in vitro differentiation of chicken osteoblasts. *Journal of Bone and Mineral Research* (1995). doi:10.1002/jbmr.5650101217
61. Yang, R. Sen, Tang, C. H., Ling, Q. D., Liu, S. H. & Fu, W. M. Regulation of fibronectin fibrillogenesis by protein kinases in cultured rat osteoblasts. *Molecular Pharmacology* **61**, 1163–1173 (2002).
62. Tang, C. H., Yang, R. Sen, Liou, H. C. & Fu, W. M. Enhancement of fibronectin synthesis and fibrillogenesis by BMP-4 in cultured rat osteoblast. *Journal of Bone and Mineral Research* (2003). doi:10.1359/jbmr.2003.18.3.502
63. Assis-Ribas, T., Forni, M. F., Winnischofer, S. M. B., Sogayar, M. C. & Trombetta-Lima, M. Extracellular matrix dynamics during mesenchymal stem cells differentiation. *Developmental Biology* (2018). doi:10.1016/j.ydbio.2018.03.002
64. Puchtler, H. & Meloan, S. N. Demonstration of phosphates in calcium deposits: A modification of von Kossa's reaction. *Histochemistry* **56**, 177–185 (1978).

65. Rungby, J., Kassem, M., Eriksen, E. F. & Danscher, G. The von Kossa reaction for calcium deposits: silver lactate staining increases sensitivity and reduces background. *The Histochemical Journal* **25**, 446–451 (1993).
66. Puchtler, H., Meloan, S. N. & Terry, M. S. On the history and mechanism of alizarin and alizarin red S stains for calcium. *The journal of histochemistry and cytochemistry* **17**, 110–124 (1969).
67. Mayer, U., Aumailley, M., Mann, K., Timpl, R. & Engel, J. Calcium-dependent binding of basement membrane protein BM-40 (osteonectin, SPARC) to basement membrane collagen type IV. *European Journal of Biochemistry* **198**, 141–150 (1991).
68. Purpura, K. A., Zandstra, P. W. & Aubin, J. E. Fluorescence activated cell sorting reveals heterogeneous and cell non-autonomous osteoprogenitor differentiation in fetal rat calvaria cell populations. *Journal of Cellular Biochemistry* (2003). doi:10.1002/jcb.10596
69. Clarke, B. Normal bone anatomy and physiology. *Clinical journal of the American Society of Nephrology : CJASN* (2008). doi:10.2215/CJN.04151206
70. Akintoye, S. O. *et al.* Skeletal site-specific characterization of orofacial and iliac crest human bone marrow stromal cells in same individuals. *Bone* **38**, 756–768 (2006).
71. Scheinpflug, J. *et al.* Journey into bone models: A review. *Genes* **9**, 247 (2018).
72. Yamamoto, N., Furuya, K. & Hanada, K. Progressive development of the osteoblast phenotype during differentiation of osteoprogenitor cells derived from fetal rat calvaria: Model for in vitro bone formation. *Biological and Pharmaceutical Bulletin* (2002). doi:10.1248/bpb.25.509
73. Jonason, J. H. & O'Keefe, R. J. Isolation and culture of neonatal mouse calvarial osteoblasts. *Methods in Molecular Biology* (2014). doi:10.1007/978-1-62703-989-5_22
74. Stringa, E., Filanti, C., Giunciuglio, D., Albini, A. & Manduca, P. Osteoblastic cells from rat long bone. I. Characterization of their differentiation in culture. *Bone* (1995). doi:10.1016/8756-3282(95)00100-R
75. Soejima, K., Klein-Nulend, J., Semeins, C. M. & Burger, E. H. Different responsiveness of cells from adult and neonatal mouse bone to mechanical and biochemical challenge. *Journal of Cellular Physiology* **186**, 366–70 (2001).
76. Rodan, S. B. *et al.* Characterization of a Human Osteosarcoma Cell Line (Saos-2) with Osteoblastic Properties. *Cancer Research* **47**, 4961–4966 (1987).
77. Saldaña, L., Bensiamar, F., Boré, A. & Vilaboa, N. In search of representative models of human bone-forming cells for cytocompatibility studies. *Acta Biomaterialia* (2011). doi:10.1016/j.actbio.2011.07.019
78. Prideaux, M. *et al.* SaOS2 osteosarcoma cells as an in vitro model for studying the transition of human osteoblasts to osteocytes. *Calcified Tissue International* **95**, 183–193 (2014).
79. Billiau, A. *et al.* Human interferon: mass production in a newly established cell line, MG 63. *Antimicrobial Agents and Chemotherapy* (1977). doi:10.1128/AAC.12.1.11
80. Friedman, R. M. Clinical uses of interferons. *British Journal of Clinical Pharmacology* (2008). doi:10.1111/j.1365-2125.2007.03055.x
81. Heremans, H., Billiau, A., Cassiman, J. J., Mulier, J. C. & De Somer, P. In vitro cultivation of human tumor tissues II. Morphological and virological characterization of three cell lines. *Oncology (Switzerland)* (1978). doi:10.1159/000225298
82. Clover, J. & Gowen, M. Are MG-63 and HOS TE85 human osteosarcoma cell lines representative models of the osteoblastic phenotype? *Bone* **15**, 585–91 (1994).
83. Lajeunesse, D., Frondoza, C., Schoffield, B. & Sacktor, B. Osteocalcin secretion by the human osteosarcoma cell line MG-63. *Journal of Bone and Mineral Research* **5**, 915–22 (1990).
84. Pautke, C. *et al.* Characterization of osteosarcoma cell lines MG-63, Saos-2 and U-2 OS in comparison to human osteoblasts. *Anticancer Research* **24**, 3743–3748 (2004).
85. Muff, R. *et al.* Genomic instability of osteosarcoma cell lines in culture: Impact on the prediction of metastasis relevant genes. *PLoS ONE* **10**, (2015).
86. Czekanska, E. M., Stoddart, M. J., Richards, R. G. & Hayes, J. S. In search of an osteoblast cell model for in vitro research. *European Cells and Materials* **24**, 1–17 (2012).

87. Czekanska, E. M., Stoddart, M. J., Ralphs, J. R., Richards, R. G. & Hayes, J. S. A phenotypic comparison of osteoblast cell lines versus human primary osteoblasts for biomaterials testing. *Journal of Biomedical Materials Research - Part A* **102**, 2636–43 (2014).
88. Bard, D. R., Dickens, M. J., Smith, A. U. & Zarek, J. M. Isolation of living cells from mature mammalian bone. *Nature* **236**, 314–5 (1972).
89. Duval, K. *et al.* Modeling physiological events in 2D vs. 3D cell culture. *Physiology* **32**, 266–277 (2017).
90. McKee, C. & Chaudhry, G. R. Advances and challenges in stem cell culture. *Colloids and Surfaces B: Biointerfaces* (2017). doi:10.1016/j.colsurfb.2017.07.051
91. Lian, J. B. & Stein, G. S. Concepts of osteoblast growth and differentiation: Basis for modulation of bone cell development and tissue formation. *Critical Reviews in Oral Biology and Medicine* **3**, 269–305 (1992).
92. Di Silvio, L. & Gurav, N. Osteoblasts. in *Human Cell Culture* (eds. Kollar, M. R., Palsson, B. O. & Masters, J.) 221–241 (Kluwer Academic Publishers, 2001).
93. Jähn, K., Richards, R. G., Archer, C. W. & Stoddart, M. J. Pellet culture model for human primary osteoblasts. *European Cells and Materials* **20**, 149–161 (2010).
94. Bara, J. J., Richards, R. G., Alini, M. & Stoddart, M. J. Concise review: Bone marrow-derived mesenchymal stem cells change phenotype following in vitro culture: Implications for basic research and the clinic. *Stem Cells* **32**, (2014).
95. Cesarz, Z. & Tamama, K. Spheroid culture of mesenchymal stem cells. *Stem Cells International* (2016). doi:10.1155/2016/9176357
96. Foty, R. A simple hanging drop cell culture protocol for generation of 3D spheroids. *Journal of Visualized Experiments* **6**, 2720 (2011).
97. Metzger, W. *et al.* Expansion and differentiation of human primary osteoblasts in two- and three-dimensional culture. *Biotechnic and Histochemistry* **88**, 86–102 (2012).
98. Kale, S. *et al.* Three-dimensional cellular development is essential for ex vivo formation of human bone. *Nature Biotechnology* (2000). doi:10.1038/79439
99. Barisam, M., Saidi, M. S., Kashaninejad, N. & Nguyen, N. T. Prediction of necrotic core and hypoxic zone of multicellular spheroids in a microbioreactor with a U-shaped barrier. *Micromachines* **9**, 94 (2018).
100. Curcio, E. *et al.* Mass transfer and metabolic reactions in hepatocyte spheroids cultured in rotating wall gas-permeable membrane system. *Biomaterials* **28**, 5487–97 (2007).
101. Potapova, I. A. *et al.* Mesenchymal stem cells support migration, extracellular matrix invasion, proliferation, and survival of endothelial cells in vitro. *Stem Cells* **25**, 1761–8 (2007).
102. Tsai, A. C., Liu, Y., Yuan, X. & Ma, T. Compaction, fusion, and functional activation of three-dimensional human mesenchymal stem cell aggregate. *Tissue Engineering - Part A* **21**, 1705–19 (2015).
103. Chen, C.-T., Shih, Y.-R. V., Kuo, T. K., Lee, O. K. & Wei, Y.-H. Coordinated changes of mitochondrial biogenesis and antioxidant enzymes during osteogenic differentiation of human mesenchymal stem cells. *Stem Cells* **26**, 960–8 (2008).
104. Almeida, M., Han, L., Martin-Millan, M., O'Brien, C. A. & Manolagas, S. C. Oxidative stress antagonizes Wnt signaling in osteoblast precursors by diverting β-catenin from T cell factor- to forkhead box O-mediated transcription. *Journal of Biological Chemistry* **282**, 27298–27305 (2007).
105. Zhu, S. *et al.* From the clinical problem to the basic research—Co-culture models of osteoblasts and osteoclasts. *International Journal of Molecular Sciences* **19**, 2284 (2018).
106. De Luca, A. *et al.* Relevance of 3d culture systems to study osteosarcoma environment. *Journal of Experimental and Clinical Cancer Research* **37**, (2018).
107. Currey, J. Collagen and the mechanical properties of bone and calcified cartilage. in *Collagen: Structure and Mechanics* 397–420 (2008). doi:10.1007/978-0-387-73906-9_14
108. Jafary, F., Hanachi, P. & Gorjipour, K. Osteoblast differentiation on collagen scaffold with immobilized alkaline phosphatase. *International Journal of Organ Transplantation Medicine* **8**, 195–202 (2017).

109. Matthews, B. G. *et al.* Enhanced osteoblastogenesis in three-dimensional collagen gels. *Bonekey Reports* **3**, (2014).
110. Datta, N., Holtorf, H. L., Sikavitsas, V. I., Jansen, J. A. & Mikos, A. G. Effect of bone extracellular matrix synthesized in vitro on the osteoblastic differentiation of marrow stromal cells. *Biomaterials* **26**, 971–977 (2005).
111. Haycock, J. W. 3D cell culture: a review of current approaches and techniques. *Methods in molecular biology (Clifton, N.J.)* (2011).
112. Amini, A. R., Laurencin, C. T. & Nukavarapu, S. P. Bone tissue engineering: Recent advances and challenges. *Critical Reviews in Biomedical Engineering* **40**, 363–408 (2012).
113. Middleton, J. C. & Tipton, A. J. Synthetic biodegradable polymers as orthopedic devices. *Biomaterials* (2000). doi:10.1016/S0142-9612(00)00101-0
114. Narayanan, G., Vernekar, V. N., Kuyinu, E. L. & Laurencin, C. T. Poly (lactic acid)-based biomaterials for orthopaedic regenerative engineering. *Advanced Drug Delivery Reviews* (2016). doi:10.1016/j.addr.2016.04.015
115. Ghassemi, T. *et al.* Current concepts in scaffolding for bone tissue engineering. *Archives of Bone and Joint Surgery* **6**, 90–99 (2018).
116. Ishaug, S. L., Yaszemski, M. J., Bizios, R. & Mikos, A. G. Osteoblast function on synthetic biodegradable polymers. *Journal of Biomedical Materials Research* **28**, 1445–1453 (1994).
117. Dhandayuthapani, B., Yoshida, Y., Maekawa, T. & Kumar, D. S. Polymeric scaffolds in tissue engineering application: A review. *International Journal of Polymer Science* **2011**, (2011).
118. Solchaga, L. A., Dennis, J. E., Goldberg, V. M. & Caplan, A. I. Hyaluronic acid-based polymers as cell carriers for tissue-engineered repair of bone and cartilage. *Journal of Orthopaedic Research* **17**, 205–13 (1999).
119. Phipps, M. C. *et al.* Mesenchymal stem cell responses to bone-mimetic electrospun matrices composed of polycaprolactone, collagen I and nanoparticulate hydroxyapatite. *PLoS ONE* **6**, (2011).
120. Bigi, A., Boanini, E., Panzavolta, S., Roveri, N. & Rubini, K. Bonelike apatite growth on hydroxyapatite-gelatin sponges from simulated body fluid. *Journal of Biomedical Materials Research* **59**, 709–15 (2002).
121. Motamedian, S. R. Smart scaffolds in bone tissue engineering: A systematic review of literature. *World Journal of Stem Cells* **7**, 657–668 (2015).
122. Liu, X. & Ma, P. X. Polymeric scaffolds for bone tissue engineering. *Annals of Biomedical Engineering* **32**, 477–486 (2004).
123. Carnachan, R. J., Bokhari, M., Przyborski, S. A. & Cameron, N. R. Tailoring the morphology of emulsion-templated porous polymers. *Soft Matter* 608–616 (2006). doi:10.1039/b603211g
124. Lerman, M. J., Lembong, J., Muramoto, S., Gillen, G. & Fisher, J. P. The evolution of polystyrene as a cell culture Material. *Tissue Engineering - Part B: Reviews* (2018). doi:10.1089/ten.teb.2018.0056
125. Knight, E., Murray, B., Carnachan, R. & Przyborski, S. Alvetex®: polystyrene scaffold technology for routine three dimensional cell culture. in *Haycock J. (eds) 3D Cell Culture. Methods in Molecular Biology (Methods and Protocols)* 323–340 (Humana Press, 2011). doi:https://doi.org/10.1007/978-1-60761-984-0_20
126. Hill, D. S. *et al.* A novel fully humanized 3D skin equivalent to model early melanoma invasion. *Molecular Cancer Therapeutics* **14**, 2665–73 (2015).
127. Clarke, K. E. *et al.* A robust and reproducible human pluripotent stem cell derived model of neurite outgrowth in a three-dimensional culture system and its application to study neurite inhibition. *Neurochemistry International* **106**, 74–84 (2017).
128. Marrazzo, P. *et al.* 3D reconstruction of the human airway mucosa in vitro as an experimental model to study NTHi infections. *PLoS ONE* **11**, (2016).
129. Huebsch, N. *et al.* Harnessing traction-mediated manipulation of the cell/matrix interface to control stem-cell fate. *Nature Materials* **9**, 518–26 (2010).
130. Kytýř, D., Petráňová, V. & Jiroušek, O. Assessment of micromechanical properties of trabecular bone using quantitative backscattered electron microscopy. in *13th Bilateral*

Czech/German Symposium (2012).
131. Lee, S. *et al.* Potential bone replacement materials prepared by two methods. *Materials Research Society Symposium Proceedings* **1418**, (2012).
132. Hardy, S. Mesenchymal stem cells as trophic mediators of neural differentiation. (Durham theses, Durham University, 2010).
133. Bokhari, M., Carnachan, R. J., Przyborski, S. A. & Cameron, N. R. Emulsion-templated porous polymers as scaffolds for three dimensional cell culture: Effect of synthesis parameters on scaffold formation and homogeneity. *Journal of Materials Chemistry* **17**, 4088–4094 (2007).
134. Zhang, L. & Chan, C. Isolation and enrichment of rat mesenchymal stem cells (MSCs) and separation of single-colony derived MSCs. *Journal of Visualized Experiments* 2–5 (2010). doi:10.3791/1852
135. He, Q., Ye, Z., Zhou, Y. & Tan, W. S. Comparative study of mesenchymal stem cells from rat bone marrow and adipose tissue. *Turkish Journal of Biology* **42**, 477–489 (2018).
136. Baghaei, K. *et al.* Isolation, differentiation, and characterization of mesenchymal stem cells from human bone marrow. *Gastroenterology and Hepatology from Bed to Bench* **10**, 208–213 (2017).
137. Banik, B. L., Riley, T. R., Platt, C. J. & Brown, J. L. Human mesenchymal stem cell morphology and migration on microtextured titanium. *Frontiers in Bioengineering and Biotechnology* **4**, (2016).
138. Wiesmann, A., Bühring, H.-J., Mentrup, C. & Wiesmann, H.-P. Decreased CD90 expression in human mesenchymal stem cells by applying mechanical stimulation. *Head & Face Medicine* **2**, (2006).
139. Simmons, P. J. & Torok-Storb, B. CD34 expression by stromal precursors in normal human adult bone marrow. *Blood* **78**, 2848–53 (1991).
140. Sidney, L. E., Branch, M. J., Dunphy, S. E., Dua, H. S. & Hopkinson, A. Concise review: evidence for CD34 as a common marker for diverse progenitors. *Stem Cells* **32**, 1380–1389 (2014).
141. Zuk, P. A. *et al.* Human adipose tissue is a source of multipotent. *Molecular Biology of the Cell* **13**, 4279–4295 (2002).
142. Wagner, W. *et al.* Comparative characteristics of mesenchymal stem cells from human bone marrow, adipose tissue, and umbilical cord blood. *Experimental Hematology* **33**, 1402–16 (2005).
143. Craig, W., Poppema, S., Little, M. T., Dragowska, W. & Lansdorp, P. M. CD45 isoform expression on human haemopoietic cells at different stages of development. *British Journal of Haematology* **88**, 24–30 (1994).
144. Karageorgiou, V. & Kaplan, D. Porosity of 3D biomaterial scaffolds and osteogenesis. *Biomaterials* **26**, 5474–5491 (2005).
145. Mastrogiacomo, M. *et al.* Role of scaffold internal structure on in vivo bone formation in macroporous calcium phosphate bioceramics. *Biomaterials* **27**, 3230–7 (2006).
146. Kim, K., Yeatts, A., Dean, D. & Fisher, J. P. Stereolithographic bone scaffold design parameters: osteogenic differentiation and signal expression. *Tissue Engineering - Part B: Reviews* **16**, 523–9 (2010).
147. O'Brien, F. J., Harley, B. A., Yannas, I. V. & Gibson, L. J. The effect of pore size on cell adhesion in collagen-GAG scaffolds. *Biomaterials* **26**, 433–41 (2005).
148. Murphy, C. M. & O'Brien, F. J. Understanding the effect of mean pore size on cell activity in collagen-glycosaminoglycan scaffolds. *Cell Adhesion and Migration* **4**, 377–381 (2010).
149. Dragan, A. I. *et al.* Characterization of PicoGreen interaction with dsDNA and the origin of its fluorescence enhancement upon binding. *Biophysical Journal* **99**, 3010–3019 (2010).
150. Tomoaia, G. & Pasca, R. D. On the collagen mineralization. A review. *Clujul Medical* (2015). doi:10.15386/cjmed-359
151. Golub, E. E. & Boesze-Battaglia, K. The role of alkaline phosphatase in mineralization. *Current Opinion in Orthopaedics* **18**, 444–8 (2007).
152. Moursi, A. M. *et al.* Fibronectin regulates calvarial osteoblast differentiation. *Journal of Cell Science* **109**, 1369–1380 (1996).

153. Calabrese, G. *et al.* Collagen-Hydroxyapatite scaffolds induce human adipose derived stem cells osteogenic differentiation in Vitro. *PLoS ONE* (2016). doi:10.1371/journal.pone.0151181
154. Rumiński, S., Kalaszczyńska, I., Długosz, A. & Lewandowska-Szumieł, M. Osteogenic differentiation of human adipose-derived stem cells in 3D conditions - comparison of spheroids and polystyrene scaffolds. *European cells & materials* (2019). doi:10.22203/eCM.v037a23
155. Li, J., Liu, X., Crook, J. M. & Wallace, G. G. Development of a porous 3D graphene-PDMS scaffold for improved osseointegration. *Colloids and Surfaces B: Biointerfaces* (2017). doi:10.1016/j.colsurfb.2017.07.087
156. Hardy, S. Establishment of in vitro MSC cultures and assessment of their functional behaviour when cultured on a novel 3D polystyrene-based scaffold. (2010).
157. Assaf, R. B. *et al.* Evaluation of the osteogenic potential of different scaffolds embedded with human stem cells originated from schneiderian membrane: An in vitro study. *BioMed Research International* (2019). doi:10.1155/2019/2868673
158. Karaoz, E. *et al.* Characterization of mesenchymal stem cells from rat bone marrow: Ultrastructural properties, differentiation potential and immunophenotypic markers. *Histochemistry and Cell Biology* **132**, 533–546 (2009).
159. Huang, Y. C. *et al.* Hypoxia inhibits the spontaneous calcification of bone marrow-derived mesenchymal stem cells. *Journal of Cellular Biochemistry* (2012). doi:10.1002/jcb.24014
160. Huang, Y. Z. *et al.* Species variation in the spontaneous calcification of bone marrow-derived mesenchymal stem cells. *Cytotherapy* (2013). doi:10.1016/j.jcyt.2012.11.011
161. Funaoka, H., Dohi, Y., Ohgushi, H., Akahane, M. & Imamura, T. Development of a high-specificity enzyme-linked immunosorbent assay (ELISA) system for the quantification and validation of intact rat osteocalcin. *Immunological Investigations* (2010). doi:10.3109/08820130903428283
162. Nakamura, A. *et al.* Osteocalcin secretion as an early marker of in vitro osteogenic differentiation of rat mesenchymal stem cells. *Tissue engineering. Part C, Methods* **15**, 169–80 (2009).
163. Tsao, Y. T. *et al.* Osteocalcin mediates biomineralization during osteogenic maturation in human mesenchymal stromal cells. *International Journal of Molecular Sciences* (2017). doi:10.3390/ijms18010159
164. Ogasawara, T. *et al.* Bone morphogenetic protein 2-induced osteoblast differentiation requires Smad-mediated down-regulation of Cdk6. *Molecular and Cellular Biology* (2004). doi:10.1128/mcb.24.15.6560-6568.2004
165. Noda, M. & Denhardt, D. T. Regulation of osteopontin gene expression in osteoblasts. *Annals of the New York Academy of Sciences* **760**, 242–8 (1995).
166. McDonald, J. A., Kelley, D. G. & Broekelmann, T. J. Role of fibronectin in collagen deposition: Fab' to the gelatin-binding domain of fibronectin inhibits both fibronectin and collagen organization in fibroblast extracellular matrix. *Journal of Cell Biology* (1982). doi:10.1083/jcb.92.2.485
167. Merceron, C. *et al.* Hypoxia-inducible factor 2α is a negative regulator of osteoblastogenesis and bone mass accrual. *Bone Research* **7**, (2019).
168. Todo, M. & Arahira, T. In vitro bone formation by mesenchymal stem cells with 3D collagen/β-TCP composite scaffold. in *Proceedings of the Annual International Conference of the IEEE Engineering in Medicine and Biology Society, EMBS* 409–412 (2013). doi:10.1109/EMBC.2013.6609523
169. Lee, A., Langford, C. R., Rodriguez-Lorenzo, L. M., Thissen, H. & Cameron, N. R. Bioceramic nanocomposite thiol-acrylate polyHIPE scaffolds for enhanced osteoblastic cell culture in 3D. *Biomaterials Science* **5**, 2035–2047 (2017).